U.S. DEPARTMENT OF THE INTERIOR
U.S. GEOLOGICAL SURVEY

Southern Monterey Bay Continental Shelf Investigations: Former Fort Ord Restricted Zone

edited by

Stephen L. Eittreim
US Geological Survey, 345 Middlefield Rd., Menlo Park, CA 94025

Open File Report 97-450

1997

Southern Monterey Bay Continental Shelf Investigations: Former Fort Ord Restricted Zone

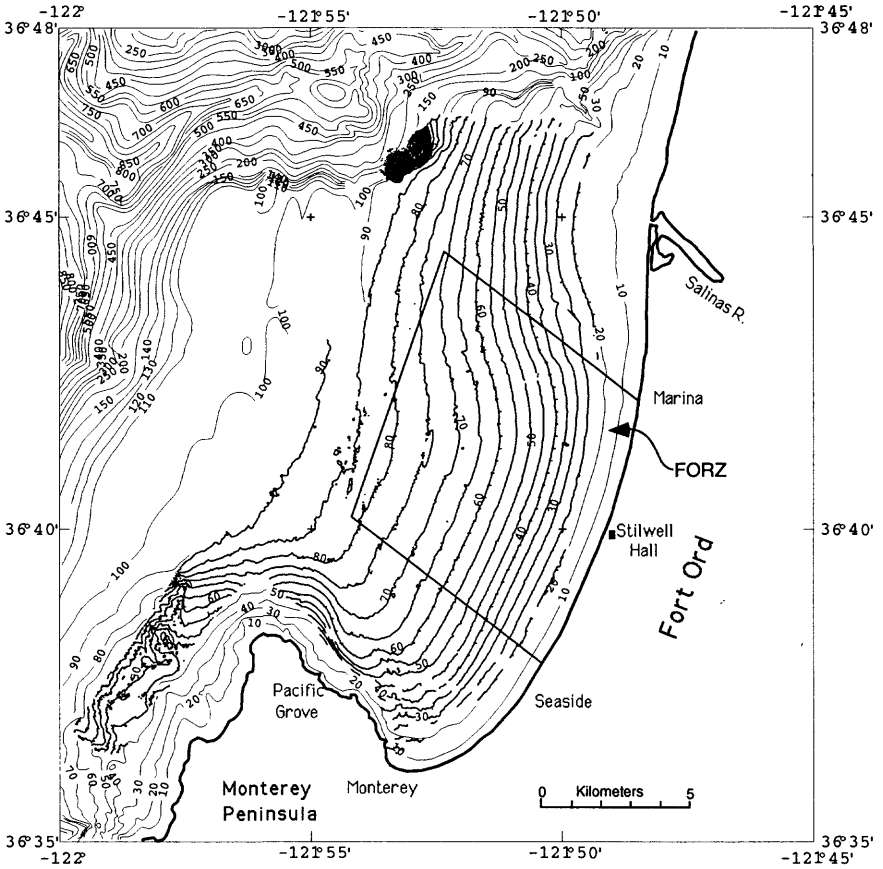

U.S. DEPARTMENT OF THE INTERIOR
U.S. GEOLOGICAL SURVEY

Stephen L. Eittreim, Brian D. Edwards, Andrew J. Stevenson, James V. Gardner and Marjorie D. Medrano
U.S. Geological Survey

Korie Ann Johnson, Gregor Cailliet, James Oakden, Chris Malzone, Russell Fairey and Stewart Lamerdin
Moss Landing Marine Laboratories

Mark Stephenson, Gary Ichikawa, Jon Goetzl, Kim Paulson and Mark Pranger
California Department of Fish and Game, Moss Landing Marine Laboratories

Ronald Tjeerdema, John Newman, Johnathon Becker and Matthew Stoetling
University of California Santa Cruz

Larry A. Mayer
University of New Brunswick, N.B., Canada

Rikk Kvitek
California State University Monterey

George Gardner
US Environmental Protection Agency, Naragansett

Open File Report 97-450

Preface

Fort Ord Army Base officially closed its doors in 1994. From 1917 to 1994 the 114 square kilometer tract on the coast of Monterey Bay was used as a U.S. Army training base and as staging area for troops in time of war. The Fort Ord Restricted Zone (FORZ) is an area extending about 7 km off the coast where access by civilian boaters was restricted. The stated purpose of the FORZ was to protect boaters from stray rifle and artillery fire that may have bypassed the coastal dunes that were used as backstops for target practice. In 1994 the FORZ was declared no longer in existence.

The plan for Fort Ord's conversion to civilian use has included extensive environmental cleanup operations onshore for spilled oil, lead bullets, ammunition shells, PCBs from transformers, and other materials that accumulated through the base's 70+ years of use (Harding Lawson Associates, 1995, Basewide Remedial Investigation/Feasability Study Fort Ord, California).

With the establishment of the Monterey Bay National Marine Sanctuary (MBNMS) in 1992, a group of scientists assembled into a committee called the Research Activities Panel (RAP). RAP offers advice to the Monterey Bay National Marine Sanctuary Office on scientific issues relating to stewardship of the Sanctuary. A spinoff group from RAP was concerned about possible seafloor hazards that may exist in the FORZ and they proposed a series of studies of the seafloor environment in and around the FORZ to come to a better understanding of "what is out there."

The result is the investigations in this report that deal with seafloor morphology and geology, toxicology of seafloor muds, and findings regarding some abnormal fish lesions that have been recovered in the FORZ area. We believe the investigations here are a good start at a detailed understanding of the seafloor environment of the southern Monterey Bay shelf seafloor. As with seafloor studies anywhere, one's definition of "detailed" is a subjective judgement of what is necessary for the job at hand, and for serious students of the seafloor the detail is never great enough; the detailed knowledge of the 1990s will likely be bypassed in the coming decades by better techniques and more surveys.

The work was funded through the offices of the U.S. Army Corps of Engineers (Dan McMindes and David Eisen). Many scientists and administrators from Fort Ord (Gail Youngblood), Envirnomental Protection Agency (John Cheshnut, Robert Hall), National Oceanic and Atmospheric Administration's MBNMS Office (Terry Jackson, Patrick Cotter, Andrew DeVogelaere, Aaron King), and Harding Lawson Associates (Ed Ticken) were involved in the planning stages of these studies. Thanks are due all the above for advice and patience through periods of funding uncertainties and with complex lines of communication. We would especially like to thank the Army for their generous and farsighted attitude in allowing studies to extend beyond the FORZ "box" to allow establishing context for the findings inside the FORZ.

Stephen L. Eittreim, *United States Geological Survey*

Contents

Multibeam Bathymetry and Acoustic Backscatter Imagery of the Southern Monterey Bay Shelf.

Stephen L. Eittreim and Andrew J. Stevenson
U.S. Geological Survey, Menlo Park, CA 94025

Larry A. Mayer
Univ. of New Brunswick, Fredericton, N.B., Canada E3B 5A3

James Oakden[1] and Chris Malzone
Moss Landing Marine Laboratories, Moss Landing, CA 95039

Rikk Kvitek
California State Univ. Monterey, Seaside, CA 93955-8001

ABSTRACT

The seafloor of the former Fort Ord Restricted Zone (FORZ) and surrounding area is a generally flat, featureless plain with the exception of a) the subtle sculpting of coarse sand troughs due to active sand transport, and b) the outcrop of older consolidated bedrock over limited areas. Outcropping bedrock surrounds the Monterey Peninsula and occurs in the Monterey Bay Fault zone, a moderately active fault zone north of Monterey that has locally tilted and disrupted the shelf stratigraphy. Within the realizable limits of detection of the EM-1000 multibeam system, no surficial debris could be identified that might be interpreted as leftover from the Army's use of this area over the last 70 years. The EM-1000 system in this water depth range has a horizontal pixel resolution of 5 m in bathymetry and 2.5 m in backscatter, and a vertical resolution better than 1 m. Higher resolution surveys using 500-kHz side-scan systems with 10-cm pixel resolution were carried out in a 1x1 km^2 core area of the FORZ. Only ephemeral features, interpreted to be biologic targets, could be found.

INTRODUCTION

The 6-km wide southern Monterey Bay shelf is typical of the wave-cut platforms that form the continental shelves of the west coast of the U.S. where the morphology is formed by subsidence or local uplift of the continental margin, the supply and deposition of sediment, and the relatively recent post-glacial raising of sealevel (Dupre', 1990). The present shelf morphology is predominantly influenced by the last sea-level lowstand at about -100 m that ended about 10,000 yr ago. Salinas River sediment, in addition to alongshore sediment transport from more distant sources, are now in the process of filling the depositional space below wave base that has been created by the raising of the sea surface to its present level (Chin et al, 1988). The rocky outcrops of the Monterey Peninsula form a buttress that offers some protection from the southwesterly open-ocean swell and also interrupts the normally southward, wind-driven, along-shore sediment transport. Seafloor sediments of the broad flat shelf north of Monterey grade from nearshore medium sands (to 20m depth), to fine sands (to 50m depth), to silts and clays at greater depths (Dingler, et.al.,1985; Edwards and Gardner, this volume). This surficial trend then reverses at about 90 m where coarse relict sediments are found over the broad outer shelf to the shelf break.

The shoreline of the former Fort Ord Restricted Zone (FORZ) is subject to large wave swell from the northwest and because of wave erosion this shoreline exhibits one of the steepest shoreface slopes found in the greater Monterey Bay area (Dingler, el. al., 1985). A series of erosional coarse-sand-floored troughs, parallel to shore, have been found in this area in the depth

[1] Also at ABA Consultants, Capitola, CA

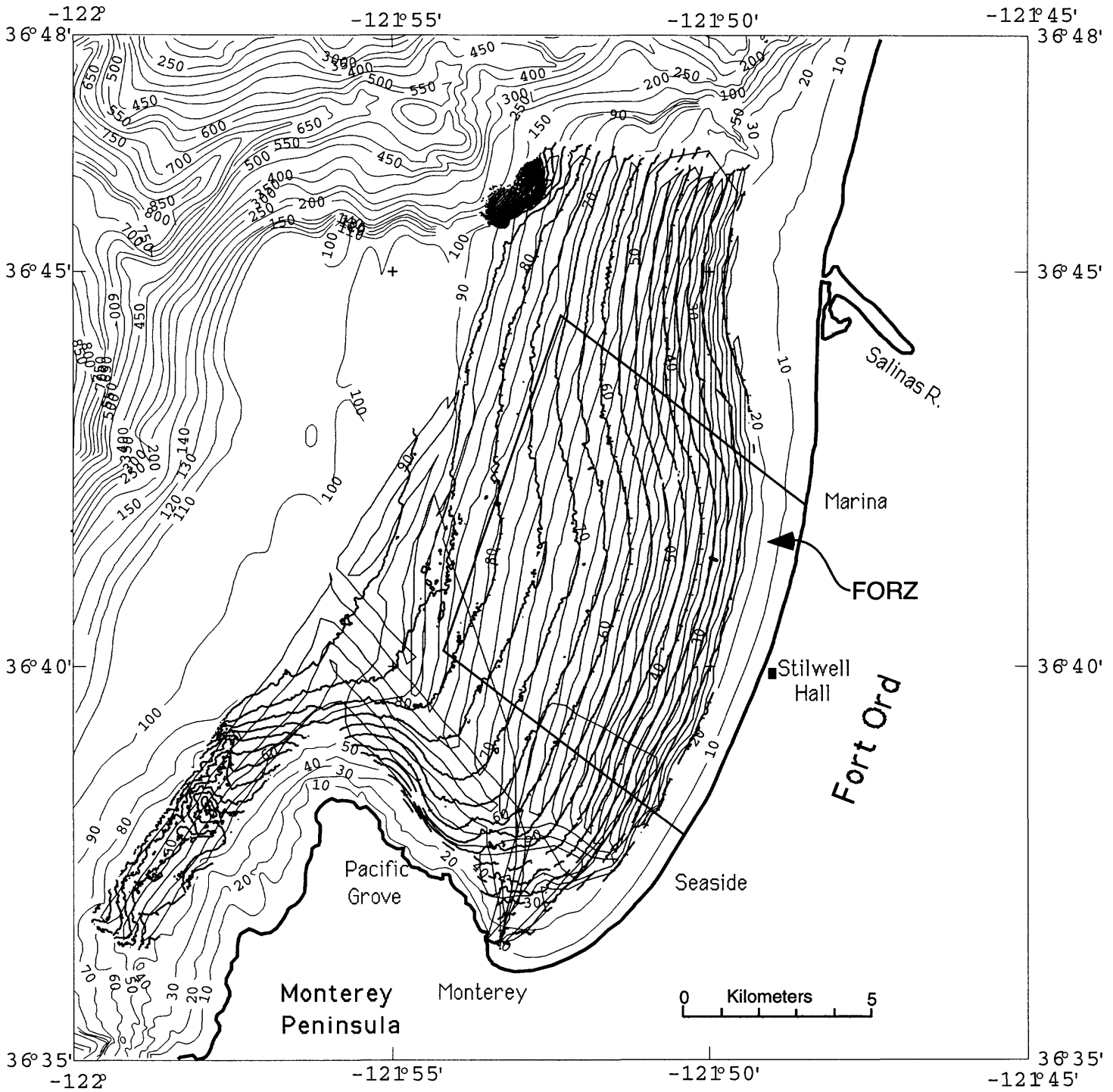

Fig. 1 Tracks of R/V Pacific Hunter, with track-spacing ranging from 80 to 300 m. 5-m contour bathymetry, in bold, from EM-1000 data in survey region, 10-m contours generalized elsewhere.

zone from 10 to 30 m; these may be related to the high-energy shoreface of this area. These troughs, also called "sand bands", or "ripple troughs", have been shown by Hunter et al (1984) and Mariant (1993) to be dynamic features that change shape and position from season to season. They are floored with 1-m wavelength coarse sand ripples. The orientation of the ripples is parallel to shore, indicating active coarse sand transport. Mariant (1993) argues that the ripple troughs are lag-deposits formed beneath the offshore rip currents that develop during high wave conditions.

The multibeam bathymetric survey reported on here was conducted as part of a series of studies to provide detailed information about the seafloor of the FORZ. Due to its designation as a "Restricted Zone" for boaters from the 1940s to 1995, the region is relatively unknown to bottom fisherman and divers. There is some concern among the public that over the many decades of use by the Fort Ord Army Base, and possibly inadequate record-keeping of offshore activities, there may be hazardous seafloor debris. Thus, the purpose of this investigation was a comprehensive investigation of seafloor morphology in the FORZ to identify any suspect targets that may be anthropogenic.

We surveyed with a multibeam bathymetric swath map system to provide a comprehensive "roadmap" to the features on the seafloor. With adequate overlap of swaths, all features above a certain size should be detected using such a swath-map system. In contrast, conventional single-beam surveys require interpolation between tracklines to arrive at a comprehensive seafloor view. In addition to the multibeam survey, higher resolution surveys were conducted with a small-boat 500 kHz system, at slower survey speeds, to look for small items in areas that were judged most promising for searches, based on the multibeam data. The slower boat speeds and higher pulse-repetition rate of collection give higher-density along-track coverage (about 12 cm), and the higher frequency sound used gave higher-density across-track coverage (about 3 cm). The greater pixel resolution of these high-frequency, slow-speed surveys results however in low rates of ground coverage and only small selected areas could be covered in the time available.

Using the multibeam system we were unable to identify any targets as anthropogenic debris, although areas of apparent seafloor lumps or "suspect targets" needing higher resolution surveys, were located. Using the higher frequency system, similarly, no targets were identified that were judged to be anthropogenic debris although many interesting ephemeral, and presumably biologic, targets were seen.

SURVEY METHODS

EM-1000 System

The Simrad EM-1000 system (Godin, et al., 1992) uses 95 kHz sound projected from a half-donut shaped transducer array that also acts as receiver. This transducer gives acoustic returns from a swath that is 3.4 to 7.4 times the water depth, depending on mode used. In ultrawide or shallow mode (150 to 200m water depths), the mode used for most of our survey, it operates with 60 beams of information radiating out at 2.5° per beam. The beams are shifted by 1.25° every other ping so that an effective total of 120 beams at 1.25° spacings is obtained for each pair of pings. The time delay of the acoustic returns determines seafloor depth at each beam location on the seafloor. For automatic bottom detection, the system uses an amplitude-detect algorithm for inner beams to detect the sharp leading edge of the returned echo, the conventional method of depth measurement by echo sounding. For outer beams, where the leading edge of the reflected pulse loses its sharpness, a phase-interferometric technique is used. By splitting each beam into two "halfbeams", the phase difference between these "halfbeams" is calculated providing a measure of the angle of arrival of the echo which can be converted to bottom depth for that beam. Both amplitude-detect and phase-detect is carried out on each beam and the best quality detection method is selected by the system software which results generally in inner-beams using amplitude-detect and outer beams phase-detect for the calculation of depth.

In addition to providing detailed bathymetric data, the EM-1000 also provides quantitative seafloor backscatter data that can be displayed in a sidescan sonar-like image and used to gain insight into the distribution of seafloor properties. Acoustic backscatter strength is a function of bottom composition and small-scale roughness, with fine-grained muds generally returning lower

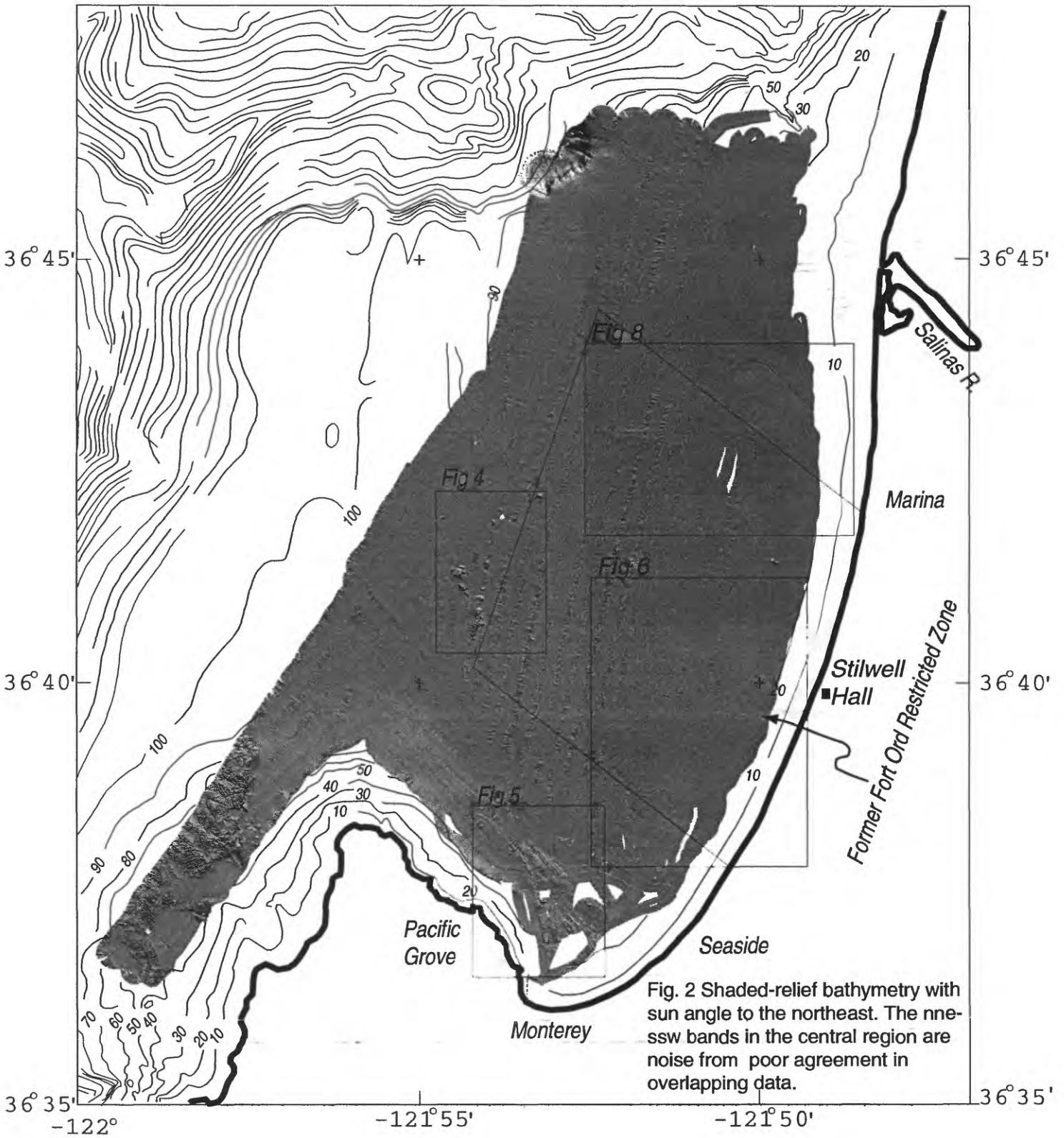

Fig. 2 Shaded-relief bathymetry with sun angle to the northeast. The nne-ssw bands in the central region are noise from poor agreement in overlapping data.

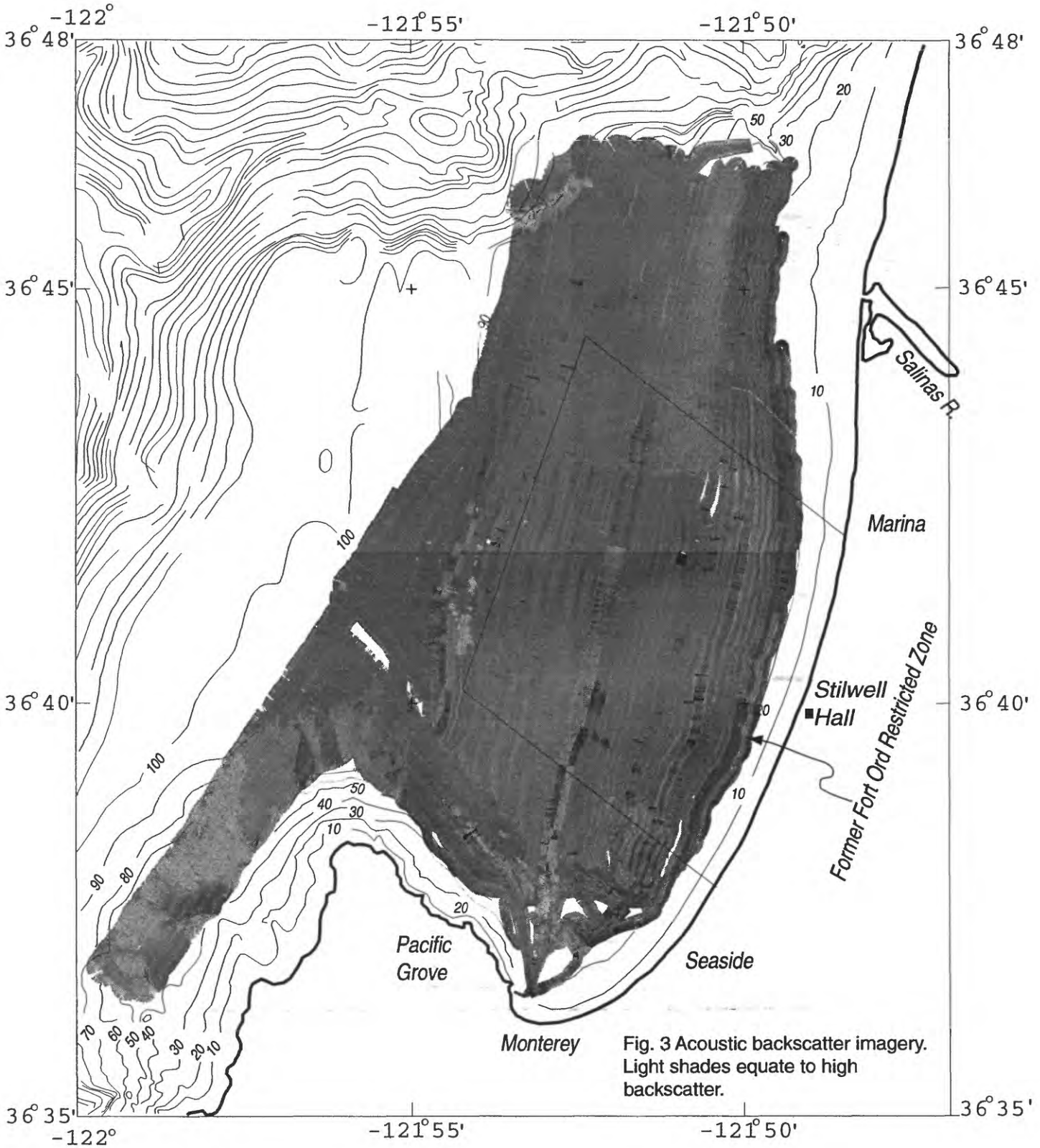

Fig. 3 Acoustic backscatter imagery. Light shades equate to high backscatter.

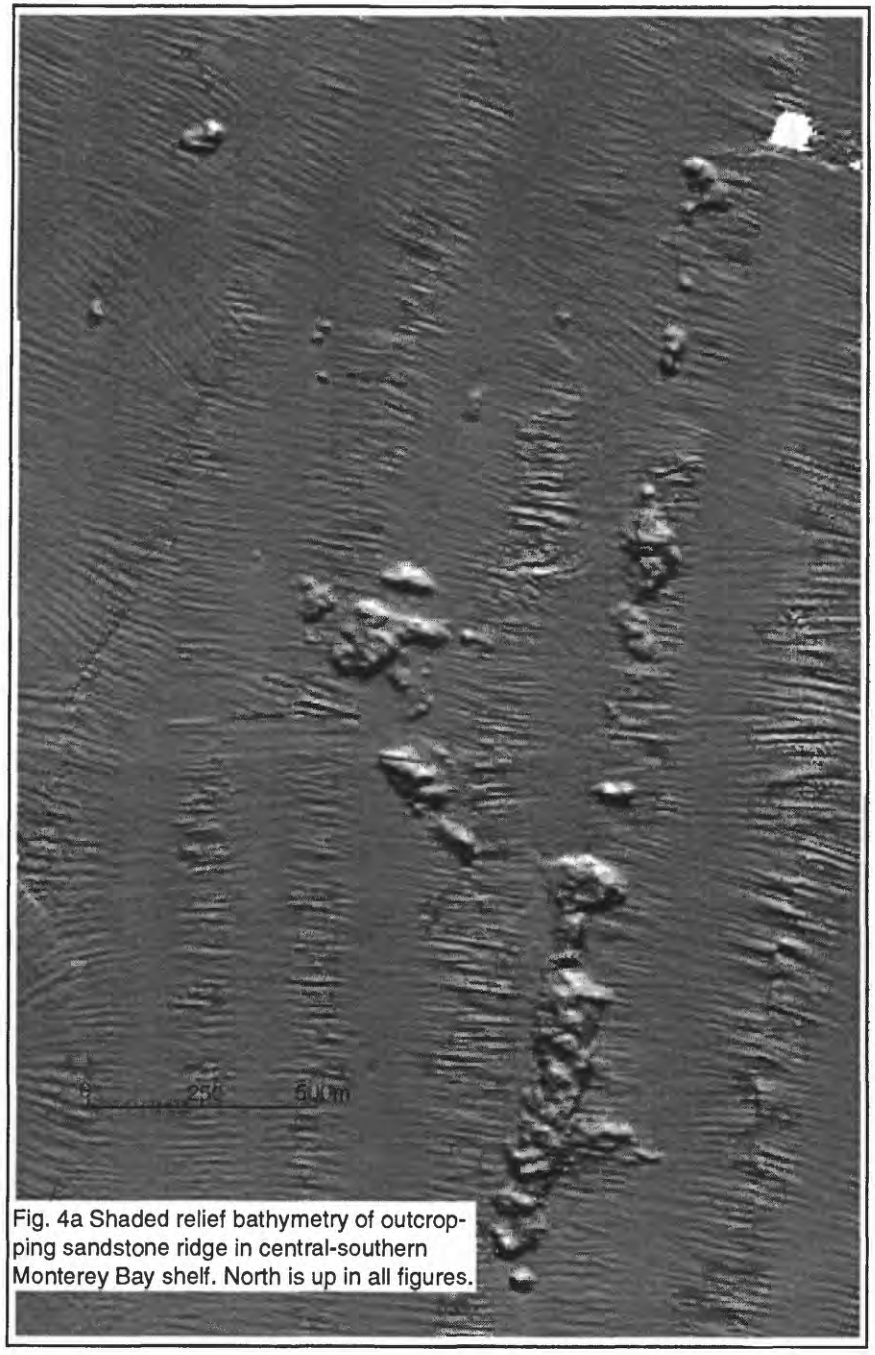

Fig. 4a Shaded relief bathymetry of outcropping sandstone ridge in central-southern Monterey Bay shelf. North is up in all figures.

Fig 4b Backscatter view of outcropping sandstone ridge, central-southern Monterey Bay shelf in 85-m water depth. North is up in all figures.

backscatter strength than sands or rock outcrops. A time series of echo amplitudes from each beam is recorded (at 0.2 to 2.0 msec sampling rate depending on the water depth). These echoamplitudes (which are sampled at an interval that is much finer than the beam spacing) can be strung together from beam to beam to produce a sidescan sonar image with the theoretical resolution of the sampling interval (15 cm at 0.2 msec). Because the angular direction of each range sample is known, the amplitude information can be placed in its geometrically correct position relative to the across-track profile. The manufacturer corrects the amplitude series for gain changes, propagation losses, predicted beam patterns and for the insonified area (with some simplifying assumptions like a flat seafloor and Lambertian scattering). Subsequent processing uses real seafloor slopes and applies empirically derived beam-pattern corrections to produce a quantitative estimate of seafloor backscatter across the swath.

In addition to the multibeam sonar, integration of a number of ancillary systems were required. These include: 1) a differential GPS positioning system; 2) a motion sensor to accurately measure the heave, pitch and roll of the vessel and transform these measurements to estimates of the motion of the transducer at the time of transmission and reception, and; 3) CTD measurements to determine the sound speed structure of the water column. Seafloor depths covered in the survey ranged from the 20 m contour on the nearshore side to about 90 m offshore. Horizontal resolution of the resulting data for this survey, given the swath widths that ranged from 80 to 300 m, and ship speeds of 6 knots, are 5 m pixels for depth and 2.5 m pixels for backscatter. However, features with vertical relief smaller than 1 m are detected, as will be shown in the data presented below.

To carry out the survey we contracted with C&C Technologies of Lafayette, LA for use and operation of their EM-1000 system and with Humboldt State University for ship support. The 125-ft R/V PACIFIC HUNTER, was outfitted with the EM-1000 transducer pod mounted 2.7-m below the ship's water line on a pole welded to the bow stem. The motion sensor system, a POS-MV, was mounted in the forward deck housing about 10-m aft of the transducer. Severe temporal and spatial changes in watermass properties were encountered during the survey and thus sound velocity profiles were made approximately every hour. Figure 1 shows the track lines that were run from 30 July -2 August, 1995 in wind conditions that ranged from 5 to 20 knots. Figures 2 and 3 show the bathymetric and backscatter results, respectively. Wind and wave swell conditions often exceeded the capacity of the pole-mounted system to maintain a rigid mechanical link between transducer and the motion sensor, resulting in a "twist" error that severely degraded the records. This degradation is most apparent in the lack of agreement at overlaps between adjacent swaths (see for example, in Figures 2 and 4a, the north-south noise bands in the central portion of the survey). This noise degrades our ability to contour the bathymetry at a less than 5 m contour interval. However, seafloor features that are less than 1 m in relief are easily identified in the data, as the relative precision of depth information is better than 1 m (see for example in Figure 6 the flat-floored troughs along the coast in 25 m water depths that are less than 1-m relief; Hunter et. al., 1984).

500 kHz side-scan sonar systems

To derive higher-resolution seafloor imagery of the FORZ, we used Klein and EG&G side-scan sonar systems in small-area surveys with a switchable 100/500 kHz-source fish towed at about 3 knots speed. All data were recorded digitally. Navigation utilized differential GPS. At tow speeds of about 3 knots, raw pixel resolutions were 3 cm and pixel resolution of processed mosaics was 12 cm. Two days on Moss Landing Marine Labs 35-ft vessel R/V RICKETS on October 20-21, 1995 and three days on USGS's 42-ft vessel R/V DAVID JOHNSTON on October 22-24, 1996 resulted in 4 surveys of approximate 1-km^2 segments of the FORZ seafloor. An area in the northern FORZ was surveyed on three separate days in 1995 and 1996.

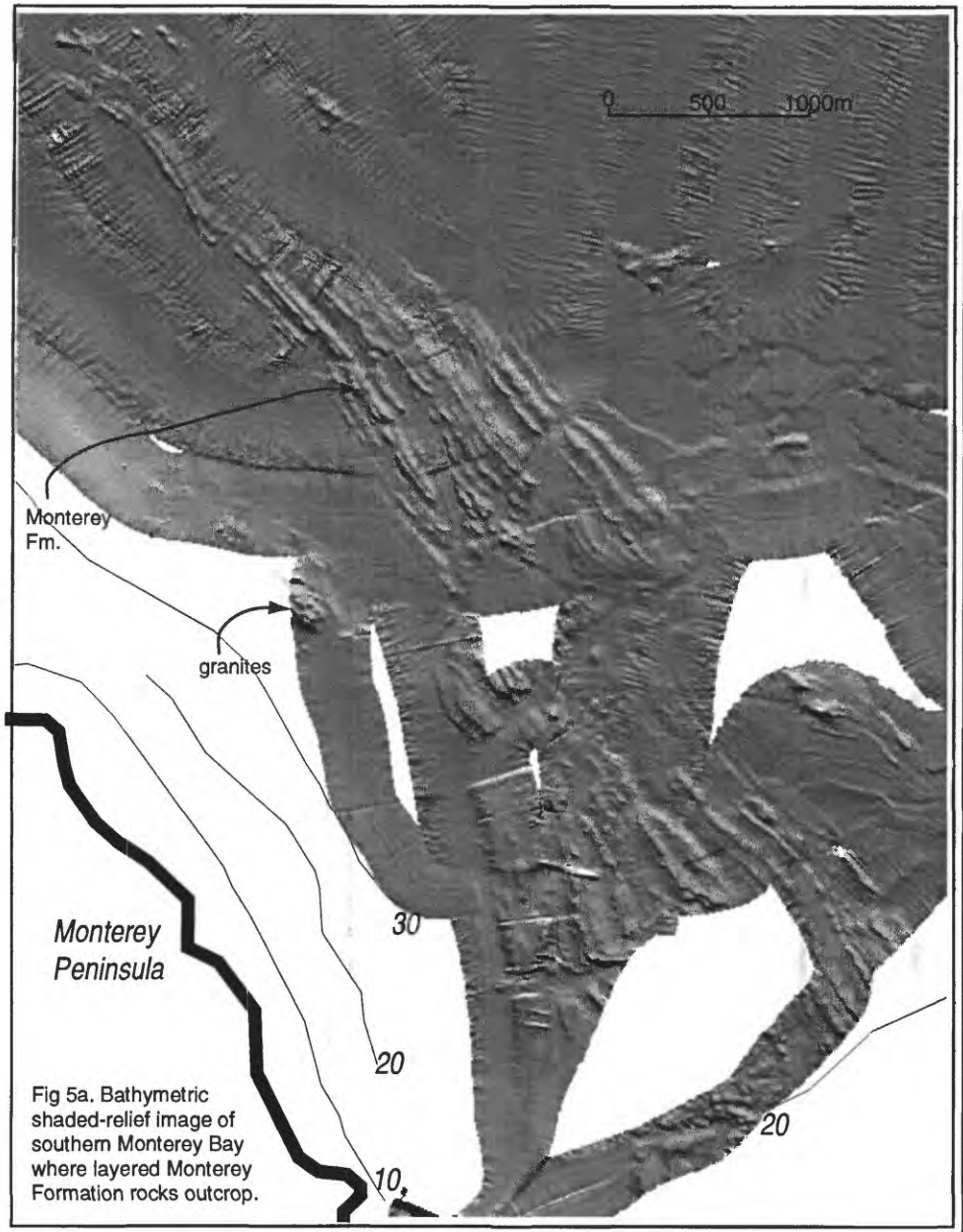

Fig 5a. Bathymetric shaded-relief image of southern Monterey Bay where layered Monterey Formation rocks outcrop.

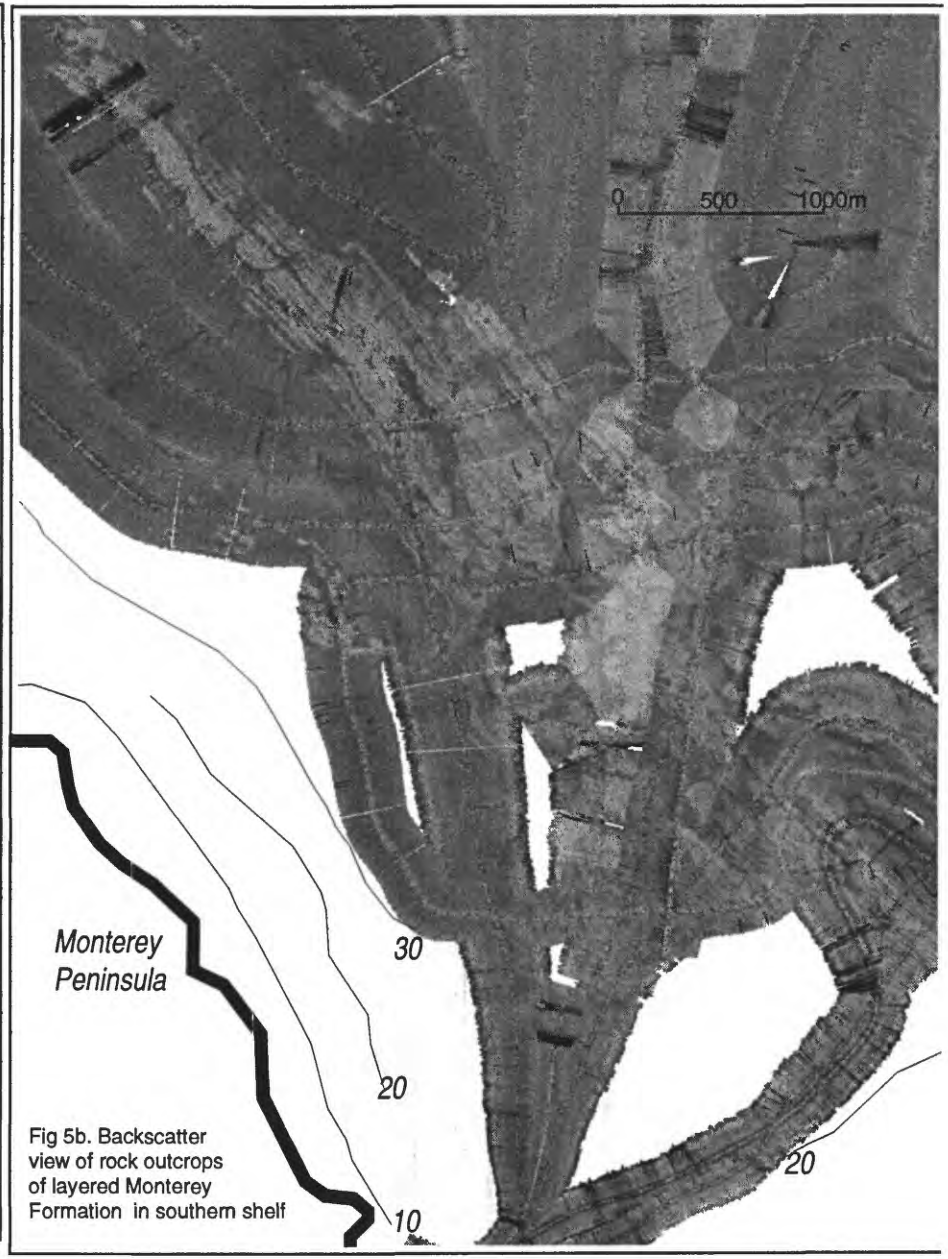

Fig 5b. Backscatter view of rock outcrops of layered Monterey Formation in southern shelf

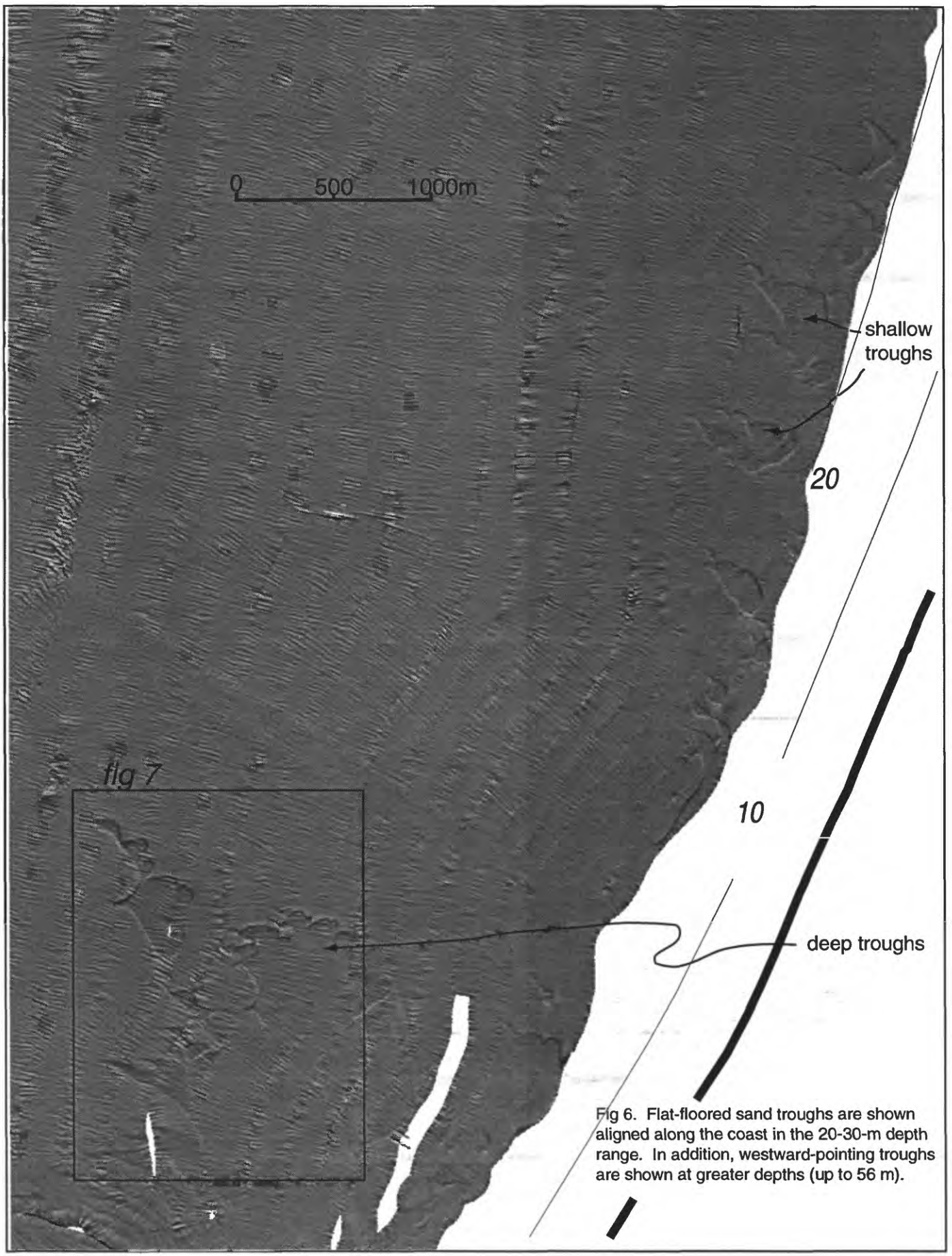

Fig 6. Flat-floored sand troughs are shown aligned along the coast in the 20-30-m depth range. In addition, westward-pointing troughs are shown at greater depths (up to 56 m).

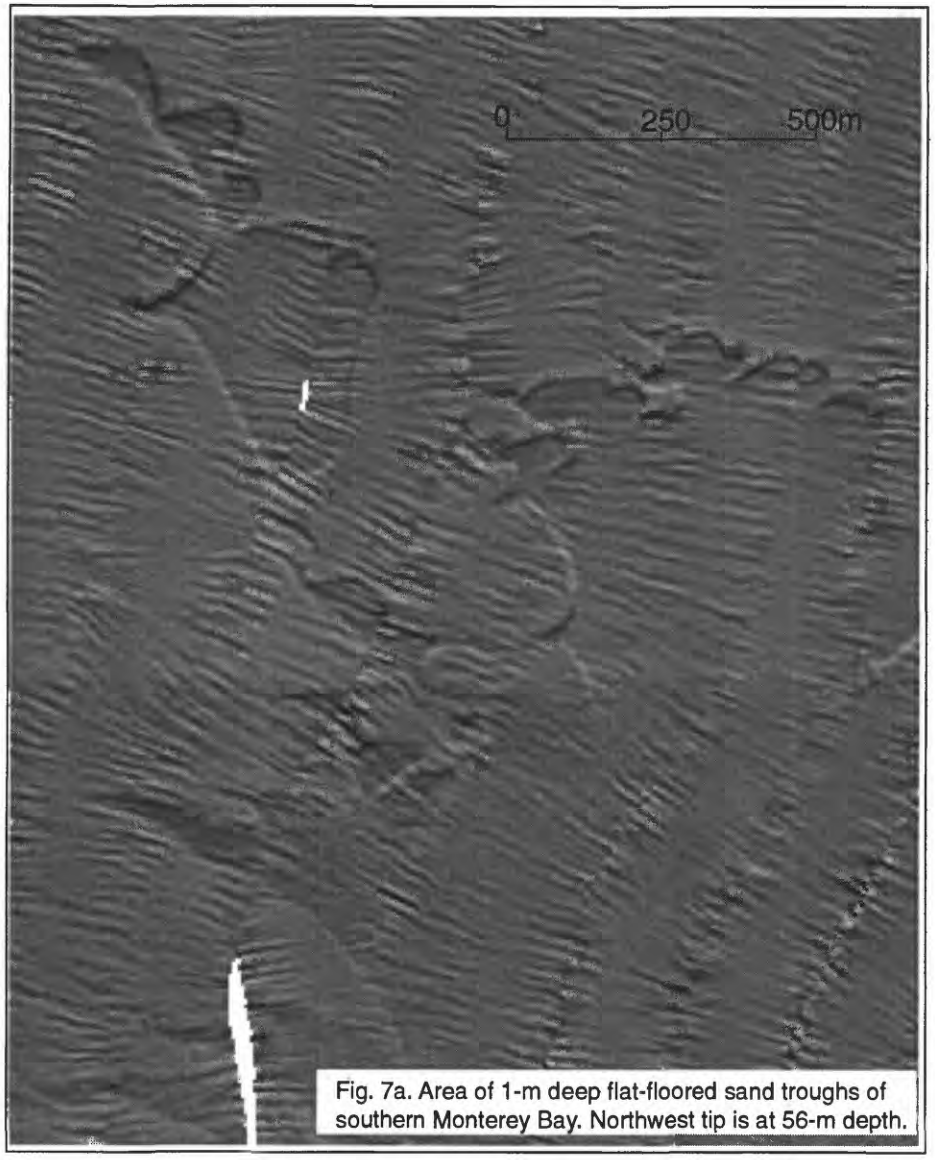

Fig. 7a. Area of 1-m deep flat-floored sand troughs of southern Monterey Bay. Northwest tip is at 56-m depth.

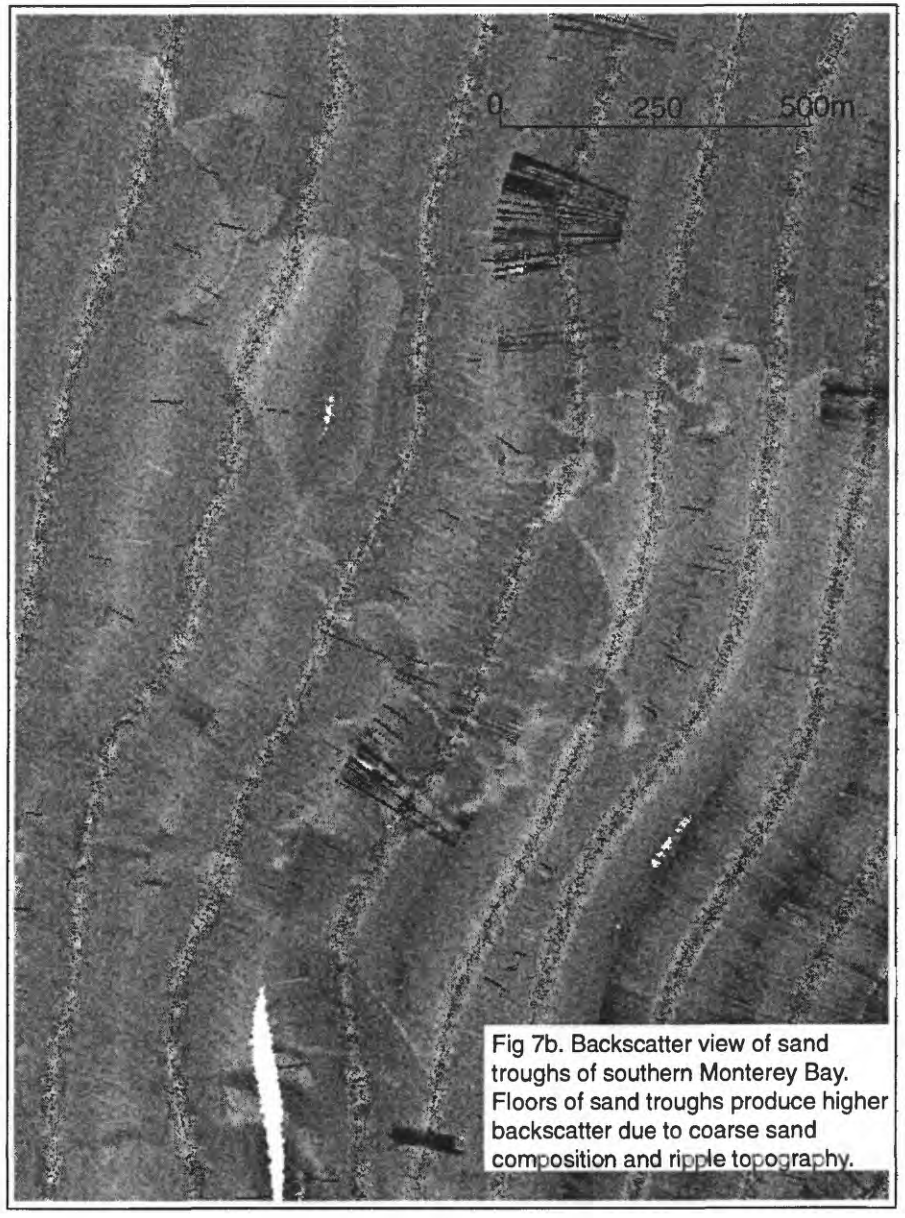

Fig 7b. Backscatter view of sand troughs of southern Monterey Bay. Floors of sand troughs produce higher backscatter due to coarse sand composition and ripple topography.

RESULTS

EM-1000 data

The EM-1000 data set covers the southern Monterey Bay shelf, except for the outermost shelf from 90 to 110-m water depths (Figure 2). Images show the seafloor of southeast Monterey Bay to be mostly a flat featureless plain with the exception of a few rocky outcrops and sedimentary features that are highlighted in figures 4 and 5 and will be discussed in later sections.

The backscatter imagery of Figure 3 shows rocky outcrops and coarse sand troughs that are features of high backscatter probably due to both high acoustic impedance contrast with the overlying water, and to the surface roughness associated with rocky outcrops and the coarser sands that are commonly rippled. The rough granitic terrain northwest of the Monterey Peninsula is of particularly high and variable backscatter. Adjacent to these outcrops northwest of the Peninsula lie areas of intermediate to high but uniform backscatter that we interpret to be sandy bottom, probably associated with the erosion of the granitic terrain of the Peninsula. The two zones of low backscatter that project north-northwest from the northern tip of the Peninsula, on close examination of the bathymetric data, are seen to be flat areas of seafloor that are about 1-m shallower than the surrounding regions. The contrast in backscatter could be due to a sand-mud contrast, with lower-backscatter muds mantling the shallower regions, or it could be a contrast between rippled sands of the deeper troughs and unrippled sands on the 1-m shallower seafloor.

The upper-most continental slope, sampled in the northwestern-most corner of the data coverage (Fig 3), shows as a high-backscatter zone, presumably due to either rocky outcrops or coarse seafloor sand deposits. Greene (1977) mapped this portion of the upper-slope seafloor as a slump scar. In the following sections, we will discuss some of the features of interest that are displayed in both bathymetric and backscatter data of the southern Monterey Bay shelf.

500 kHz side-scan data

Results of the higher-resolution small-area surveys included a survey of the "Fort Ord Ridge", a Y-shaped ridge of outcropping sandstone ledges (Eittreim et al, 1995) along the western edge of the FORZ, and three separate surveys of an area in the core of the FORZ where "suspect" targets (i.e., possibly anthropogenic) had been imaged with the EM-1000 system. Of the three surveys, one was completed in November, 1995, and the other two were completed on two subsequent days in October, 1996. The third survey of this core area revealed that targets that were considered "suspect" were in fact ephemeral biologic targets (see below).

Fort Ord Ridge

This ridge lies just outside the western edge of the FORZ and appears as two intersecting linear ridges each of about 5-m relief (Figure 4a) and of high acoustic backscatter (Figure 4b). Rock outcrops that occur on the outer shelf to the southwest, outside the boundaries of our EM-1000 coverage, may be similar and related features and are known by the informal name of Portugese Ledge, a favorite groundfishing location on the outer shelf and upper continental slope (Greene et al, 1995). Fort Ord Ridge occurs in 84 m water depth on an otherwise flat and featureless outer shelf. The north-south arm of the ridge is about 3 km in length and the rock outcrops are about 50-100 m across. High-resolution sub-bottom reflection profiles (Chin et al, 1988) show that the ridge consists of eroded remnants of planar strata that dip to the west at about 5°. Video images and rock samples of the ridge were collected on an ROV dive using the Monterey Bay Aquarium Research Institute's R/V Ventana (D. Orange, chief scientist). These images verified that the ledges dip gently westward and consist of indurated medium to coarse sandstone layers, cemented with carbonate, from a few centimeters to a half meter in thickness. The likely source of these outcropping sandstone ledges are stratigraphic units of the lower Monterey Formation that have been uplifted. The Monterey Formation are layered clastic rocks with thin sandstone layers at its base. It is thought to underlie the southeast Monterey Bay shelf (Greene and Hicks, 1990). Its uplift above the shelf surface was probably caused by tectonic elevation among the various blocks and slivers of crust involved in the multi-strand Monterey Bay fault zone, a northwest-southeast trending fault zone that extends from Seaside to the region south of Davenport, west of Santa

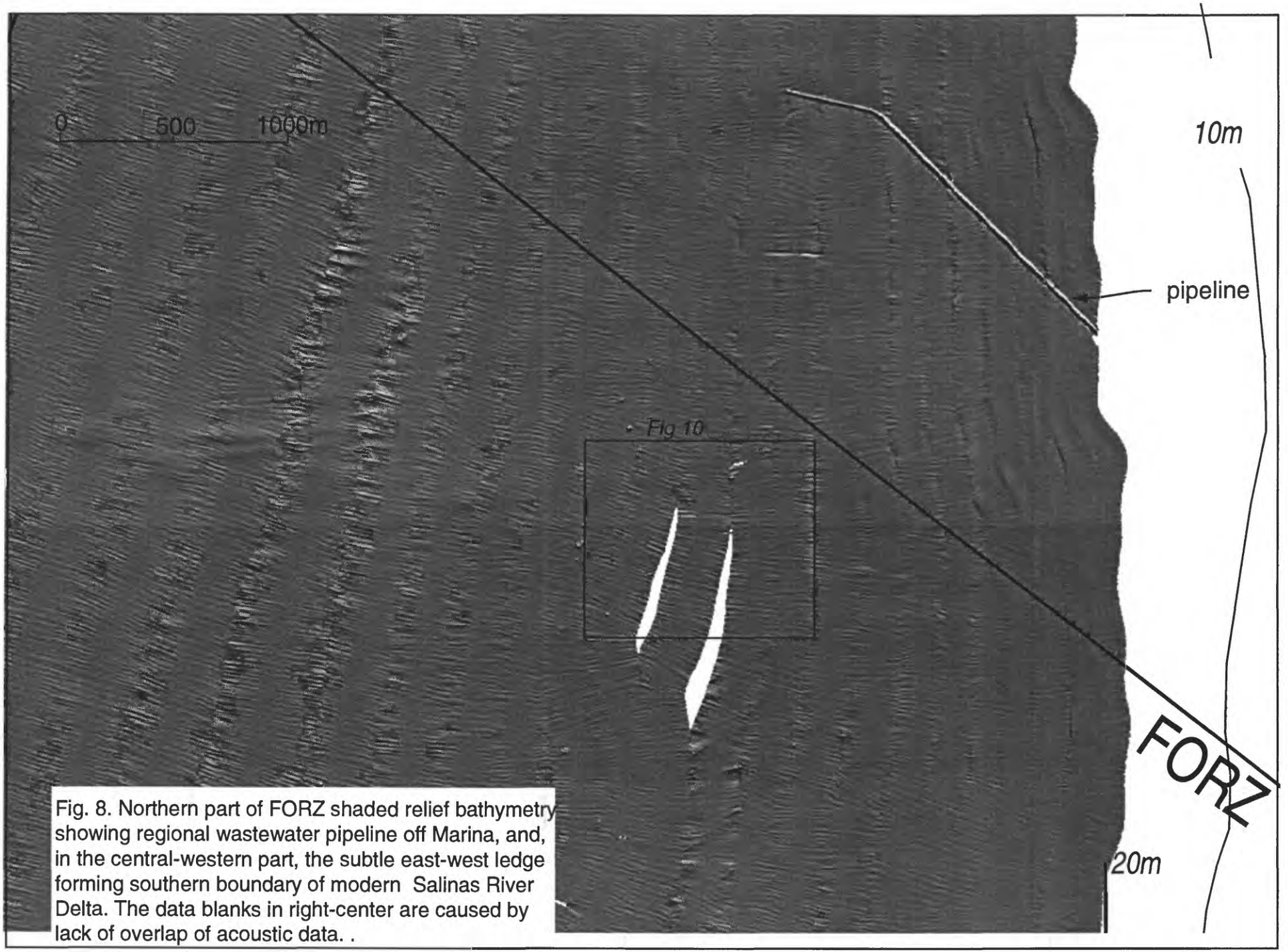

Fig. 8. Northern part of FORZ shaded relief bathymetry showing regional wastewater pipeline off Marina, and, in the central-western part, the subtle east-west ledge forming southern boundary of modern Salinas River Delta. The data blanks in right-center are caused by lack of overlap of acoustic data. .

Cruz. The fault zone is part of the left-lateral San Andreas Fault system and is still moderately active today, with occasional earthquakes (Greene, 1990).

Monterey Formation outcrops north of Monterey

The Miocene Monterey Formation is the highly stratified sequence of clastic sedimentary rock that overlies the granitic rocks forming the structural backbone of the Monterey peninsula. Surveys by Gardner-Taggart, et.al. (1993) showed that the seafloor north of the city of Monterey is composed of broad areas of outcrop of this Formation. The view of these Monterey Formation outcrops from the EM-1000 data is shown in both bathymetry and backscatter in Figures 5a and 5b, respectively. The outcrops occur over a broad zone widening to the south to over 1 km with southeast-northwest striking layers that dip gently northeastward. The backscatter imagery shows the erosion-resistant layers as high backscatter, with ponded sediment between these layers as low backscatter. To the southwest, closer to the peninsula shoreline, the Monterey Peninsula granites (Greene and Hicks, 1990) outcrop and are imaged as knobby, rough terrain, similar to the more extensive granitic outcrops to the northwest of the peninsula seen in Figure 2.

Erosional Sand Troughs

Erosional sand-floored troughs have been observed on many continental shelves of the world including the northern California shelf (Cacchione et. al., 1984). We observe two types of flat-floored depressions in the FORZ (Figure 6). The first type located just beyond the surf zone, from 10 to 30 m depth, are troughs that tend to be shore-parallel, but can be equidimensional. These have been described previously by Hunter et.al. (1984) and Mariant (1993). The above authors documented their changing shapes on time scales of months to years, they documented their 1 m or less relief and their coarse-sand floors that contrast with the fine sands or silts of the inter-trough areas. The distinct recording of these troughs by the EM-1000 bathymetry system shows that the vertical resolution of this system is better then 1 m. The troughs at 10 to 30-m depth have flat floors whose coarse sands are corrugated into 1-m wavelength ripples. The second type of trough, in deeper water and located along the southern boundary of the FORZ, are a series of offshore-trending flat-floored troughs, culminating in one trough that extends to 59-m depth (Figure 7a). Both types of troughs are depressed about 1-m or less below the surrounding seafloor and both types are floored by 1-m wavelength ripples composed of coarse sand. The second type has all the characteristics of the first type, except that they occur in deeper water and do not appear to change shape or location (on a months-to 15-month time scale; see below). The higher backscatter produced by the floors of the troughs (Figure 7b) is presumed to be caused by the rippled coarse sand, which is more reflective than the fine-sands and silts of the adjacent seafloor between troughs. The deeper trough shown in Figure 7a, in one repeat survey after a 15-month interval, was found to have not changed position or shape (Eittreim et.al., 1997). The deepest and farthest-offshore points of both types of troughs are marked by finely tapered ends that point offshore. The sand waves of the floors of similar features on the northern California shelf have been shown to be caused by sands moving in response to oscillatory bottom flow that is driven by the passage of long-period winter-time swell as this swell shoals onto the mid and inner shelf (Cacchione et. al., 1984).

In the vicinity of the 59-meter-deep trough (Fig 7a), Dorman (1968) and Mariant (1993), proposed a nodal zone of offshore flow forced by the generally southerly alongshore flow on the north and northerly flow on the south. Mariant (1993) proposed this nodal zone to be a concentration of offshore rip-current flow and is centered over the coarse lag-deposits of the trough floors where coarse-sand offshore-transport is focused. The process proposed by Mariant (1993) is speculative and has not been modelled as of yet. If the process is a feasible mechanism to focus the offshore transport of sand from the nearshore, its feasability at up to 59-m water depths is more speculative, as it would call for a maintenance of offshore flow at depths and distances far beyond that of known rip-current processes.

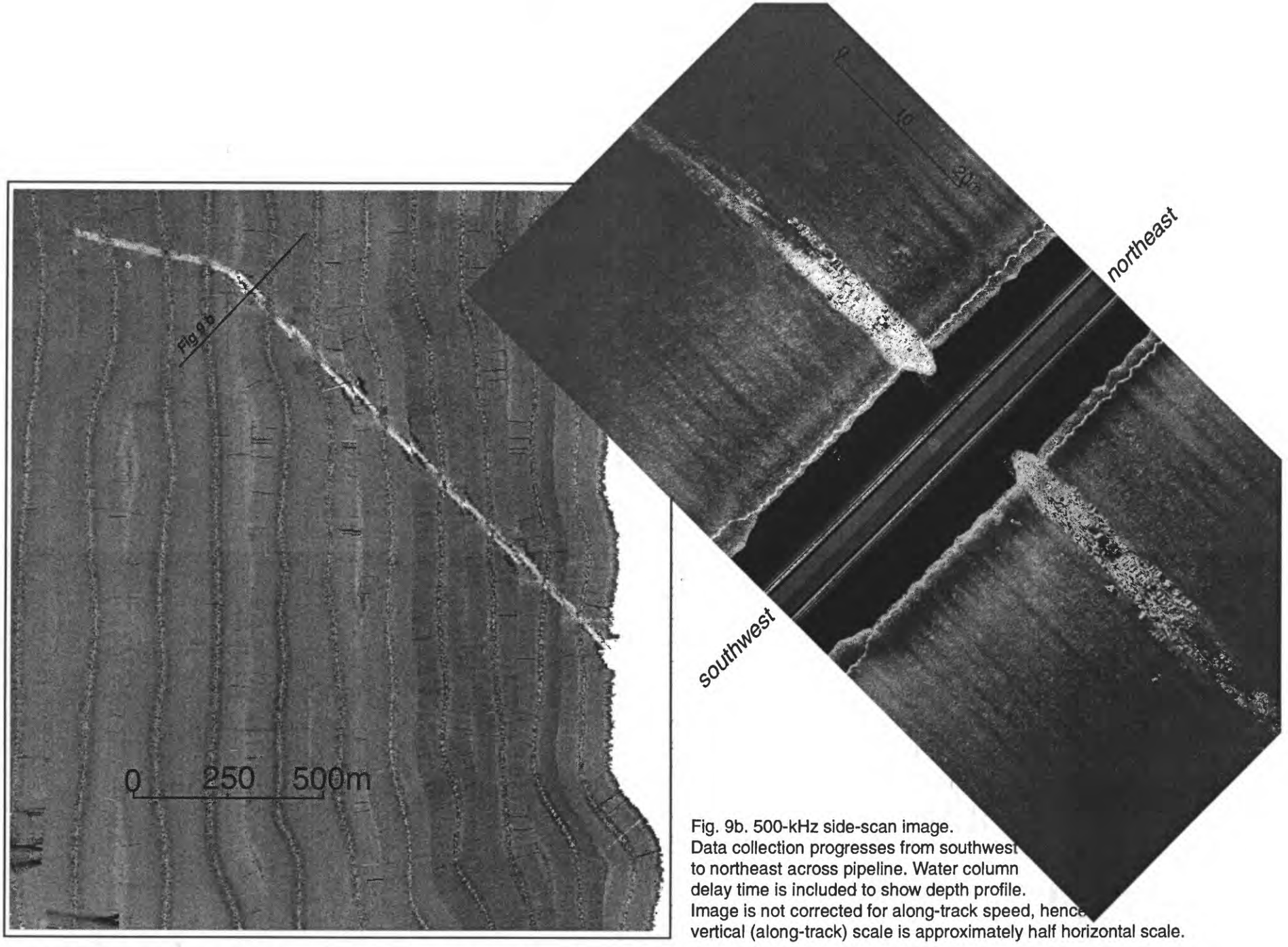

Fig. 9b. 500-kHz side-scan image.
Data collection progresses from southwest
to northeast across pipeline. Water column
delay time is included to show depth profile.
Image is not corrected for along-track speed, hence
vertical (along-track) scale is approximately half horizontal scale.

Fig. 9a. Backscatter image of Monterey Regional Water Pollution Control Agency pipeline.

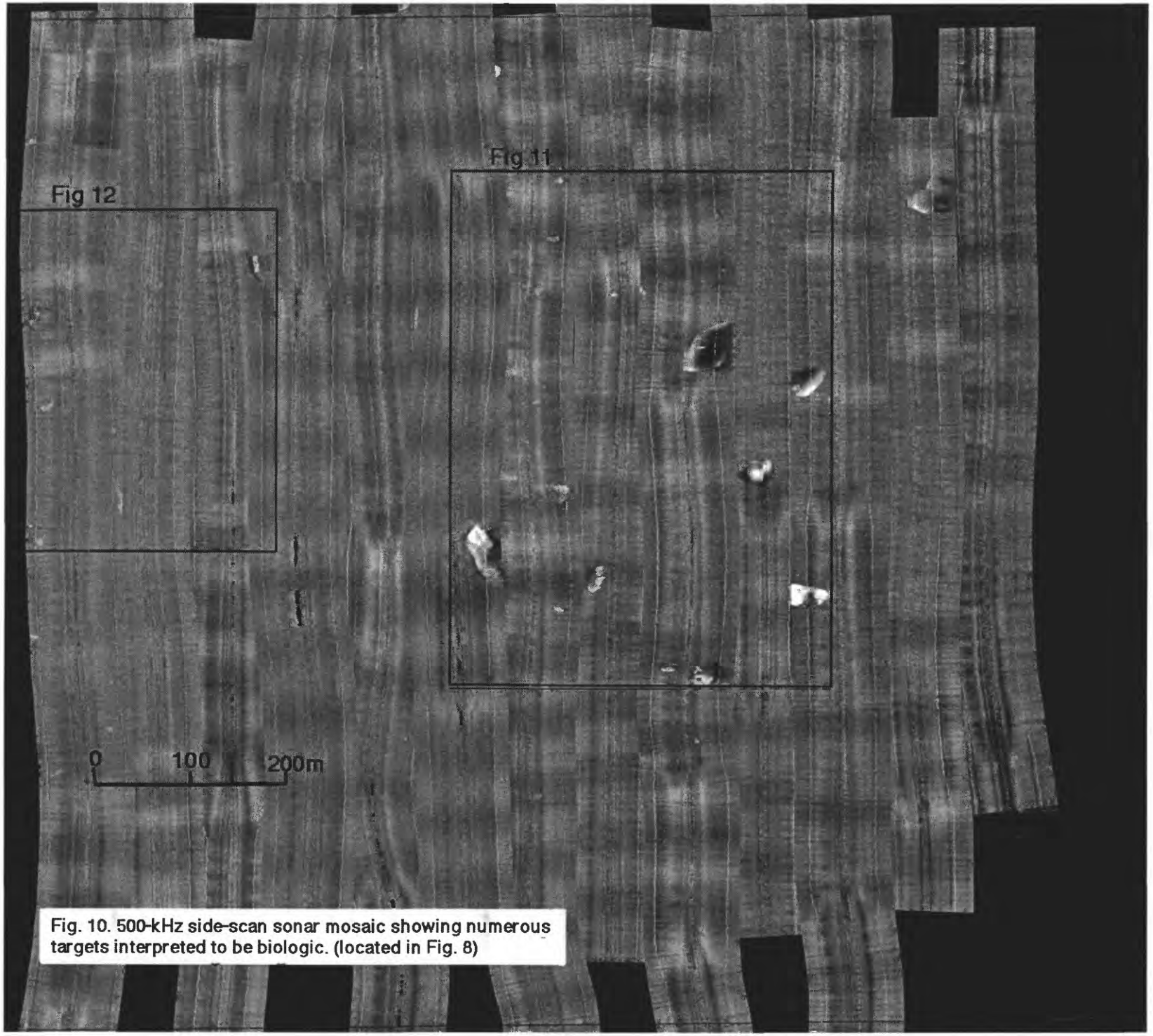

Fig. 10. 500-kHz side-scan sonar mosaic showing numerous targets interpreted to be biologic. (located in Fig. 8)

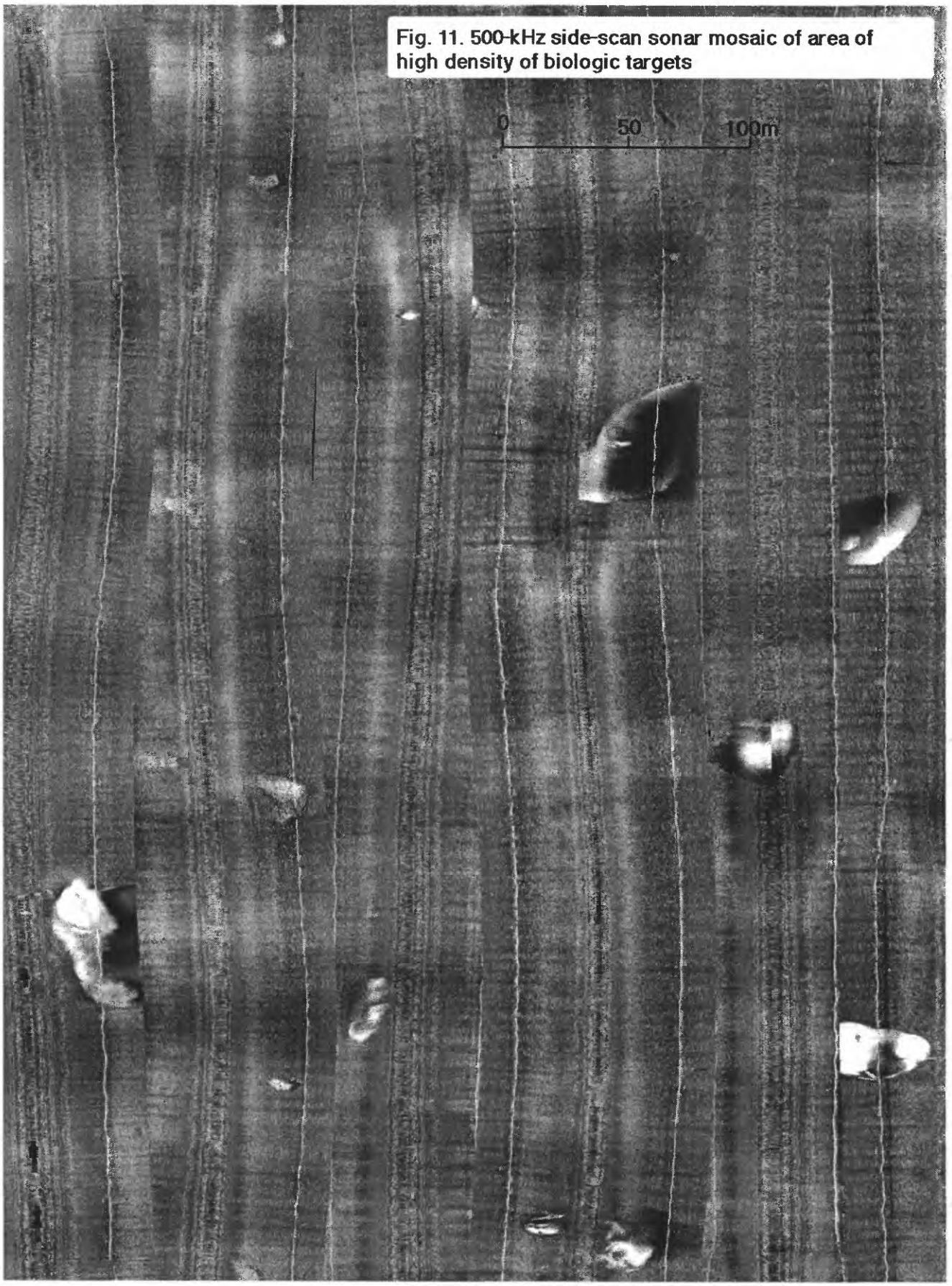

Fig. 11. 500-kHz side-scan sonar mosaic of area of high density of biologic targets

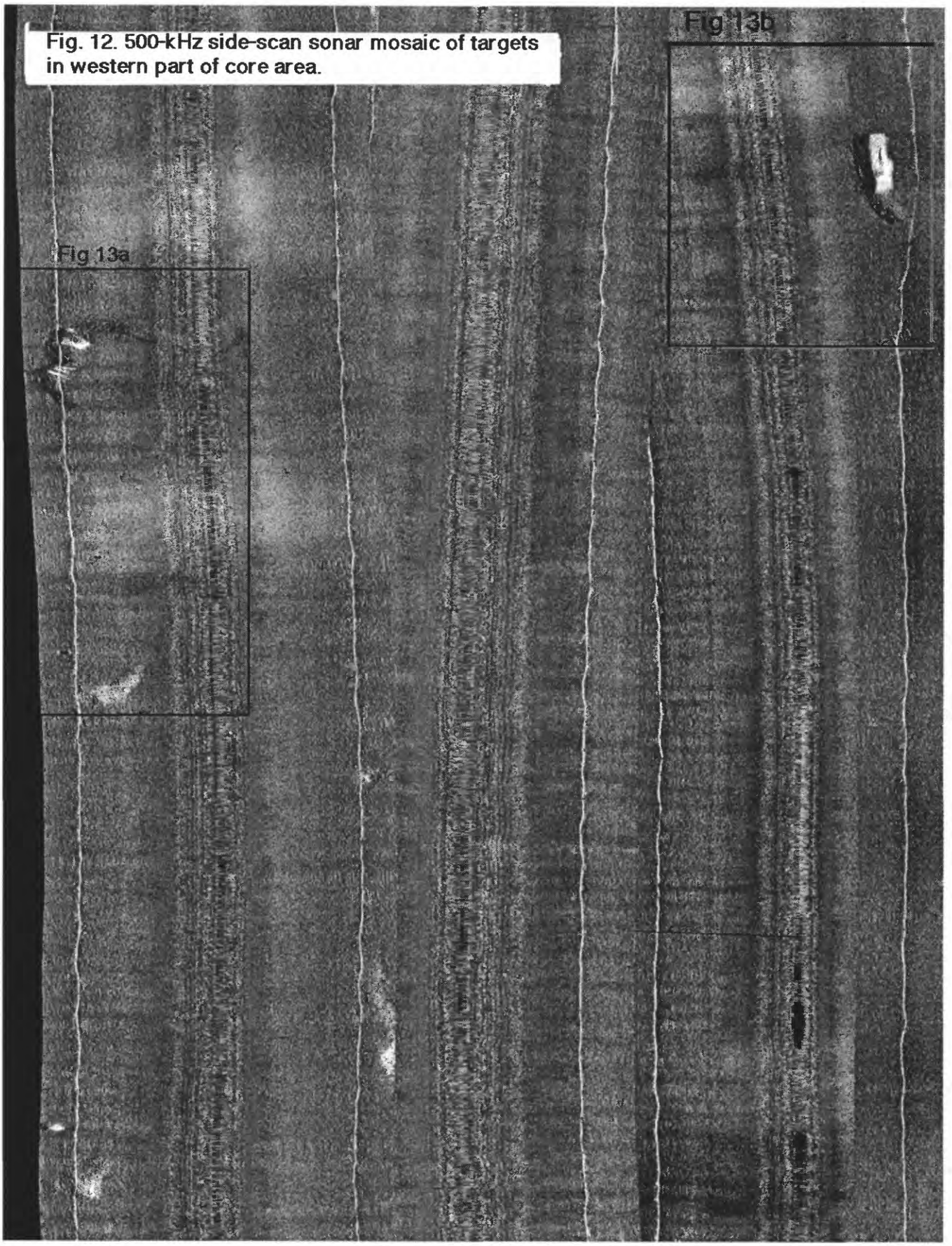

Fig. 12. 500-kHz side-scan sonar mosaic of targets in western part of core area.

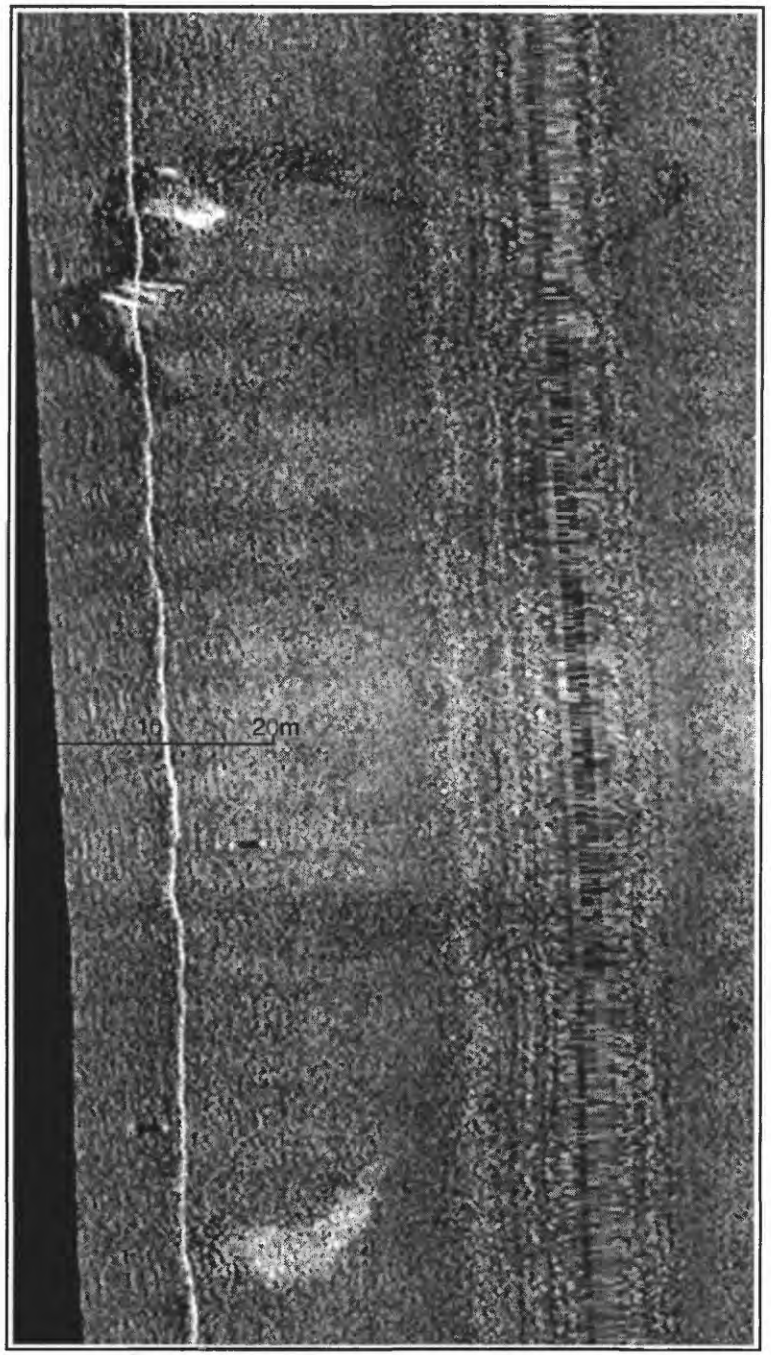

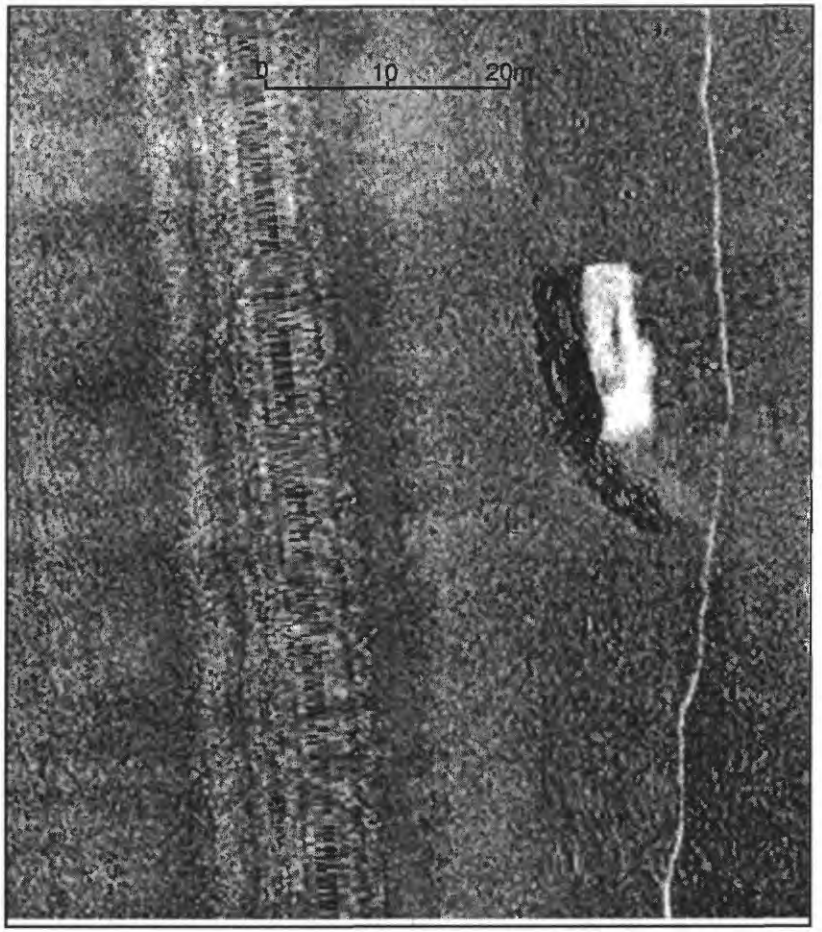

Fig 13a (left) and 13b (right). Initially classified as "suspect" targets, these targets were not present on following day's survey and thus were judged to be biologic targets.

Northern FORZ

In the generally flat and featureless seafloor in the northern FORZ, mounds of a few meters or less in size appear in the imagery (Figure 8, west and southwest of the two data-gaps crescents). To determine the nature of these features, they were investigated with higher resolution side-scan systems at a slower speed. The high-resolution surveys showed that the suspect features were not mounds, but ephemeral biologic targets (see below).

Chin et. al. (1988) mapped the Salinas River delta lobe using high-resolution sub-bottom acoustic sounding. This lobe of sediment represents clastic material that has been deposited in storm/flood deposits from the Salinas River since the rise of sea-level 10,000 years ago. The sediment lobe represents what has remained behind after erosion by waves and currents on the shelf and forms a deposit up to 35-m thick. In the area south of the pipeline and just south of the northern border of the FORZ the bathymetric imagery shows a subtle morphologic step (down to the south) in the sediments of the Salinas River delta. This would appear to be a sedimentary feature caused by some undocumented pattern in flow conditions on this part of the shelf, as there are no known stuctural controls from underlying geologic structure in this area (Chin et.al., 1988; Greene and Hicks, 1990).

Figure 8 includes a bathymetric image of the Monterey Regional Water Pollution Control Agency pipeline northwest of Marina. This pipeline is a 2-m diameter concrete pipe buried and surrounded by a triangular apron of broken rock that is 10-m wide at its base. The pipeline image provides an independent guage of the EM-1000 system's horizontal resolution. The two circular-shaped 15-m diameter backscatter features south of the pipeline terminus, seen in Figure 9a, are anchor materials that were used for surface buoys during the construction phases of the pipeline. Dark patterns are seen along both sides of the pipeline and are caused by an acoustic shadow on the far side of the high-standing pipeline ediface itself and, on the near side, by a moat or depression in the sediment along the edge of the pipeline debris pile. Bright patterns are also observed parallel to the pipeline that are caused by the high-reflectivity of the steep facing side of the pipeline ediface.

In contrast to the image of Figure 9a, a higher-resolution 500 kHz side-scan image of the pipeline is shown in Figure 9b. The water-column time delay has not been removed from this image, so that the third dimension, depth, is visualized along the trackline. The pipeline ediface stands about 3-m high with a slight moat along the sediments at its base. Note that the seafloor along the north side of the pipeline is about 1-m shallower than along the south side, apparently the result of faster sediment accumulation rates along the north, or "upstream," side, according to studies of alongshore transport (Dingler, et.al.,1985; Dorman, 1968; Wolf, 1970). This difference in apparent accumulation was noted one year after the pipeline was constructed in 1984 (ABA Consultants, 1985), and the differential amount between north and south has not increased significantly since, based on surveys in 1988, 92, 94 and 95.

The image on the right of Fig. 9b looks along the straight-line of the pipeline towards the southeast. The image on the left shows the bend in the pipeline from an azimuth of 315° to 282°. At this bend the pipeline changes from rock-covered to exposed along its upper half, with diffuser holes along its sides (R. Holden, Monterey Regional Water Pollution Control Agency, personal communication). The uncovered pipeline can be seen beyond the bend on the far upper left of the image. The conclusion from this excercise is that features between 0.1 and 1 meter in size (eg., some of the rock fragments at the base of the pipeline ediface) can be distinctly imaged by the 500 kHz system.

The processed mosaic of data from the 500 kHz system is shown in Fig. 10. Numerous targets, most of them cloud-like,without sharp edges, and some clearly in the water column rather than on bottom, are characteristic of biologic targets such as schools of fish (Fig.11). Targets from features in the water column are frequently truncated either below the ship track (nadir) where data from the water column time-delay has been removed, or at the overlap between adjacent swaths due to movement of the target during the appoximate half-hour separating the data collection between swaths. A few of the targets however have sharp-edged geometric shapes that suggest non-biologic bottom debris, such as those shown in Figs. 12, 13a and 13b. A resurvey with the same side-scan system on the day following that during which the Figs. 10-13 data were obtained,

including a check on navigation and system performance by collection of a repeat pipeline image, showed these targets to be ephemeral features. Thus they also are apparently biologic in nature.

SUMMARY OF FORZ SEAFLOOR ACOUSTIC IMAGERY

The seafloor in the FORZ and the surounding southern Monterey Bay shelf is a flat featureless plain, typical of quasi-protected embayments of the western California coast, with a gently sloping modern sandy seafloor whose gradients are determined by the wave and current erosional conditions that prevail here. Erosional troughs, floored with coarse sands that are set in motion in 1-m symmetrical ripples during large wave conditions, are testament to the dynamic environment on the seafloor here, especially at depths shallower than 30 m. The same testament is given by the eroding cliffs under Stillwell Hall. South of the southern FORZ boundary the underlying bedrock, the Miocene Monterey Formation, emerges from below the modern sand cover. Along the western border of the FORZ, deeper stratigraphic units, probably also parts of the lower Monterey Formation, are tectonically exposed in ledges that provide about 5-m of relief above the adjacent seafloor. To the north of the FORZ the large pipeline that extends from the coast northwest of Marina is well imaged by the EM-1000 and 500-kHz side-scan systems and confirms a maximum (best) resolution for the two systems of about 1 m and about 10 cm, respectively. The pipeline appears to have developed moats along its sides due presumably to the concentration of current flow; this has also resulted in preferential sedimentation along its northern side. In the northern FORZ a subtle ridge and down-to-the-south step forms what appears to be an unexplained southern boundary of the Salinas River lobe in the area to the south and west of the pipeline.

No evidence of anthropogenic debris has been detected with the EM-1000 system. However the limits of pixel resolution, 5m horizontal and 1 m or less vertical for bathymetry, and 2.5 m horizontal for backscatter, need to be kept in mind. It is doubtful that piles of debris or single objects on the seafloor that are 1-m or higher and 10 m or more in horizontal dimension would have avoided detection. Higher resolution surveys (500 kHz) with resolution down to the 0.1 m level were carried out in some areas that were considered most likely for anthropogenic debris. No such debris was found although it should be kept in mind that less than 10% of the area of the FORZ was imaged with the higher-resolution systems.

ACKNOWLEDGEMENTS

This study was funded by the Army Corps of Engineers and the program of studies of which it is a part was stimulated by discussions with personnel from the Environmental Protection Agency, the National Oceanic and Atmospheric Agency's Monterey Bay National Marine Sanctuary Office through it's advisory "RAP" committee, and personnel from the the U.S. Army's Fort Ord. John Chin reveiwed the manuscript and offered many suggestions for improvements.

REFERENCES

ABA Consultants, 1985, North Monterey County Regional Outfall Monitoring Report, Monterey Regional Water Pollution Control Agency, Marina, CA, 32 pp.

Cacchione, D.A, D.E. Drake, W.D. Grant and G.B. Tate, 1994, Rippled Scour depressions on the inner continental shelf off central California: *J sediment. petrology*, 54: 1280-1291.

Chin, J.L., H.E, Clifton and H.T. Mullins, 1988, Seismic stratigraphy and late Quaternary shelf history, south-central Monterey Bay, California: *Marine Geology*, 81: 137-157.

Dingler, J.R., B.L. Laband and R.J Anima, 1985, Geomorphology framework report, Monterey Bay: U.S. Army Corps of Engineers Report no. CCSTWS 85-2, 108 pp.

Dorman, C.E., 1968, The southern Monterey Littoral cell: A preliminary sediment budget study: unpublished Masters Thesis, U.S. Naval Postgraduate School, 234 p.

Dupre', W.P., 1990, Quaternary Geology of the Monterey Bay Region: In: Garrison, R.E., et. al. (editors), *Geology and Tectonics of the Central California Coast region, San Francisco to Monterey*, Pacific Section Amer. Assoc. Petrol. Geol. Volume and Guidebook, 185-192.

Edwards, B.D. and J.V. Gardner, (this volume), Seafloor Composition in southern Monterey Bay.

Eittreim, S.L., A.J. Stevenson and H.G. Greene, 1995, Outer-shelf ridge in southern Monterey Bay: (abs.): Trans., Amer. Geophys. Un., 76: 328.

Eittreim, S.L., K.Kinoshita, G.B. Tate, and D.A. Cacchione, 1997, Rippled scour depressions of the southern Monterey Bay shelf, (abs): in 5th Annual MBNMS Symposium Proceedings: p.24.

Gardner-Taggart, J.M, H.G. Greene and M.T. Ledbetter, 1993, Neogene folding and faulting in southern Monterey Bay, Central California, USA: *Marine Geology*, 113: 167-177.

Greene, H.G., 1977, Geology of the Monterey Bay region: U.S. Geol. Survey Open File Report no. 77-718, 347pp.

Greene, H. G., 1990, Regional tectonics and structural evolution of the Monterey Bay region, Central California: In: Garrison, R.E., et. al. (editors), *Geology and Tectonics of the Central California Coast region, San Francisco to Monterey*, Pacific Section Amer. Assoc. Petrol. Geol. Volume and Guidebook, 31-56.

Greene, H.G., M.N. Yoklavich, D. Sullivan, and G.M. Cailliet, 1996, A geophysical approach to classifying marine benthic habitats: Monterey Bay as a model: in: V. O'Connell and W. Wakefield (editors), *Applications of side-scan sonar and laser line-scan systems in fisheries research,* Alaska Dept. of Fish and Game Spec. Publ. no. 9, 15-30.

Godin, A., B. Tessier, P. Hally, and D. Hains, 1992, Simrad EM1000 and SWATH vessel technology: The perfect match?, Proceedings of the Intl. Hydrographic Conference, December 1992, Copenhagen, Denmark, 16pp.

Hunter, R. E., J.R. Dingler, R.J. Anima, and B.M. Richmond, 1988, Coarse sediment bands on the inner shelf of southern Monterey Bay, California: *Marine Geology*, 80: 81-98.

Mariant, J.J., 1993, Origin of sediment ripple bands and zones on the inner shelf of southern Monterey Bay, California: M.S. Thesis, San Jose State Univ., 49 pp.

Wolf, S.C., 1970, Coastal currents and mass transport of surface sediments over the shelf regions of Monterey Bay, California: *Marine Geology*, 8: 321-336.

Grain Size, Organic Carbon, and $CaCO_3$ of Surface Sediments from the Southern Monterey Bay Continental Shelf Seafloor

Brian D. Edwards, James V. Gardner, and Marjorie D. Medrano
U.S. Geological Survey, Menlo Park, CA 94025

ABSTRACT

Forty-six coring sites were occupied on the continental shelf south of Monterey Canyon as part of the Fort Ord Restricted Zone (FORZ) study. The recovered sediment was evaluated for geological, geochemical, and geotechnical characteristics. The data show surface sediment grain size to decrease offshore with clearly developed nearshore sand bodies and a mid-shelf/outer shelf mud belt. These findings are consistent with the view that finer-grained sediment (e.g., flood sediment) from the Salinas River either bypasses the inner shelf and is deposited at mid- to outer shelf depths or bypasses the shelf entirely and is deposited in the adjacent Monterey Canyon. Organic carbon and calcium carbonate contents are generally unremarkable except in the exposed bedrock area north of the Monterey peninsula (high backscatter on the SIMRAD EM-1000 data) where $CaCO_3$ values are >30%. Photographs taken simultaneously with the cores show bioturbation and physical structures that are typical of mid-latitude terrigenous shelf environments.

INTRODUCTION

The Western Region Coastal and Marine Geology Team of the U.S. Geological Survey (USGS) initiated a five-year project in 1994 to study aspects of the newly declared Monterey Bay National Marine Sanctuary (MBNMS). Also during 1994 the U.S. Army closed the military reservation at Fort Ord, CA, a site located immediately east of the central MBNMS. Approximately 62 km^2 of the continental shelf south of Monterey Canyon was periodically maintained by the U.S. Army as "prohibited" and "restricted" use zones for six decades to protect the public during beach training and live firing exercises conducted in the vicinity of Fort Ord (Figure 1). The entire continental shelf was incorporated in the MBNMS following the Fort Ord base closure and reopened for public use (Harding Lawson Associates, 1995).

Two sampling cruises during 1995 occupied sites throughout the study area (Fig. 1). The first cruise (M1-95-MB) conducted aboard the NOAA ship McARTHUR, departed San Francisco, CA, on April 2, 1995, and returned to Monterey, CA, on April 11, 1995. Operations included: 1) coring with a USGS NEL box corer and 2) seismic-reflection profiling between coring stations using a Datasonics high-resolution CHIRP system. The second cruise (P2-95-MB) conducted aboard the Moss Landing Marine Laboratory (MLML) ship R/V POINT SUR, departed Moss Landing, CA, on September 6, 1995, and returned to Moss Landing, CA, on September 12, 1995. Operations included: 1) coring with a USGS Navel Electronics Laboratory (NEL) box corer and an Ocean Instruments multi-corer, 2) bottom photography with a USGS camera system attached to the corers, and 3) seismic-reflection profiling between coring stations using the R/V POINT SUR's hull-mounted 3.5-kHz transducers controlled by an ODEC high resolution signal-processing system. Subsamples from selected stations were provided to Dr. Mark Stephenson of the California Department of Fish and Game for analysis of contained contaminants (Stephenson et al., this report).

This report describes textural, geotechnical, geochemical, and photographic data from stations occupied on the southern continental shelf of Monterey Bay (10 to 140 m water depth) Figure 1 shows the station locations and Table 1 provides core identifier, location, length of recovery, and water depth.

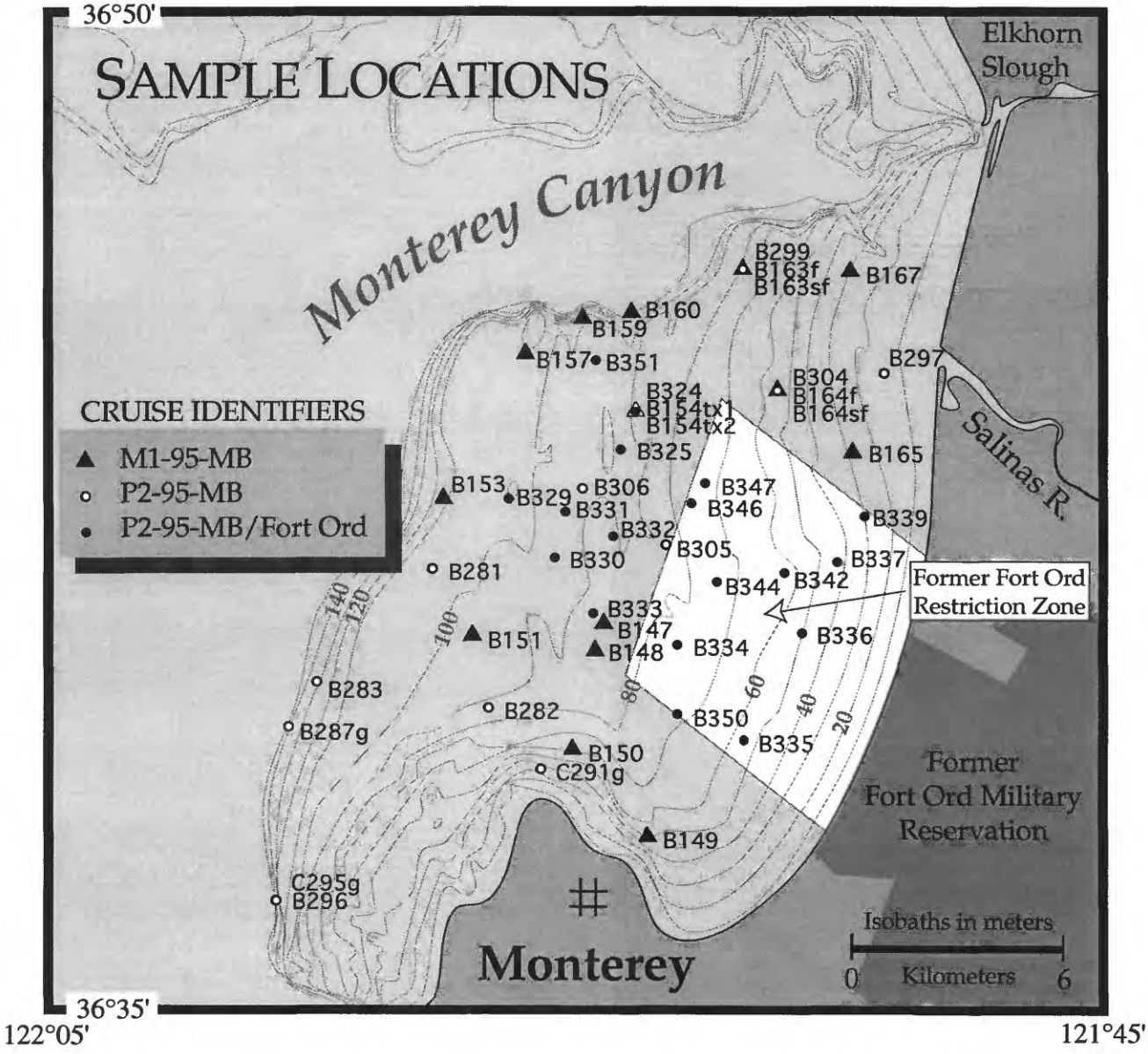

Figure 1. Location map showing coring sites occupied on the southern Monterey Bay continental shelf during crises M1-95-MB and P2-95MB. Note the boundaries of the former Fort Ord Military Reservation and the offshore Fort Ord Restricted Zone (FORZ).

METHODS

Navigation

Navigation for these cruises was provided by a differential global positioning system (DGPS). GPS is a 3-dimensional measurement system based on radio signals transmitted for the Department of Defense's (DoD) NAVSTAR system. Accuracy for the standard positioning service (SPS) is approximately +/- 100 meters horizontally (Wells and Kleusberg, 1990). DGPS uses two GPS receivers to remove the SPS errors deliberately introduced into the data by DoD. One receiver (the reference station) is at a fixed, known and stable location. The other receiver (the remote station) is located on the ship. The observed ranges from the satellites are recorded at both DGPS stations. The difference between the computed ranges and the observed ranges for the reference station are the corrections that are applied to the remote station data. With DGPS, positional accuracy is on the order of +/- 10 meters horizontally (Wells and Kleusberg, 1990).

Coring and Deck Handling

Twenty six of the 44 sites occupied on the southern Monterey Bay continental shelf were chosen from a statistical grid developed by EPA's EMAP design criteria and were funded as part of the USGS Monterey Bay National Marine Sanctuary project. An additional 18 stations were funded by the U.S. Army.

The primary bottom sampling tool for the southern Monterey Bay continental shelf was the NEL box corer (Lee and Clausner, 1979). The box corer is the industry and academic community standard for obtaining undisturbed samples of the uppermost sediment column. The corer is constructed of mild steel, is coated with an inorganic zinc compound, and holds a 0.06 m^2 stainless steel box. The unit has a flow-through head design with closing door flaps and recovers a relatively short (< 60 cm), undisturbed sample of seafloor sediment. Maximum effective penetration is about 55 cm.

The gimbaled support frame weighs approximately 1500 lbs in air and has the attached hollow steel-walled rectangular sampling box mounted beneath a weight column. The box dimensions are 20 cm X 30 cm X 60 cm. The corer is lowered with a wire-rope winch. When contact is made with the seafloor, the weight column slides between guides and drives the box into the sediment. A separate cable attached to a spade arm and pulley system on the corer closes as the winch is hauled-in and slides the spade (with detachable base plate) through the sediment and beneath the box thereby sealing the sample from the ocean during the ascent to the ship's deck. A camera and strobe system, attached to the corer frame, is triggered just prior to impact and takes a picture of the segment of seafloor that is about to be cored.

On deck, the steel box with base plate is removed from the corer frame, placed in a large wooden containment box, and subsampled. Supernatant water is siphoned off and then 9.5-cm diameter polybuterate subcores are driven into the box core by means of a motorized linear actuator. A piston fixed inside each subcore provides a vacuum and minimizes compression and disturbance of the sample during subcoring. Additional surface (0 to 1 cm) samples are taken from the remaining box surface area with a spatula or spoon and placed in labeled containers.

Each subcore section was tested immediately after sampling using a GEOTEK Multi-Sensor Logging (MSL) system. The bottom of each subcore was capped prior to testing and the piston was left in the subcore to serve as a seal. The piston was removed after testing by cutting the subcore flush with the sediment surface using a circumferential cutter. The subcore top was then capped. All subcores were logged and stored horizontally.

GEOTEK Multi-Sensor Logging System

The GEOTEK Multi-Sensor Logging (MSL) system nondestructively measures the acoustic velocity, density, and magnetic susceptibility of the whole core. Because acoustic

velocity and density are properties of state and change with time, the whole cores were tested aboard ship during each cruise. The MSL data were collected at 1-cm intervals downcore and were used as a preliminary method to identify sedimentary layers (sands, muds, etc) and to correlate layers between cores.

The GEOTEK MSL system is described in detail by Kayen (1994) and Cowen et al. (1994) and many of the principles are described in Boyce (1970). The following is excerpted from those reports. The USGS version of the GEOTEK MSL consists of a 4-m-long tracking system, a compression-wave (P-wave) velocity and core-diameter sensor, a gamma-ray attenuation porosity evaluator (GRAPE), and a magnetic-susceptibility sensor (Fig. 2), all controlled by a Macintosh SE/30 computer driven by acquisition software written as a HyperCard© stack (Kayen and Phi, in press). Whole-core sections up to 1.5 m in length can be logged with the MSL.

The tracking system is run by a computer-controlled stepper motor that advances the core section at a selectable interval that was set to 1 cm during each cruise. Each core section was run consecutively through the sensors, starting with the top (sediment surface) and progressing to the bottom of the core.

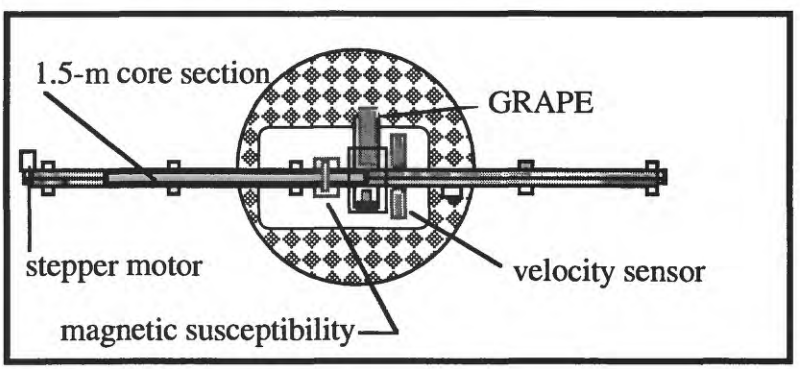

Figure 2. Plan view of USGS Multi-Sensor Logger showing position of each device. Electronics and computer not shown.

P-wave velocity sensor

The P-wave velocity sensor is a two-component station. In addition to the sonic transducers, the station incorporates a very accurate (± 0.1 mm) distance-measuring sensor that precisely determines the separation of the P-wave velocity transducers. The total face separation distance is measured by two rectilinear displacement transducers, each calibrated to the face of the two acoustic transducers. The displacement transducers precisely monitor the separation of the transducer heads, thus measuring the outside diameter of the section being measured.

The P-wave velocity sensor is composed of two identical 500-kHz transducers that measure travel time of a sonic pulse through the liner and the sediment. The 500-kHz pulse is produced at a pulse-repetition rate of 1 kHz. P-wave velocity is very sensitive to temperature, so sediment temperature was measured just prior to, and just after, each core section was run. The system was calibrated repeatedly to water at a measured temperature during both cruises.

The P-wave velocity of the sediment is calculated from the measured core diameter and P-wave travel time, correcting for liner thickness, electronic-signal delays, and core-liner travel time. The P-wave velocity (V_p) is calculated as:

$$V_p = \frac{D-2L}{T-2T_{liner} - T_{electronics}} \quad (1)$$

where D is the whole core outer diameter, L is the liner thickness, T is the total travel time, T_{liner} is the liner travel time, and $T_{electronics}$ is the electronic signal delay within the transducers, wiring, and electronics packages.

Gamma-Ray Attenuation Porosity Evaluator (GRAPE) sensor

The GRAPE sensor utilizes a 12 milli-curie ^{137}Cs capsule (active element CsCl) to produce gamma rays at 0.662 MeV. The source capsule is housed in a 70-mm-diameter primary lead shield and collimator. The collimating hole is about 11 mm in diameter and 52-mm long. Additional lead shielding is fitted around the base of the source (Fig. 3) and, during logging operations, a lead-lined box is placed over both the detector and the source. A Harshaw-type 6S6/1.5B NaI(TI) scintillation detector, with photo-multiplier tube and dynode chain, is used for counting gamma rays.

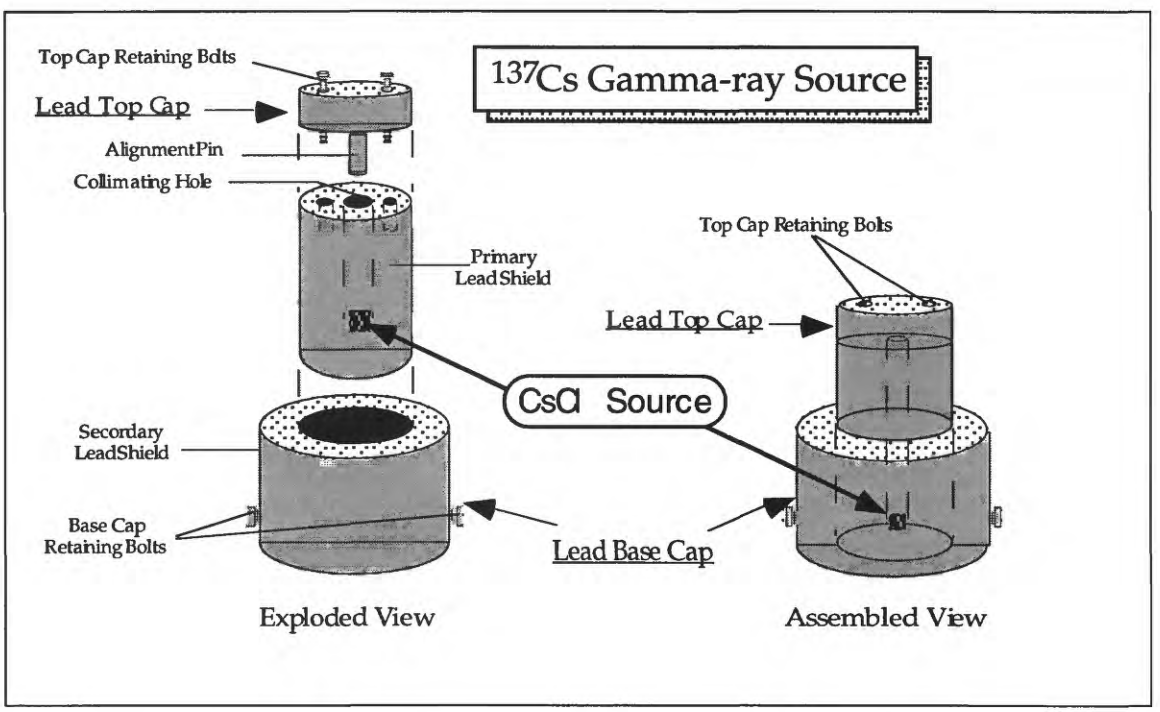

Figure 3. Exploded and assembled views showing the construction and lead shielding of the ^{137}Cs source.

Core (sediment and liner) bulk density (ρ_c) is calculated as a Lambert's Law attenuation of the gamma-ray and Compton scattering of gamma rays by hydrogen (in pore water) (Whitmarsh, 1971). The number of gamma rays that pass through the core is detected during a defined time interval. This count is termed the attenuated counts (I). The number of gamma rays that pass through only air is termed the unattenuated counts (I_o). For a core of thickness d, the attenuated gamma-ray count can be related to the unattenuated count, sediment thickness, core bulk density (ρ_c), and the Compton scattering coefficient (μ), by using Lambert's Law as follows:

$$I = Io^{(-\mu \rho_c d)} \qquad (2)$$

Then, the bulk density of the core can be determined as:

$$\rho_c = \frac{I}{\mu d} \ln \frac{I_o}{I} \tag{3}$$

However, to obtain an accurate determination of the sediment wet bulk density, corrections must be made to account for the influence of the core liner. This is done empirically using standards (water and aluminum) to determine separate Compton-scattering coefficients and, hence, a bulk-density correction for the liner. The full expression for the sediment bulk density (ρ_b), accounting for the core liner is:

$$\rho_b = \frac{\{\ln \frac{I_o}{I} - 2L\ \rho_{liner} * \mu_{liner}\}}{\mu_{sed}(D-2L)} \tag{4}$$

where D is the outside diameter of the core liner, L is the liner thickness, ρ_{liner} is the liner density, μ_{liner} is the liner Compton scattering coefficient, and μ_{sed} is the sediment Compton scattering coefficient. Although neither calculated nor displayed in this report, porosity (η) can be calculated from wet bulk density (ρ_b), density of sea water (Gsw), and average grain specific gravity (Gs) by the relationship :

$$\eta = \frac{\rho_b - Gs}{Gsw - Gs} \tag{5}$$

Magnetic-susceptibility sensor

Magnetic susceptibility of the sediment is directly measured by a 125-mm diameter Bartington MS-2 transducer coil. No liner corrections are required when using non-magnetic polybuterate liner material. The sensor was electronically zeroed at the beginning of each section scan.

System Calibration

Diameter Calibration

The electronic distance-measuring system of the outside diameter of the liner was calibrated with a stainless steel cylinder machined to two diameters, one exactly 80-mm and the other 90-mm. Throughout the cruises, the calibration was confirmed with the machined standard.

Velocity Calibrations

Compressional-wave velocity (V_p) was calibrated to water, which has a known velocity similar to that of many fine-grained surface marine sediments. The compressional-wave velocity of distilled water at standard pressure and temperature is 1.4917 km/s. The water-filled standard used for the calibration was constructed of the same polybuterate core liner used for the subcores. Because compression-wave velocity is sensitive to temperature, we measured the water temperature and corrected the raw calculated velocity to an equivalent velocity at 23°C at standard pressure using known correction factors (U.S. Naval Oceanographic Office, 1962). We empirically determined a travel-time delay ($2T_{liner} + T_{electronics}$) that corrects the measured raw compressional-wave velocity to the

standard's known velocity. The empirically determined travel-time delay was applied to each measured velocity to derive a corrected sediment V_p (see equation 1 above).

Density Calibrations

Density measurements of the sediment were calibrated to the known densities of water and aluminum. These two standards serve as end-members that fully bracket the densities typical of near-surface marine sediment. The density of water represents the lower bound and aluminum represents the upper bound. In addition, the respective Compton scattering coefficients of water and aluminum are similar to that of the primary sediment constituents (solid-phase alumino-silicate minerals and liquid-phase water).

The water-aluminum standard was constructed by inserting a solid cylinder of machined 6250-Aluminum into a section of the polybuterate core liner. The 15-cm-long aluminum cylinder was press-fit and caulked into the end of the liner so that the 25-cm long uppermost section could be filled with water. A calibration run consisted of recording the number of scintillation per second through a) liner and water, b) liner and aluminum, and c) air alone. Finally, an empirical Compton scattering coefficient was determined for the water and aluminum that gave water densities of 1.00 g/cm^3 and aluminum densities of 2.70 g/cm^3.

Calibration standards were repeatedly run during both cruises. If the standard was found to be out of calibration then multiple calibrations were run until we obtained acceptable values. If an out-of-calibration condition occurred, the appropriate data files were modified with the appropriate calibration adjustments to obtain corrected values.

Magnetic Susceptibility Calibrations

Magnetic susceptibility was calibrated before and after each core using a reference standard provided with the sensor by the manufacturer, Bartington. The sensor detects the calibration standard as far as 13 cm away as the standard approaches the sensor and reaches a peak in the middle of the sensor (Fig. 4). Similarly, non-zero readings were measured when the calibration standard was as far as 13 cm beyond the sensor. This relatively broad directional sensitivity is built into the Bartington magnetic-susceptibility loop and can not be electronically adjusted.

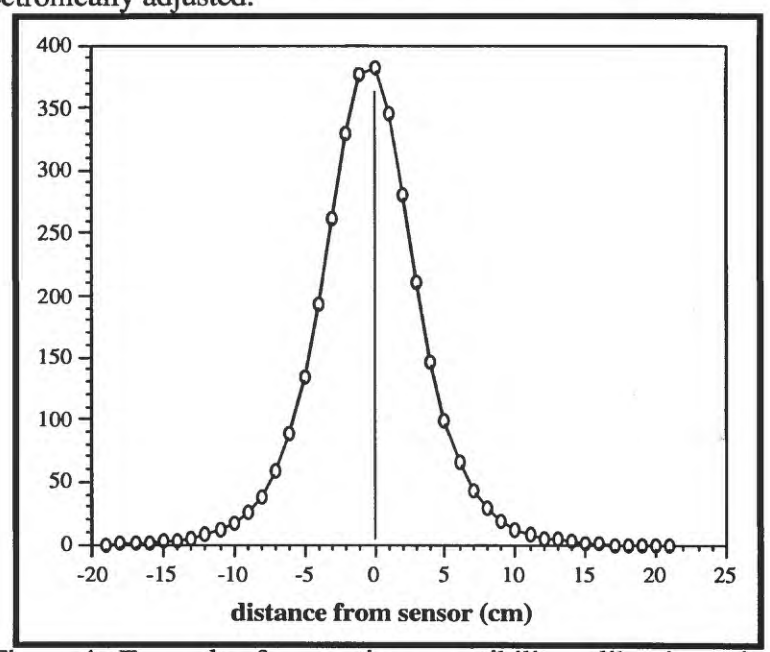

Figure 4. Example of magnetic-susceptibility calibration using the Bartington standard of 390 * 10^{-6} cgs. Vertical scale is magnetic susceptibility in 10^{-6} cgs.

A calibration was run before and after each core by placing the standard at the center of the loop and recording readings for about 10 seconds.

Textural Analysis

Textural analyses were completed in USGS laboratories located at Palo Alto, CA, using standard sedimentological procedures. The samples were not allowed to dry between recovery and testing. A representative split of the sample was digested in hydrogen peroxide overnight, then heated for two to three hours to drive off the remaining peroxide. The sample was washed and centrifuged two to three times to remove soluble components, then wet sieved through 2-mm and 62-micron screens to separate the gravel, sand, and mud fractions.

The sand fraction was oven dried, and a representative split was obtained by use of a microsplitter. The split sample was tested with a USGS-built Rapid Sediment Analyzer (RSA) to obtain the hydraulic-equivalent diameter of the sand components in each size class. The sample was placed at the top of the water-filled 10-foot-tall RSA, and the settling grains were captured on a plate at the base of the RSA. A strain gauge measured the accumulating mass of sediment with time. The fine fraction (< 62 microns) was tested using a Sedigraph™, an analytical instrument that measures grain-size by detecting changes in the penetration of X-rays as sediment falls through a water column. Sediment was dispersed with Calgon and allowed to saturate overnight in a graduated cylinder. The volume was adjusted to 100 ml and agitated for 2 minutes. A 20-ml aliquot representative of the entire fine fraction was taken by pipette at a depth of 20 cm. This aliquot was oven dried to determine the total weight of fine fraction. The remaining 980 ml were centrifuged, decanted, and made ready for testing with the Sedigraph™. The concentration was adjusted to approximately 4 grams of sediment per 75 ml of solution, Calgon was added as a dispersant, the solution stirred for two to three minutes with a magnetic stirrer, and a representative 50 ml aliquot was taken and tested. The data from the gravel, sand, and fine fraction were then combined to provide the textural information presented in this report.

The results of the textural analysis are presented as moment measures of grain size. This method uses computational rather than graphical techniques to otain a measure of mean grain size as well as other descriptors of textural data. Details of the computations involved are given in Krumbein and Pettijohn (1938).

Organic Carbon/Carbonate Carbon Analysis

The organic carbon and carbonate data were determined with a Coulometrics Coulometer™. A representative sediment sample was oven dried and powdered with mortar and pestle. A representative subsample was analyzed to determine the total-carbon content. The sample was heated to 1000 °C and the evolved gases were passed through scrubbers and titrated to obtain the total-carbon content (based on the amount of carbon dioxide driven off during the oven digestion). A second representative sample was acid digested and the amount of carbon dioxide produced was measured to give the percentage of mineral (carbonate) carbon. The difference between the total carbon and the carbonate carbon is the organic carbon. Repeated analyses of standards give precision and accuracies of ±0.1% for both organic carbon and total carbon.

Bottom Photography

Bottom photographs were obtained at some sites by use of a bottom tripped Benthos camera and strobe system attached to the box corer. The camera and strobe were connected by an electrical harness and hard-mounted on opposite sides of the corer frame. A line attached to a magnetic read-switch suspended a weight about 1.5 m below the corer. A switch triggered the synchronized strobe and camera shutter as the weight contacted the

bottom to photograph the area of seafloor about to be cored. Two lasers attached to the corer provide reference spots on each image that are separated by 10 cm.

The film negatives were scanned onto Kodak Photo CD-ROM's for archival storage. These scanned images were then digitally manipulated (sharpened, contrast enhanced, and adjusted for dynamic range) in Adobe Photoshop™ and placed in Adobe Illustrator™ files to produce the images in this report. Digital copies of the images are available upon request.

Trend Surface Analysis

Systematic changes in numerous attributes of shelf sedimentary systems are commonplace. We used trend surface analysis to map changes in sedimentary texture (mean grain size), percent organic carbon, and percent carbonate carbon. In a general sense, trend surface analysis is a procedure that divides an attribute (e.g., mean grain size) into "large-scale" changes that extend across the entire mapped area, and "small-scale" nonsystematic fluctuations that are superimposed on the large-scale patterns (Krumbein and Graybill, 1965). We fit a first-order, or linear surface, to the data to define the large-scale (area-wide) trend and the small-scale (residual) nonsystematic fluctuations. Results from the application of this technique are presented as figures and are discussed in the Results section.

RESULTS

Texture

Textural analyses of the surface sediment show two major textural regions: a mid-shelf/outer-shelf mud belt and an inner sand-rich zone that central and north-central parts of the continental shelf in southern Monterey Bay is mud-rich with a mean grain size finer than 16 microns (6 phi). A thin (0.5 to 2 cm-thick) soupy, oxidized surface sediment layer in this region indicates the area is a center of deposition for Salinas River sediment. Mean grain size (Fig. 5) increases both seaward and shoreward and becomes sand-dominated at about the 40-meter isobath. The area just seaward of the mouth of the Salinas River is covered by fine to very fine sand (mean grain size 62 to 125 microns) indicating that the fine-grained fraction of the mud-rich Salinas River sediment bypasses the inner shelf due to the high energy of the coastal wave regime. Mean grain size also increases toward the Monterey peninsula, in the area of bedrock outcrop (Eittreim *et al.* , this report). Here, the seafloor is relatively sediment-starved, and the coarse grain size is dominated by bioclastic (e.g., coral, echinoderm spicules, and broken gastropod shells) debris.

The first-order trend surface of grain size shows a well-behaved tendency of textural fining away from the Monterey Peninsula and toward the upper Monterey Canyon (Fig. 6). Residuals of the trend (Fig. 7) identify anomalous areas and show the mid-shelf mud belt to be more than 62 microns (1 phi) finer than predicted by the trend. This finding underscores the importance of this region as a center of deposition of fine grained sediment. The mouth of the Salinas River and the area immediately adjacent to the Monterey peninsula are significantly coarser than predicted by the trend. These regions reflect bypassing of fine-grained sediment near the river mouth and sediment-starved bedrock with the accumulation of large bioclastic debris, respectively.

Figures 8 and 9 show the percentage of sand and mud. Figures 10 and 11 show the silt and clay components of the mud size fraction. Although the mid-shelf mud belt is more than 60% mud (silt + clay) and is dominantly silt, sand content can be high with values to 40% (Fig. 8). The most clay-rich sediment (over 45% clay) is restricted to the edge of Monterey Canyon. Sediment off the mouth of the Salinas River is more than 80% sand with less than 5% of the material in the clay-size class. Samples collected from the coarse area north of the Monterey Peninsula are more than 90% sand size.

Figure 12 shows the moment mean grain size date for surface (0 to 1 cm) sediment overlaid on the SIMRAD EM1000 backscatter data (discussed in detail by Eittreim *et al.*. this report). Note that the low (darker tone) backscatter characteristic of the mid-shelf area

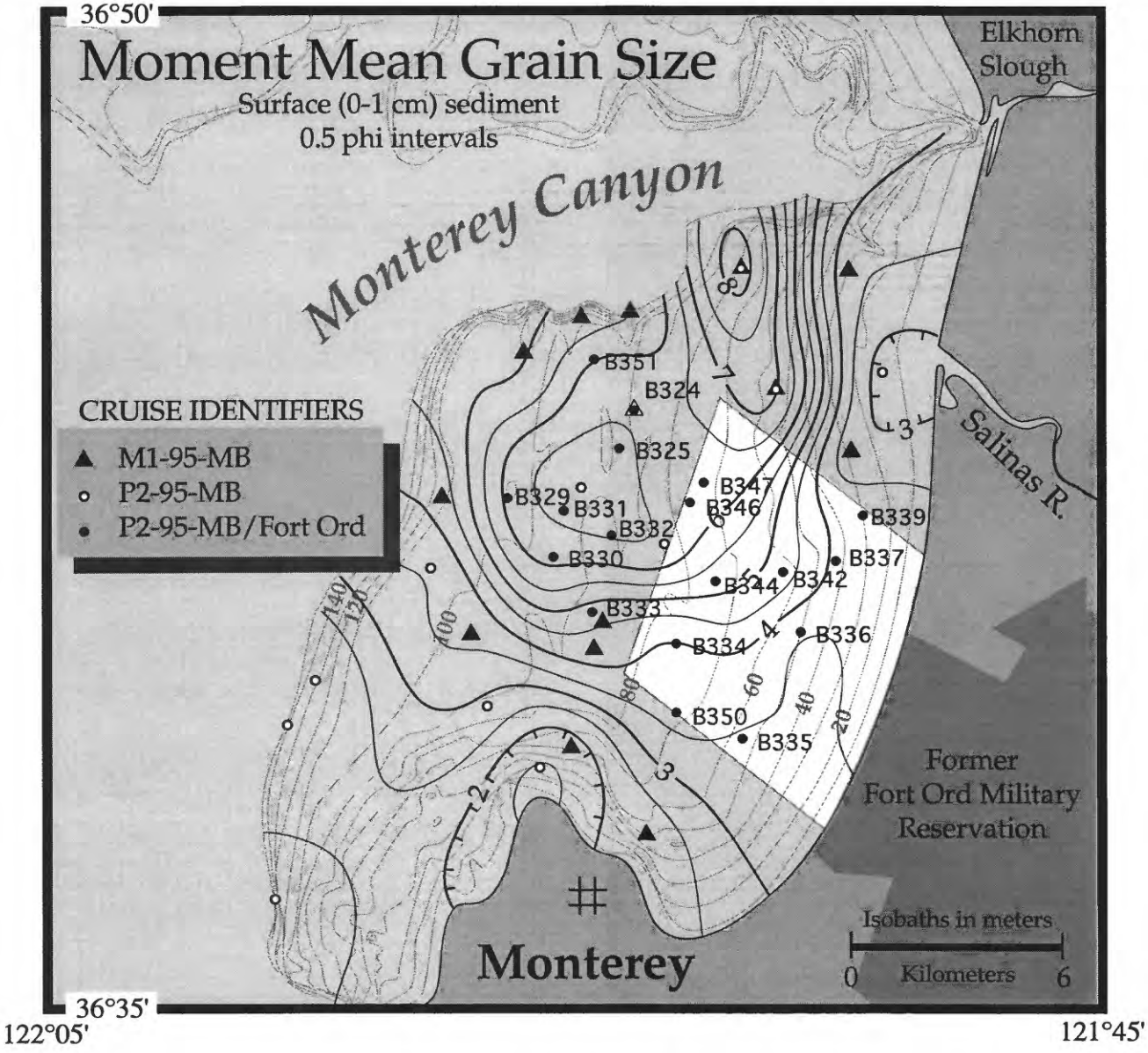

Figure 5. Areal distribution of moment mean grain size (in phi units) of surface (0 to 1 cm) sediment. Note the fine-grained sediment (< 16 μ; 6ø) located in the mid-shelf area and the eastward transition to sand at about the 40 meter isobath. Note also the sand-rich character of the southernmost part of the shelf.

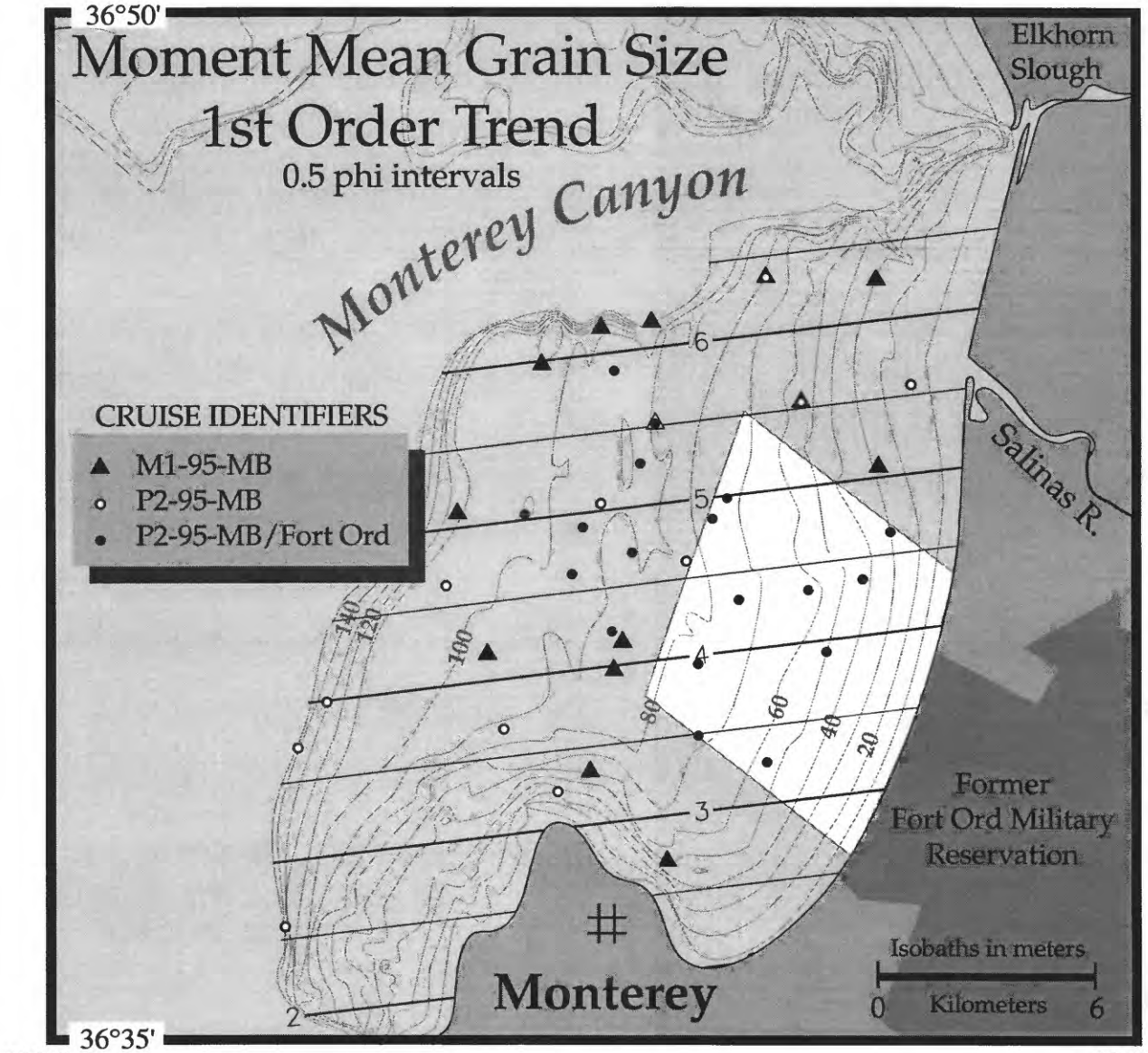

Figure 6. First order trend surface applied to the moment mean grain size. Note the northward fining trend toward the axis of the Monterey Canyon.

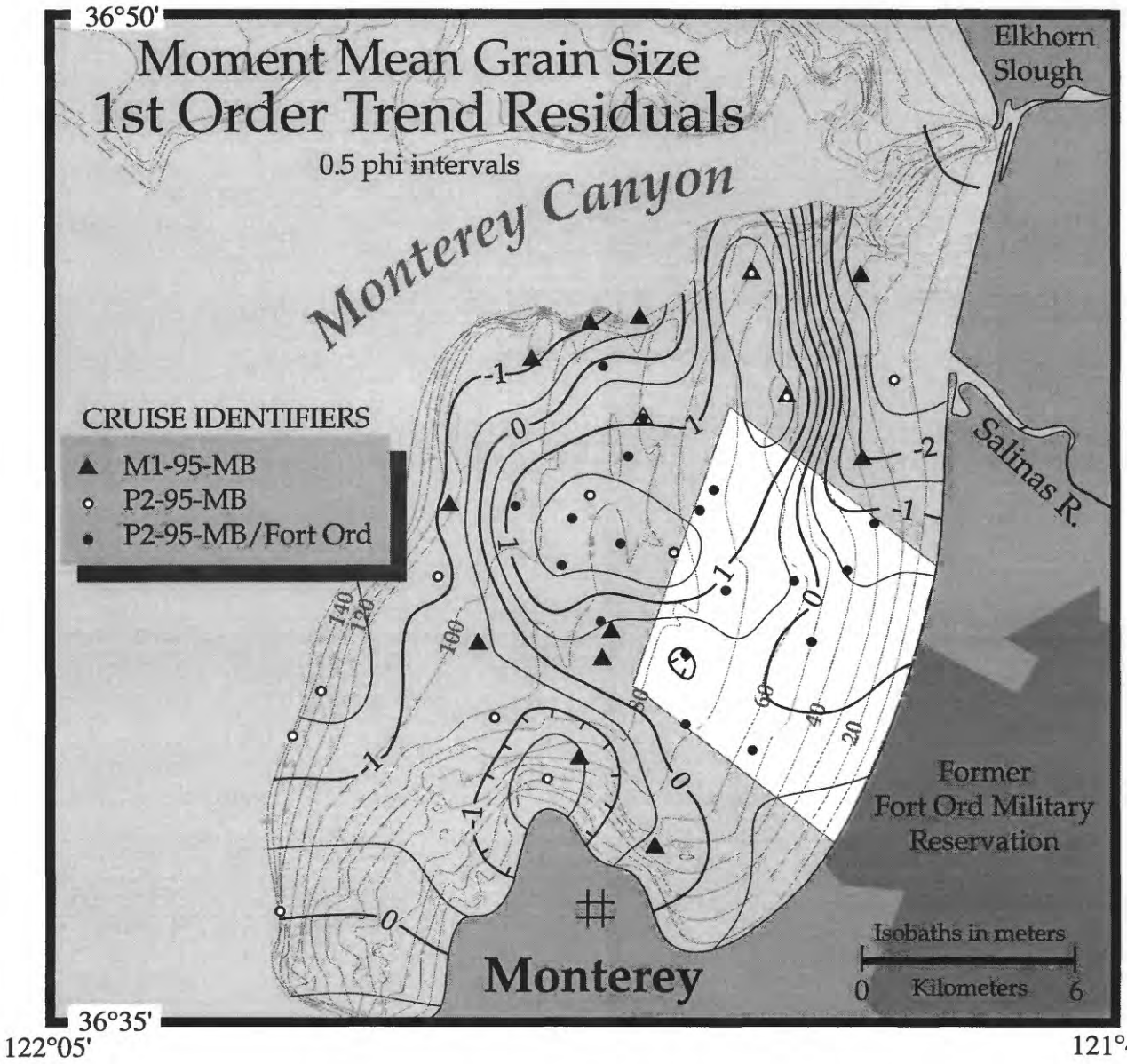

Figure 7. Areal distribution of residuals of the first order trend surface applied to the moment mean grain size. Note that the mid-shelf mud belt is finer than predicted by the trend. Note also the sands at the mouth of the Salinas River and immediately north of the Monterey Peninsula are coarser than predicted by the trend surface.

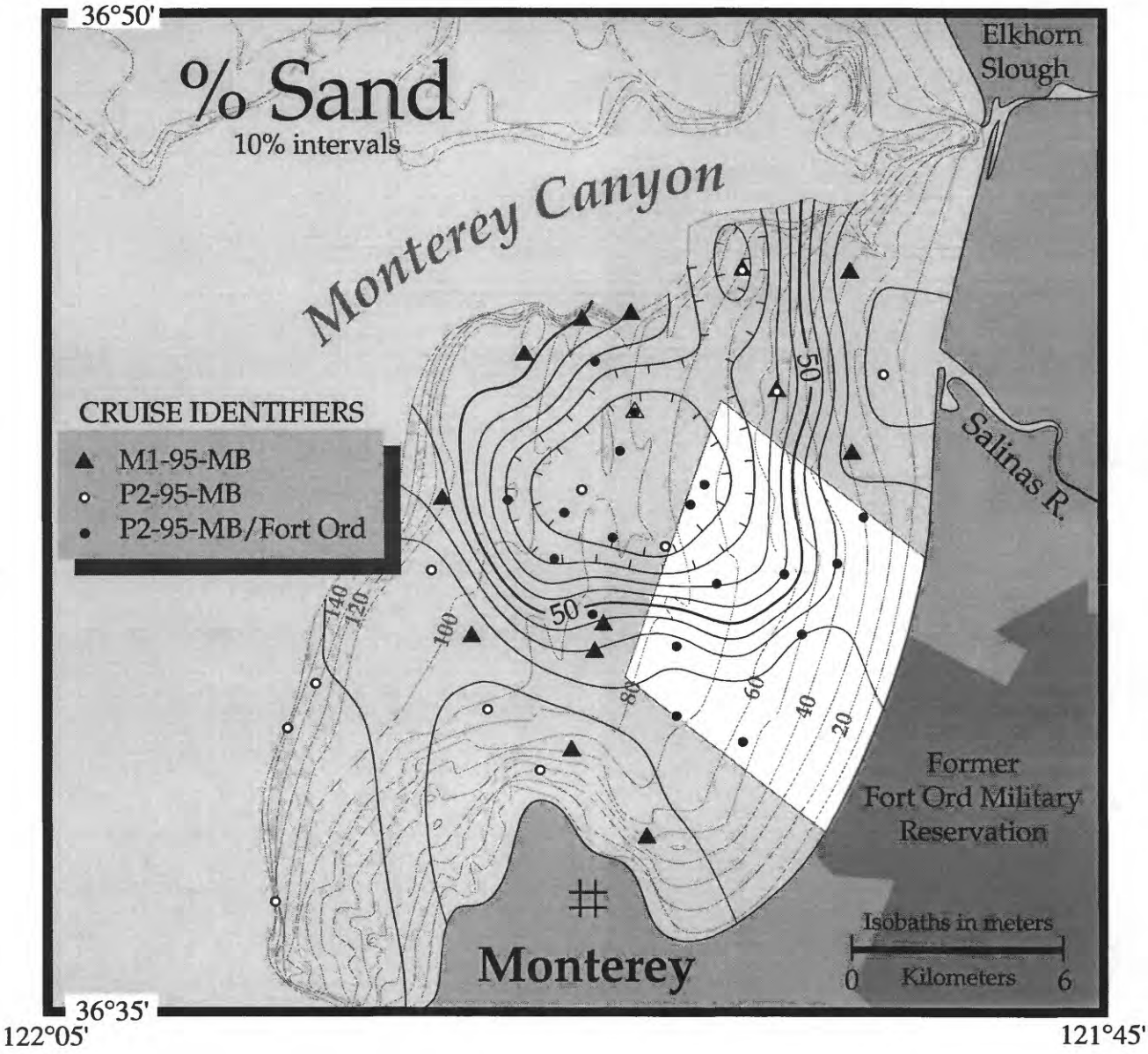

Figure 8. Areal distribution of % Sand (> 62 μ) in surface sediment (0 to 1 cm) on the Monterey Bay shelf. Note that the mid-shelf mud belt contains 10% to 20% sand.

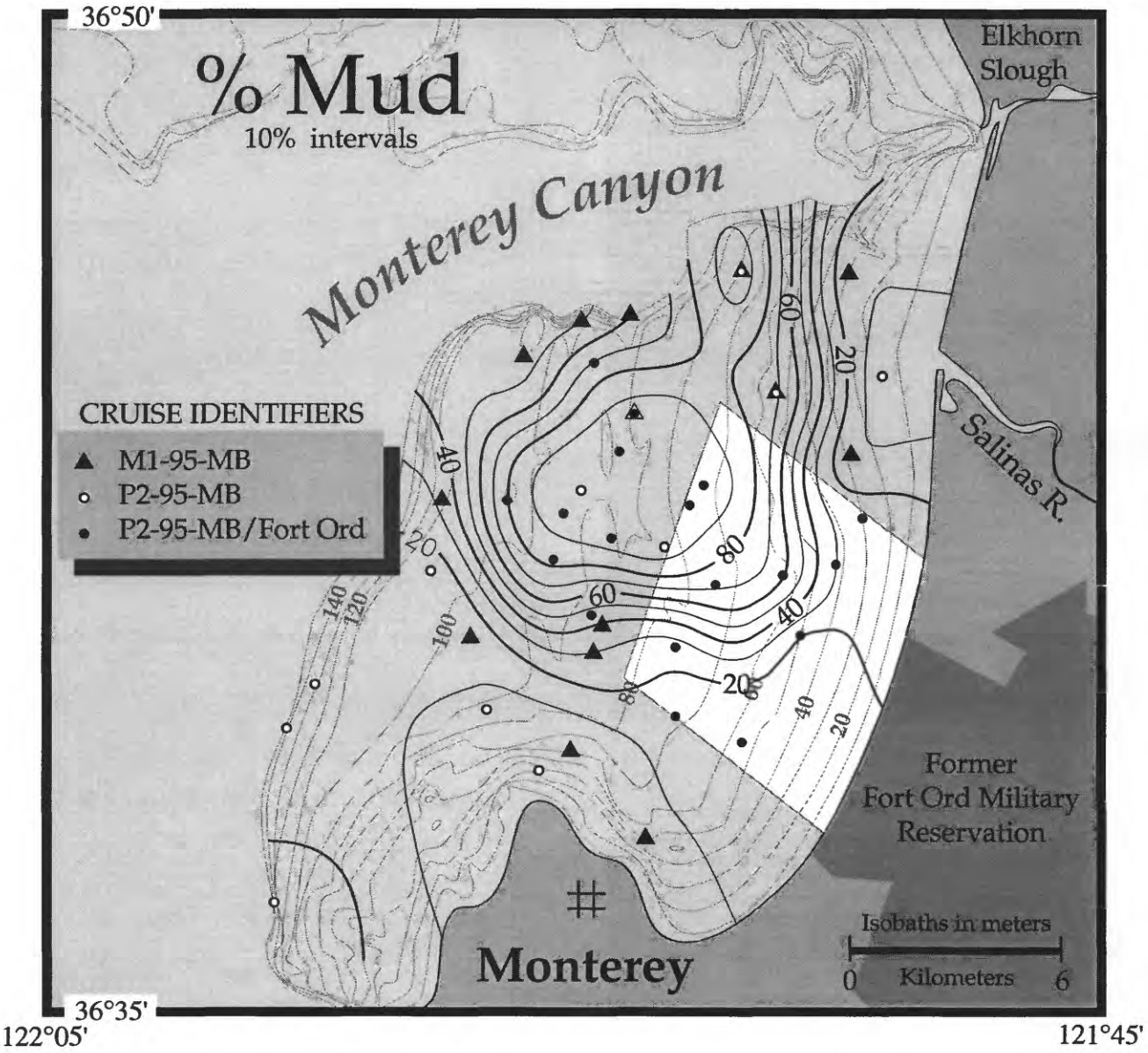

Figure 9. Areal distribution of % Mud (< 62 μ) in surface sediment (0 to 1 cm) on the Monterey Bay shelf. Note that the sand-rich sediment off the mouth of the Salinas River contains 10% to 20% mud.

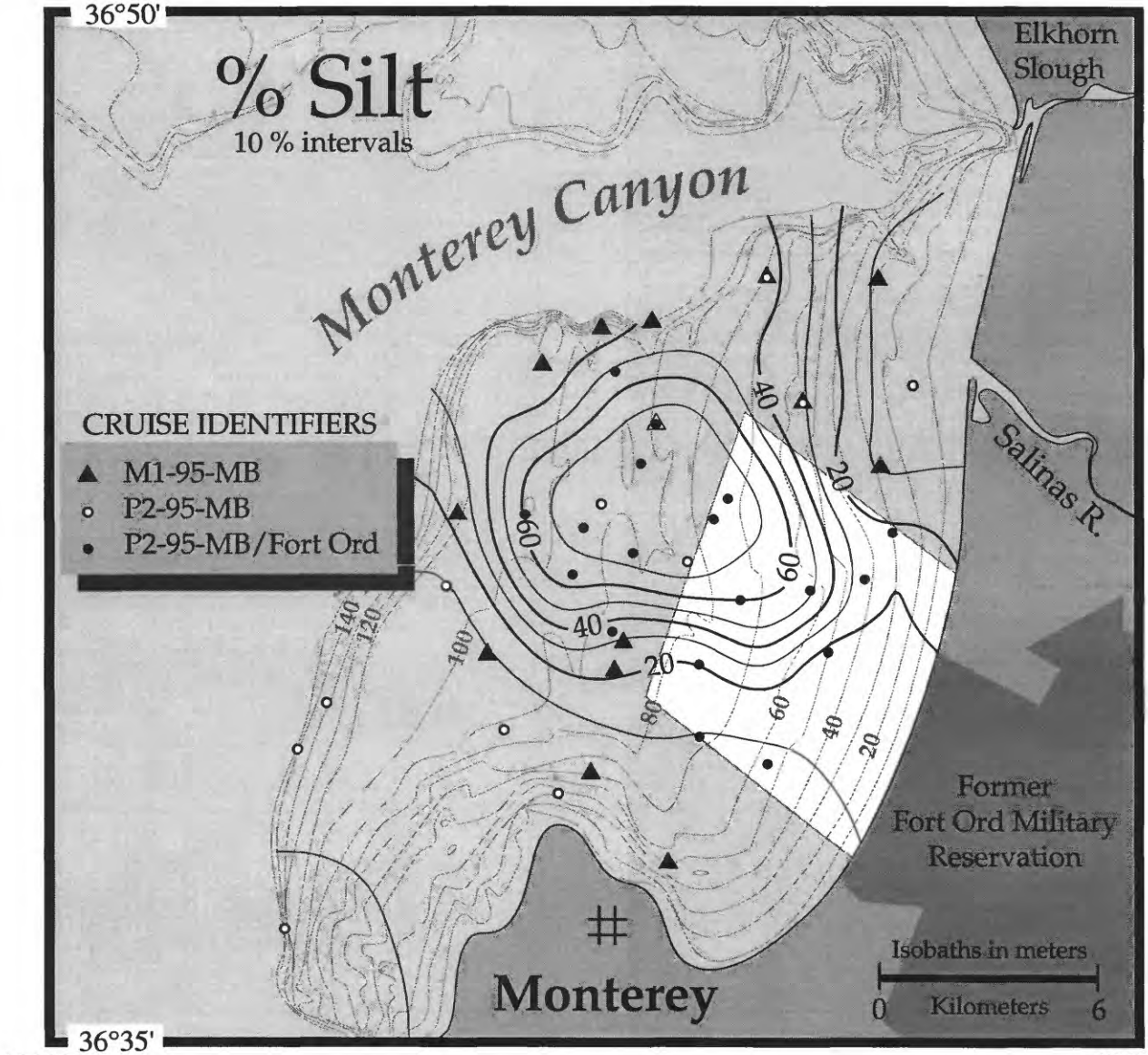

Figure 10. Areal distribution of % Silt (62 μ to 4 μ) in surface sediment (0 to 1 cm) on the Monterey Bay shelf. Note that the mid-shelf mud belt is dominated by silt-sized sediment.

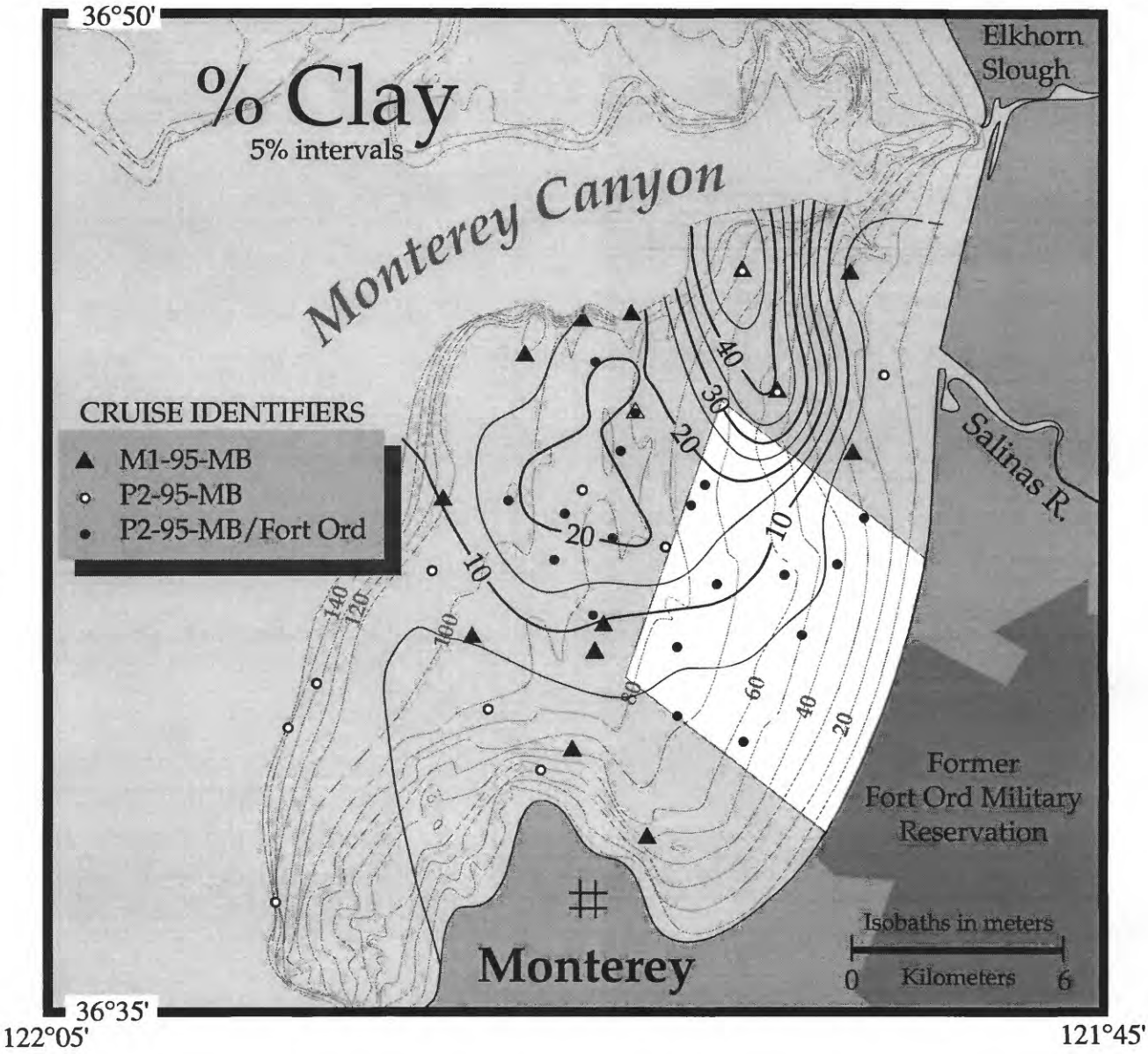

Figure 11. Areal distribution of % Clay (< 4 μ) in surface sediment (0 to 1 cm) on the Monterey Bay shelf. Note that the clay content is highest near the edge of the Monterey Canyon in the region offshore of the Salinas River. Surface sediment in this area was soupy and highly oxidized indicating deposits of flood-deposited sediment.

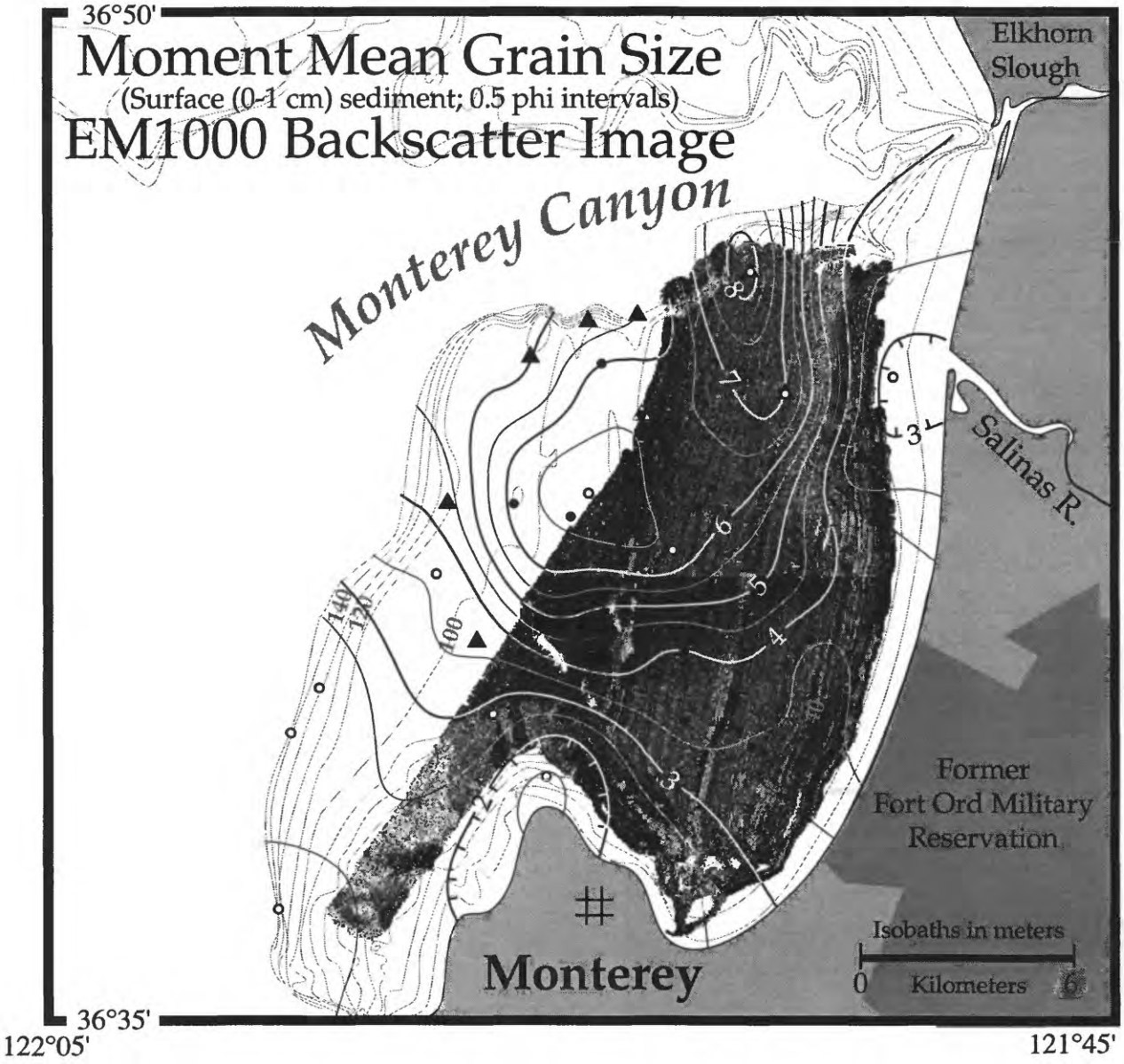

Figure 12. Moment mean grain size of surface (0 to 1 cm) sediment plotted on top of the EM1000 backscatter image. See text for discussion.

correlates with the fine-grained sediment of the mid-shelf mud belt. The higher backscatter areas offshore the Salinas River between the two lower backscatter regions correlates to a region of rapid textural change. The low backscatter region located closest to the mouth of the Salinas River correlates with sand-rich sediment. These observations show that, in these areas, low backscatter correlates with both fine silt and fine sand. More generally, however, the higher backscatter correlates with sediment in the sand-size class.

Table 2 presents the textural data in tabular form. Digital copies of the data (in 0.5 phi intevals) are available upon request.

Carbon/Carbonate

Figures 13 through 15 show the percent organic carbon, the first order trend surface, and residuals to the trend. Figures 16 through 18 show the percent $CaCO_3$, the first order trend and residuals to the trend, respectively. In general, the southern Monterey Bay continental shelf is dominated by terrigenous material and is unremarkable both in terms of organic carbon and $CaCO_3$ (percentages on the order of 1% in both cases). The midshelf mud belt is slightly enriched in organic carbon relative to the rest of the shelf area. The distribution of carbonate carbon is strongly dominated by the accumulation of bioclastic debris near the Monterey peninsula. The importance of this small area is shown by the large (> 20%) "bulls-eye" residual observed in Figure 18. However, the majority of the shelf is typified by $CaCO_3$ values less than 1%. Table 3 lists the organic carbon and $CaCO_3$ data. Digital copies are available upon request.

Bottom Photography

Obtaining good quality bottom photographs in a continental shelf setting can be an uncertain process. Much of the southern Monterey Bay continental shelf was blanketed by a near bottom turbid layer during the days we were working in the area. As a result, backscatter of the strobe light from the suspended particulates resulted in poor photographic images. The twelve images shown in Figure 19 are the highest quality images obtained on the southern Monterey Bay shelf during P2-95-MB. These images are shown in larger format in Figures 20 (A through L).

Enlarged photographs are shown for each of the three major sedimentary provences of the shelf: the mid-shelf/outer-shelf mud belt (Figs. 20E, F, G, H, I, and L), nearshore sands off the former Fort Ord Military Reservation (Figs. 20D, J, and K), and the carbonate-rich sands north of the Monterey peninsula (Figs. 20A, B, and C).

Mid-shelf/Outer-shelf Mud Belt:

Figure 20E, station B299, 79 m. Generally smooth seafloor with numerous small, sharp-edged depressions (pock marks), occasional distinct burrow depressions with open burrows. Note the sea pen(?) in the lower left corner of the image.

Figure 20F, station B304, 56 m. This station is located west of the Salinas River and the image is poor quality due to the turbidity of the water. Generally smooth seafloor with indistinct burrows and pockmarks. Occasional worm tubes(?).

Figure 20G, station B329, 105 m. Station is located near the seaward edge of the mud belt. Uniform seafloor with approximately 2-cm-diameter burrow depressions. Note the asteroid (star fish) in upper left part of the image.

Figure 20H, station B332, 92 m. Station is located in the center of the mid-shelf mud belt. Note the poor image quality due to turbidity of the water column. Generally smooth seafloor with occasional burrow depressions. Sea pen(?) in upper left part of image.

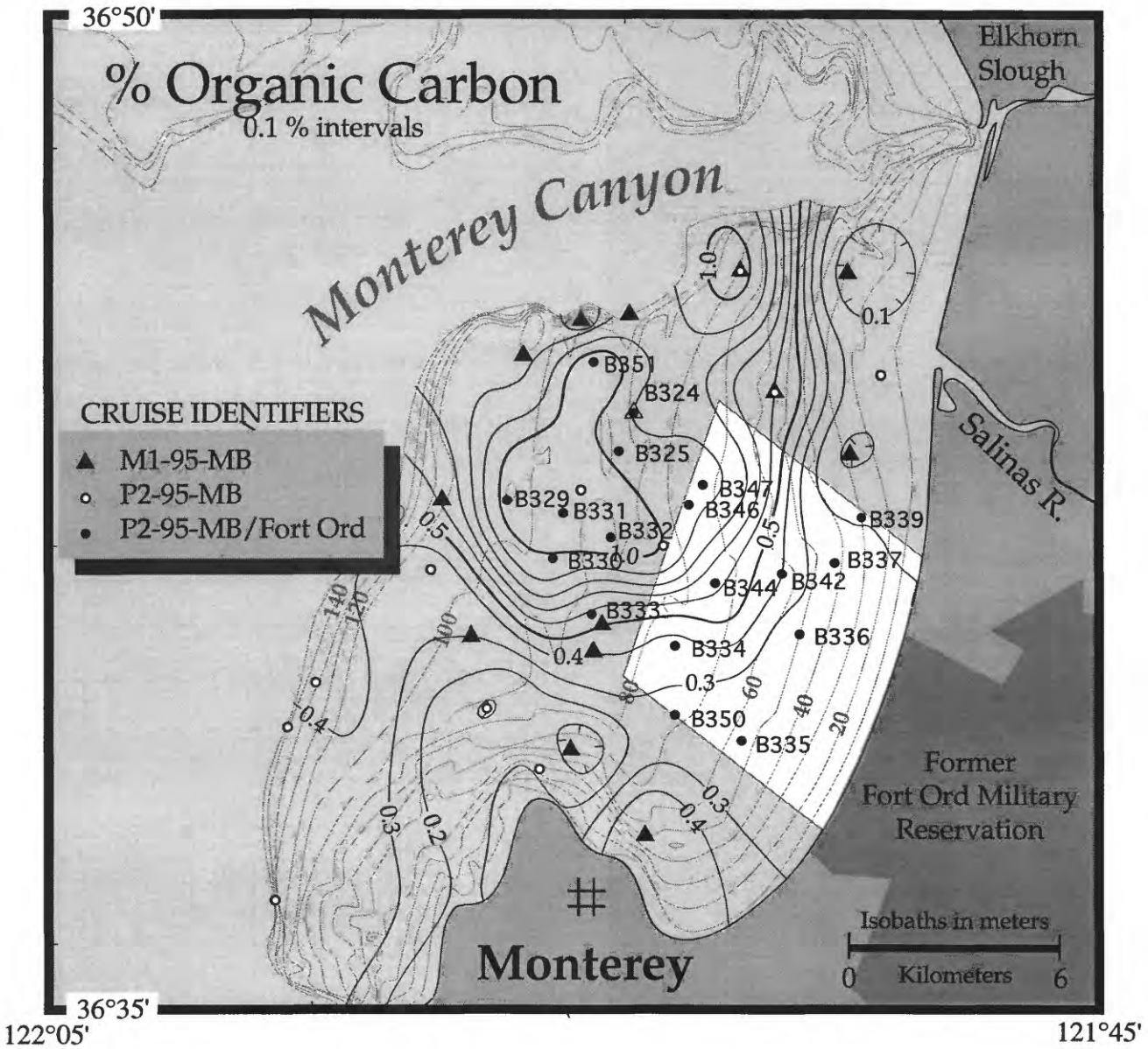

Figure 13. Areal distribution of % Organic Carbon in surface sediment (0 to 1 cm) on the Monterey Bay shelf. Note that the percentages are low (1 % or less) throughout the study area but are highest in the mid-shelf mud belt.

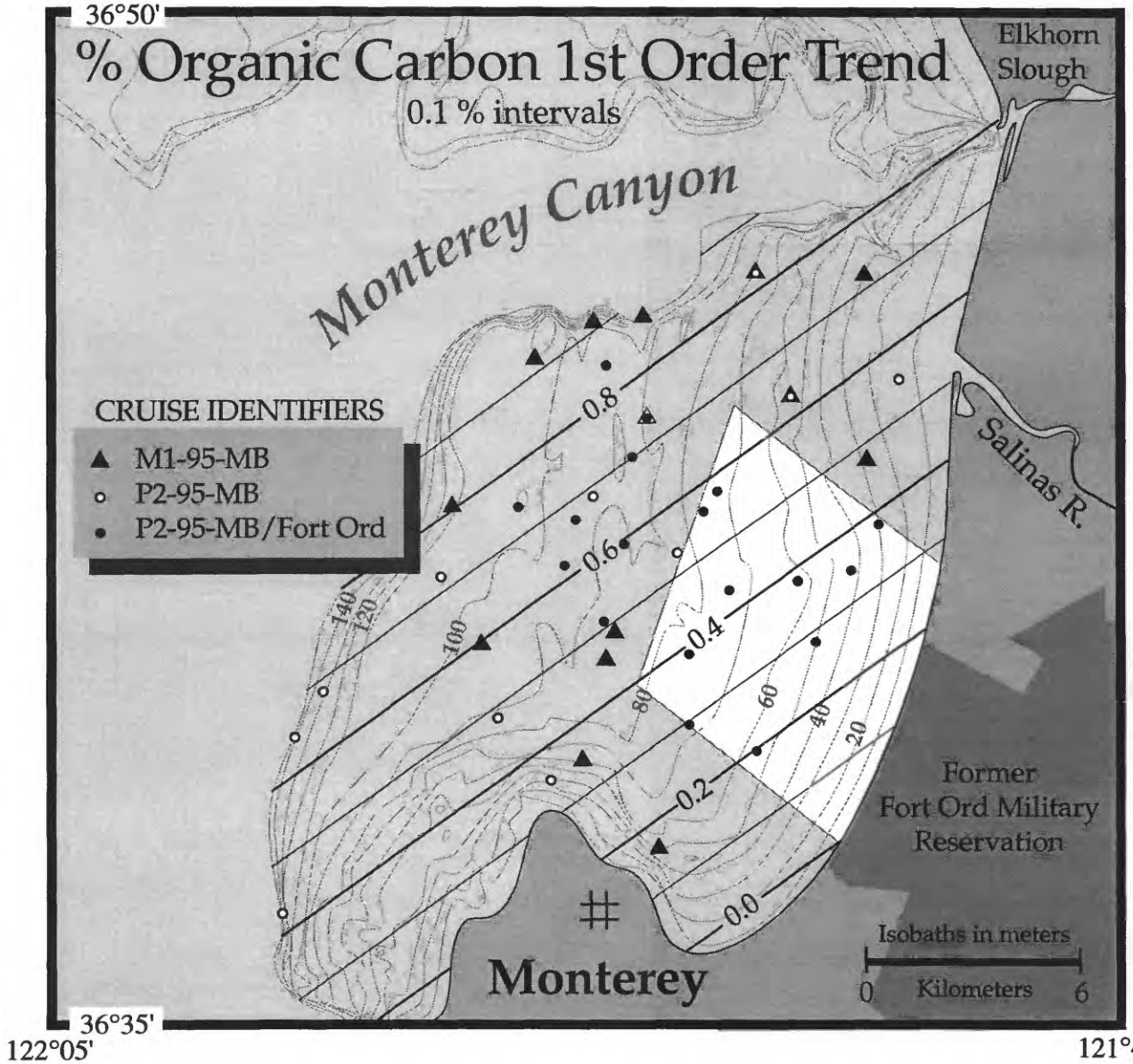

Figure 14. First order trend surface applied to % organic carbon in surface sediment (0 to 1 cm) on the Monterey Bay shelf. Note the northwestward increase in organic carbon toward the axis of Monterey Canyon, a trend that is generally in accord with that of moment mean grain size.

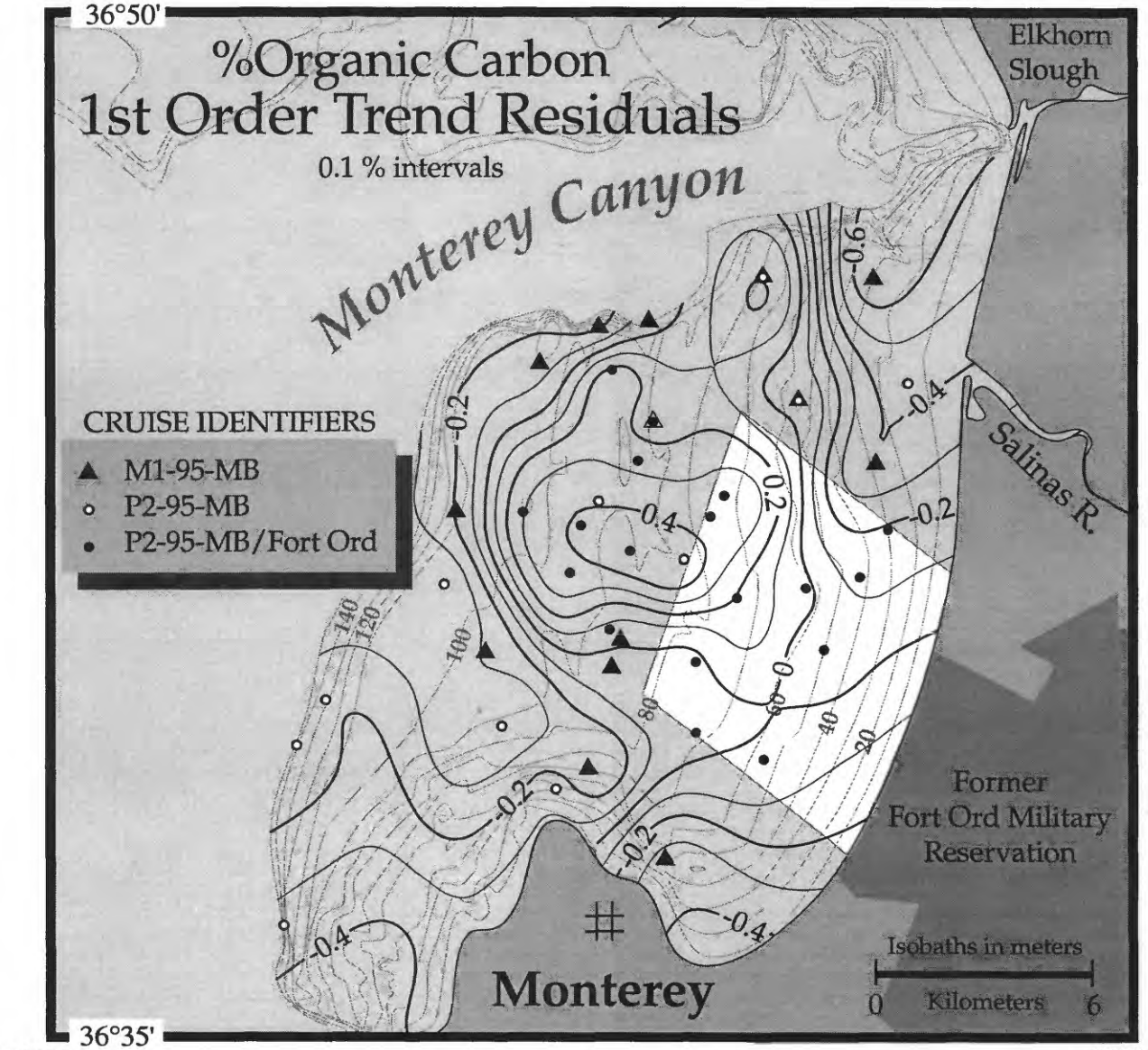

Figure 15. Areal distribution of residuals on the first order trend surface applied to % organic carbon. Note that the region of the mid-shelf mud belt is slightly higher than that predicted by the trend, a finding that correlates with the finer grained nature of this sediment.

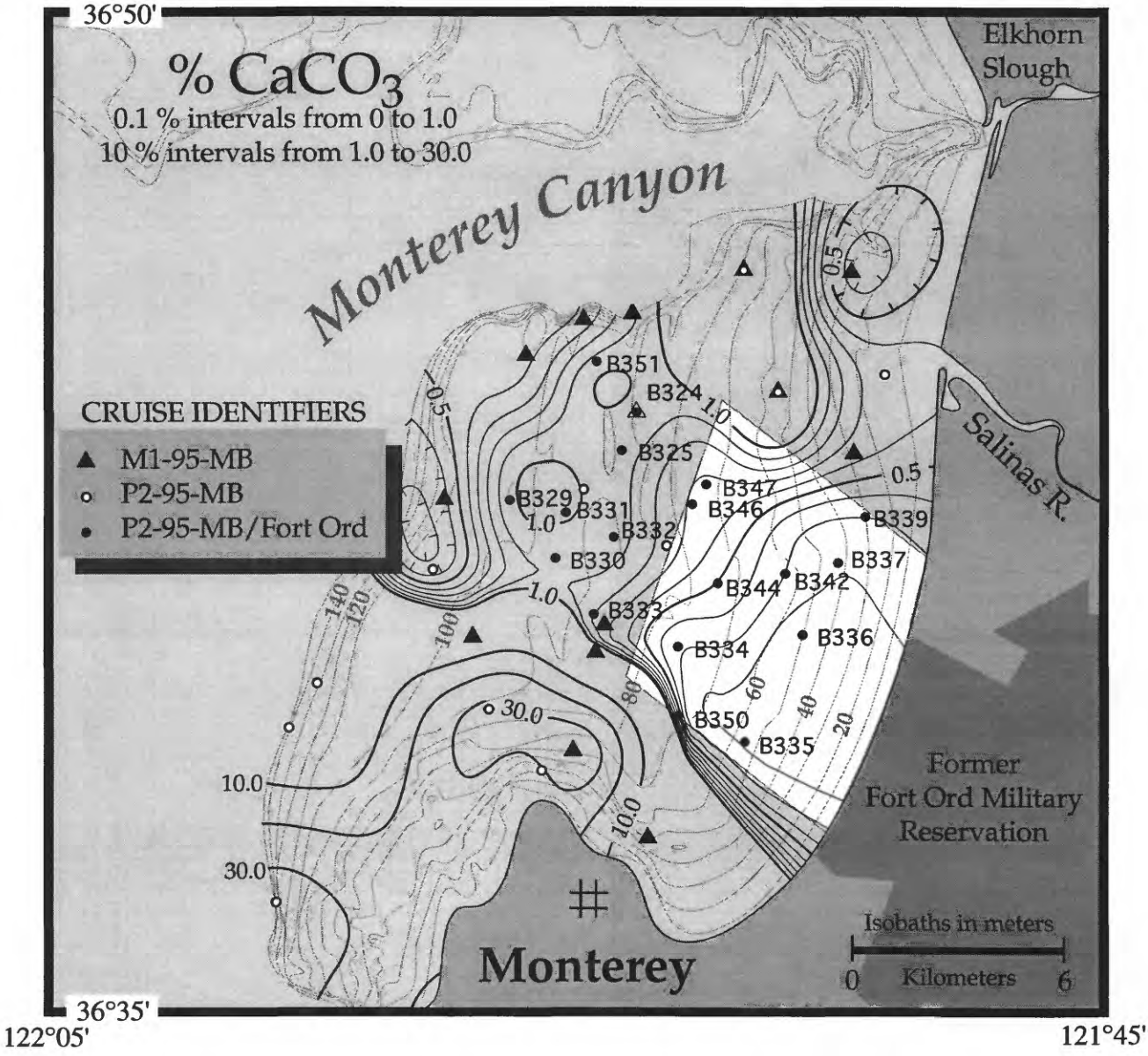

Figure 16. Areal distribution of % Carbonate Carbon in surface sediment (0 to 1 cm) on the Monterey Bay shelf. Note that the percentages are low (1 % or less) throughout most of the study area but increase dramatically near the Monterey Peninsula, in the region of bedrock outcrop seen in the SIMRAD EM1000 data.

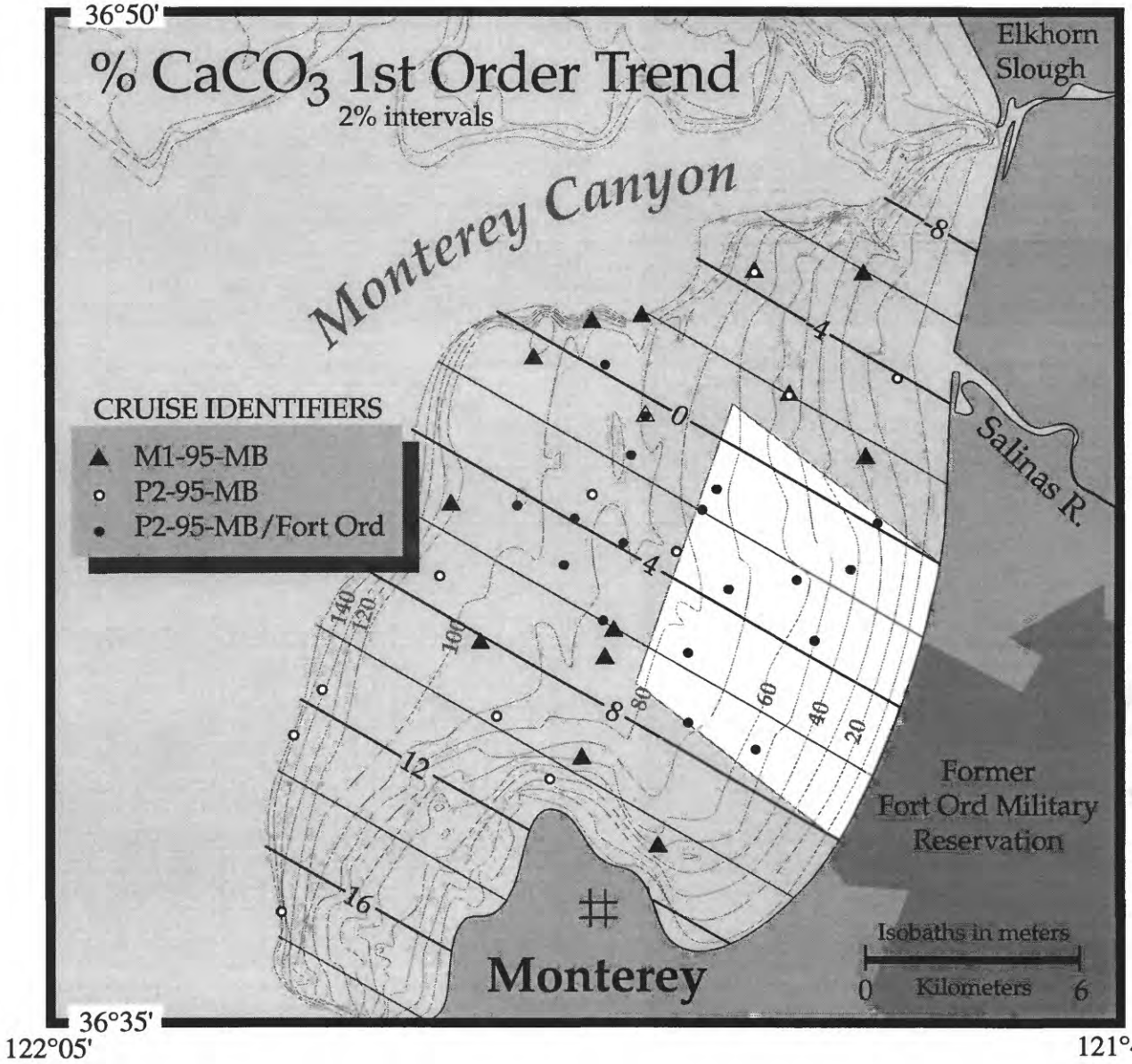

Figure 17. First order trend surface applied to % carbonate carbon in surface sediment (0 to 1 cm) on the Monterey Bay shelf. Note the increase in the trend southwestward, away from Elkhorn Slough and toward the Monterey Peninsula.

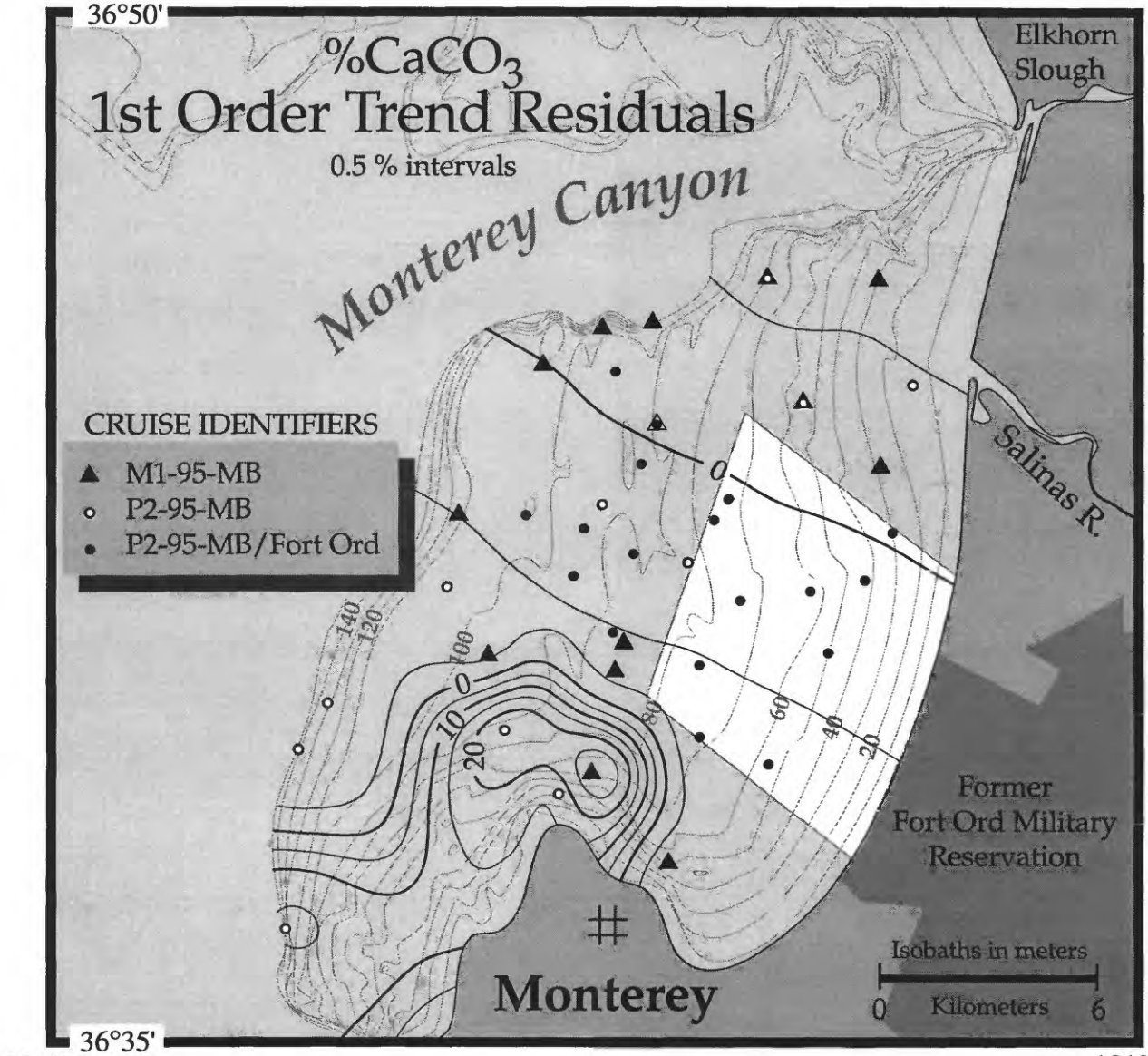

Figure 18. Areal distribution of residuals on the first order trend surface applied to % carbonate carbon. Note the anomalously high nature of the values in the vicinity of the Monterey Peninsula.

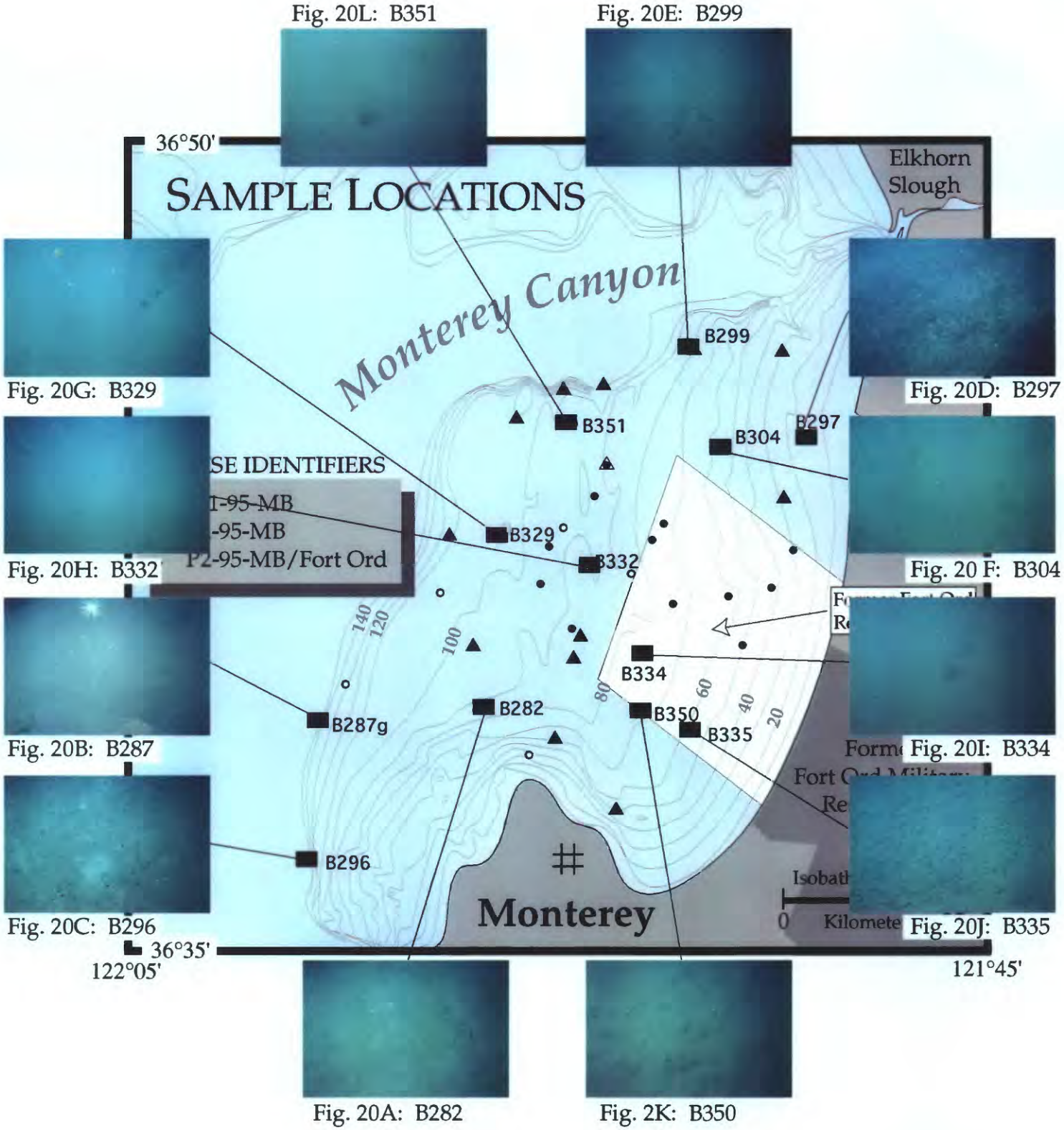

Figure 19. Location map showing thumbnail images of bottom photographs discussed in this report. Enlarged versions of the photographs are presented in Figure 20 (A-L).

A: B282 - Sand belt north of Monterey peninsula
90 m; Mean = 2.92ø; 93% sand; 30% CaC03

B: B287 - Shelf break west of Monterey; 125m;
Mean = 2.49ø; 14% gravel, 69% sand; 8% CaCO3

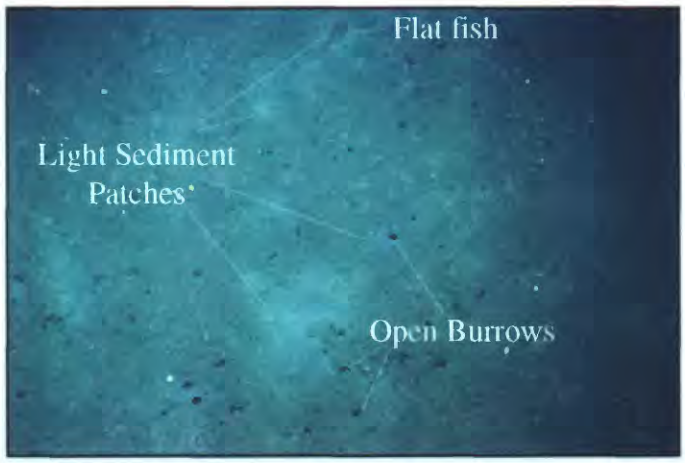

C: B296 - Shelf break west of Monterey
117m; Mean = 3.19ø; 75% sand; 30% CaCO3

D: B297 - Mouth of the Salinas River
18 m; Mean = 2.63ø; 98% sand

E: B299 - In mid-shelf mud belt at southern edge of
Monterey Canyon; 79 m; Mean = 6.61ø; 63% sand

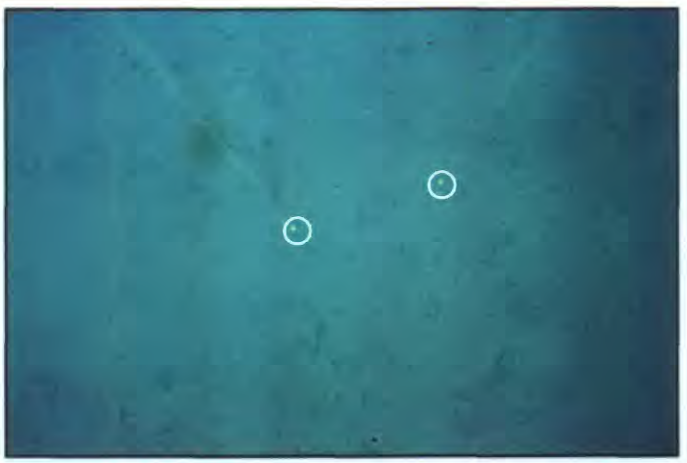

F: B304 - At edge of mid-shelf mud belt west of Salinas
River 56 m; Mean = 4.97ø; 44% sand, 45% silt

Figure 20 (A-F). Seafloor photographs at selected box coring stations. Circles identify laser points on bottom (10 cm separation). See text for description.

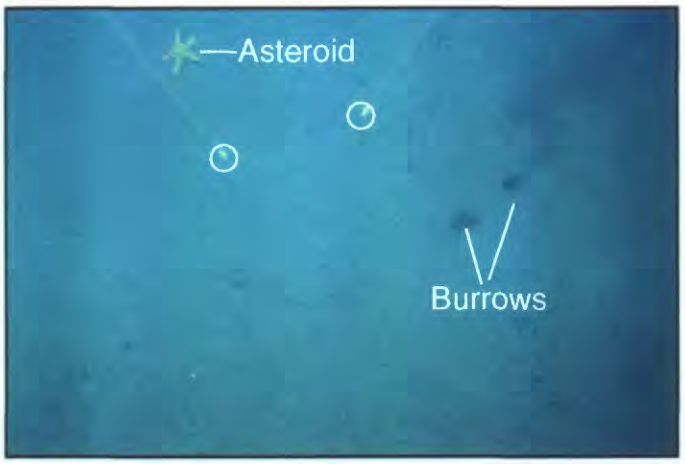

G: B329 - Outer shelf mud belt
105 m; Mean = 6.39ø; 65% silt

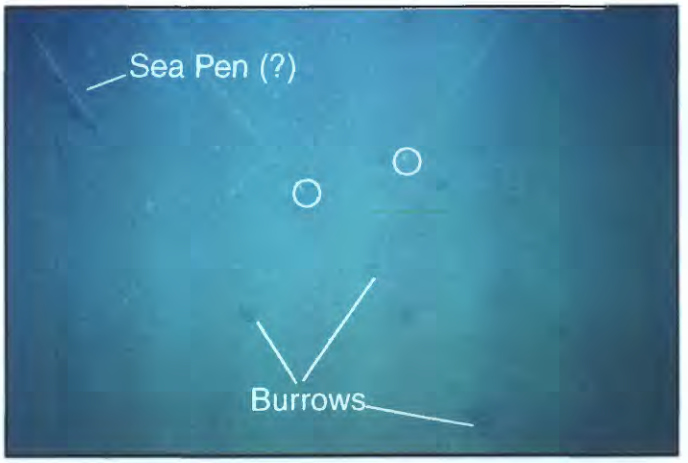

H: B332 - Inside mid-shelf mud belt
92 m; Mean = 6.6ø; 76% silt

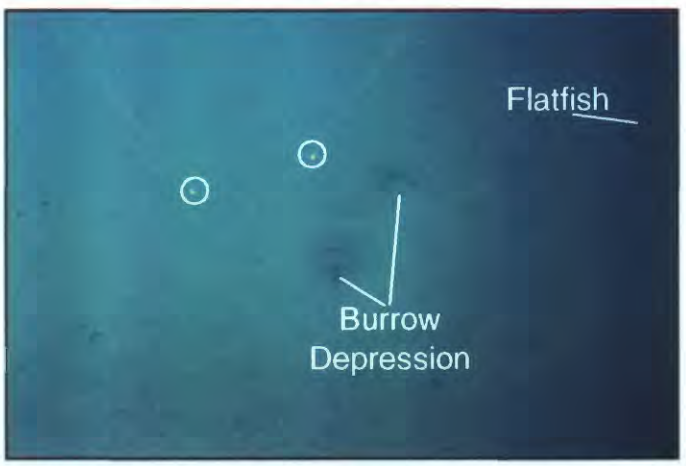

I: B334 - Central shelf at nearshore edge of mid-shelf mud belt; 81 m; Mean = 3.8ø; 80% sand

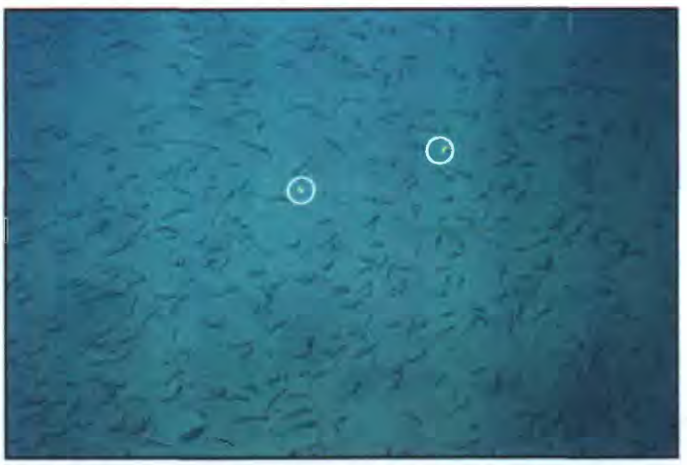

J: B335 - Nearshore sands west of former Fort Ord
57 m; Mean = 3.5ø; 89% sand

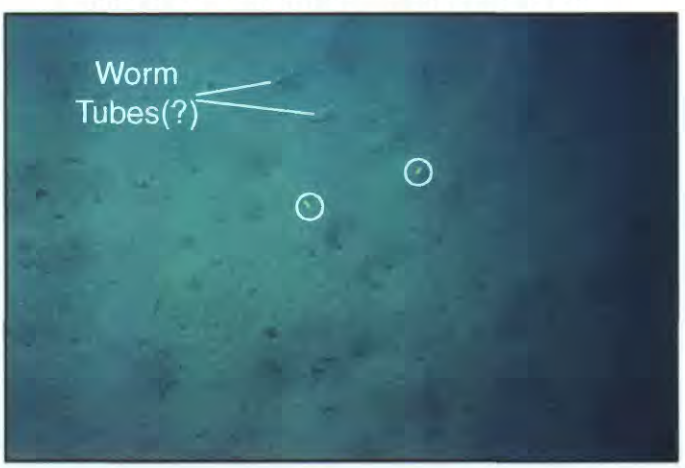

K: B350 - Nearshore sands west of former Fort Ord
75 m; Mean = 3.6ø; 88% sand

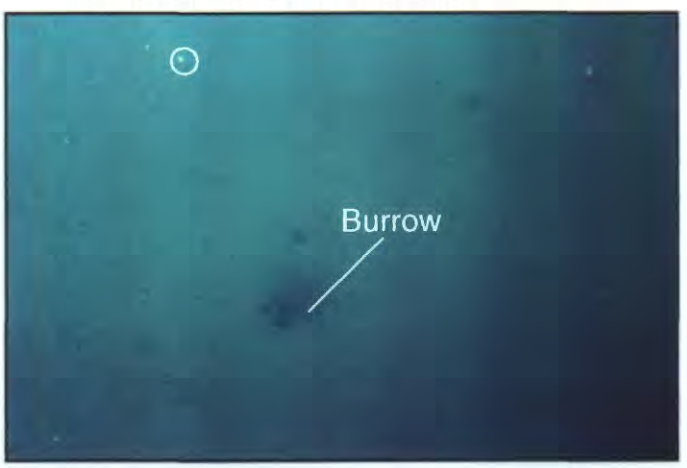

L: B351 - Mid-shelf mud belt south of Monterey Canyon; 99 m; Mean = 6.5ø; 63% silt

Figure 20 (G-L). Seafloor photogràphs at selected box coring stations. Circles identify laser points on bottom (10 cm separation). See text for description.

Figure 20I, station B334, 81 m. Generally smooth to slightly irregular seafloor with occasional burrow depressions. Note flatfish in upper right part of image. Interactions of flatfish with the bottom are known to produce irregularities of the seafloor and also mix sediment into the water column.

Figure 20L, station B351, 99 m. Generally smooth seafloor with occasional oppen burrows. No observed epifauna.

Nearshore Sands:

Figure 20D, station B297, 18 m. Water turbid leading to relatively poor image quality. Dense field of sand dollars on generally uniform substrate.

Figure 20J, station B335, 57 m. Generally smooth seafloor with numerous shallow, indistinct depressions, small burrows, and occasional worm tubes(?).

Figure 20K, station B350, 75 m. Generally smooth seafloor with numerous irregular depressions, small open burrows, and occasional worm tubes(?).

Carbonate-rich Sands:

Figure 20A, station B282, 90 m. Station is located in south-central Monterey shelf, 30% $CaCO_3$. Irregular, mottled appearance to seafloor with numerous small burrows and depressions.

Figure 20B, station B287, 125 m. Station is located at the shelf break west of the Monterey peninsula, 8% $CaCO_3$. Generally uniform seafloor with occasional open burrows. Echinoderms (basket star, asteroid, and ophiuroid) in upper part of image. Biogenically encrusted boulders at bottom of image.

Figure 20C, station B296, 117 m. Station is located at the shelf break west of the Monterey peninsula, 30% $CaCO_3$. Generally smooth seafloor with mottled coloring, numerous irregular depressions and open burrows. "Bright" spots (high reflectivity) likely are shell debris. Light-colored sediment patches

Physical Properties

Physical properties were measured with the GEOTEK MSL as a means of correlating between cores and to measure properties that change with time (bulk density and acoustic velocity). Bulk density can be combined with age dates to determine the vertical flux of sediment to the seafloor. Age dates (210Pb technique) are not yet available; hence, we cannot calculate vertical fluxes of sediment at this time. The logger data can also be used to infer sediment textures of unsplit core segments.

Appendix A presents the physical property logs from the MSL for the 18 US Army stations occupied during the study. The plots shown on each log show the measured property versus core depth in centimeters. The first plot shows compressional (P) wave velocity, the second shows bulk density, the third plot presents sediment magnetic susceptibility, and the fourth presents acoustic impedance (the product of velocity and density) a property that relates to acoustc reflectors in seismic reflection profiles.

Mud-rich sediment on this shelf segment typically has P-wave velociities of about 1500 m/s and bulk densities of about 1.5 to 1.6 g/cc (e.g., Appendix A, core B324). In contrast, nearshore sands on this shelf segment more typically have higher P-wave velocities (about 1700 m/s) and higher bulk densities (1.8 to 2.1 g/cc) (e.g., Appendix A, core B335). Most of the cores are well behaved down core; that is velocities and bulk densities increase monotonically as expected in normally consolidated sediment and the apparent texture (mud or sand) is relatively uniform throughout. A number of cores (e.g.,

B329, B330, and B346) show distinct variations in properties indicating mixed layers of muds and sands. One core (B333) looses P-wave velocity data at about 20 cm subbottom and exhibits a dramatic decrease in bulk density. These findings likely indicate a physical break or rupture of the sediment occurred during the subcoring process. In a number of cores (e.g., B342 from the eastern edge of the mid-shelf mud belt), a mud-rich sediment overlies a sand-rich unit that continues to the bottom of the core.

SUMMARY

Analysis of samples collected at 46 coring sites shows that surface sediment on the seafloor of the southen Monterey Bay continental shelf can be divided into three major sedimentological regions: 1) nearshore sands, 2) a mid-shelf/outer-shelf mud belt, and 3) carbonate-rich nearshore sands adjacent to the Monterey peninsula. The nearshore sediment is coarsest (medium sand) near the Monterey peninsula but more typically is fine to very fine sand (e.g., offshore of the Salinas River mouth). The mean grain size of sediment on the mid-shelf and outer-shelf is a very fine to coarse silt that contains significant amounts of sand. The primary source of terrigenous sediment appears to be the Salinas River where muds bypass the inner shelf and are deposited in the mid-shelf mud belt. Organic carbon and $CaCO_3$ contents are unremarkable throughout the study area. Somewhat higher organic carbon values are associated with the mid-shelf mud belt and high (over 30%) $CaCO_3$ values occur north of the Monterey peninsula. Bottom photographs taken during coring show a generally uniform seafloor with limited epifaunal activity and moderate amounts of burrowing by infauna.

ACKNOWLEDGMENTS

The U.S. Army has contributed financially to both our ship time and laboratory analytical work in an effort to help characterize the surface sediment on the southern Monterey Bay continental shelf. In addition to the U.S. Army, we are working cooperatively with representatives and scientists of the National Oceanic and Atmospheric Administration (NOAA), Environmental Protection Agency (EPA), the University of California at Santa Cruz (UCSC), and Moss Landing Marine Laboratory (MLML) a part of the California State University system. We thank the officers and crew of the NOAA ship McARTHUR and the R/V POINT SUR for their support in collecting samples discussed in this report.

REFERENCES

Boyce, R.E., 1970, Appendix I. Physical properties - methods. *in,* Edgar, N.T., A.G. Kaneps, and J.R. Herring (eds.) *Initial Reports of the Deep Sea Drilling Project,* Washington (US Government Printing Office), v. 15, p. 1115-1125.

Cowen, E.A., R.D. Powell, P.R. Carlson, R.E. Kayen, J. Cai, D.C. Seramur,, and S.D. Zellers, 1994, Cruise Report: R/V ALPHA HELIX CRUISE -173 to western Prince William Sound, Yakutat Bay, and Glacier Bay National Park, northeastern Gulf of Alaska, August 17- September 3, 1993. U.S. Geological Survey Open-File Report, 94-258, 94 p.

Eittreim, S.L., A.J. Stevenson, L.A. Mayer, J. Oakden, C. Malzone, and R. Kvitek (this volume), Multibeam bathymetry and acoustic backscatter imagery of the southern Monterey Bay shelf.

Harding Lawson Associates, 1995, Basewide remedial investigation/feasibility study Fort Ord, California.

Kayen, R.E., and T.N. Phi, in press, HYPERSCAN: a HyperCard™ Interface for instrument control and data acquisition of the U.S. Geological Survey's Multi-Sensor Ocean Sediment Core Logger. Proc. of the Scientific and Engineering Applications on the Macintosh™, 3rd Annual Conference, San Francisco, CA. Jan. 9-10, SciTech Journal, Worchester, MA.

Kayen, R.E., 1994, Mass physical and geotechnical properties of sediment on the Palos Verdes Margin: Appendix B to *The Distribution and Character of Contaminated Effluent-effected Sediment, Palos Verdes Margin, Southern California*, USGS Administrative Report.

Krumbein, W.C., and F.A. Graybill, 1965, An Introduction to Statistical Models in Geology: McGraw-Hill Book Company, San Francisco, 475 p.

Krumbein, W.C., and F.J. Pettijohn, 1938, Manual of Sedimentary Petrography, Appleton-Century-Crofts, Inc., New York.

Lee, H.J. and J.E. Clausner, 1979, Seafloor sampling and geotechnical parameter determination handbook, Civil Engineering Laboratory, Naval Construction Battalion Center, Report No. TR-873, Port Hueneme, CA. 128 p.

Stephenson, M., G. Ichikawa, J. Goetzl, K. Paulson,, M. Pranger, R. Fairey, S. Lamerdin, R. Tjeerdema, J. Newman, J. Becker, and M. Stoetling, (this volume), Distribution and concentration of selected contaminants in Monterey Bay sediments.

U.S. Naval Oceanographic Office, 1966, Handbook of Oceanographic Tables, U.S. Naval Oceanographic Office, SP-68, 427 p.

Wells, D. and A. Kleusberg, 1990, GPS: A multipurpose system. GPS World. January/February, p. 60-63.

Whitmarsh, R.B., 1971, Precise sediment density determination by gamma-ray attenuatin alone. Jour. Sedimentary Petrology, v. 41, p. 882-883.

Table 1. Station Metadata

Core ID	Latitude	Longitude	Depth (m)	Recovery (cm)
B147	36° 40.80'	121° 54.44'	85	37
B148	36° 40.40'	121° 54.58'	86	33
B149	36° 37.61'	121° 53.61'	51	32
B150	36° 38.90'	121° 55.04'	60	18
B151	36° 40.62'	121° 56.94'	95	29
B153	36° 42.67'	121° 57.50'	111	21
B154	36° 43.98'	121° 53.84'	88	55
B157	36° 44.85'	121° 55.94'	104	45
B159	36° 45.37'	121° 54.83'	95	48
B160	36° 45.47'	121° 53.87'	98	15
B163	36° 46.13'	121° 51.79'	75	56
B164	36° 44.29'	121° 51.13'	52	36
B165	36° 43.38'	121° 49.69'	28	19
B167	36° 46.07'	121° 49.73'	30	17
B281	36° 41.64'	121° 57.69'	110	29
B282	36° 39.55'	121° 56.62'	90	33
B283	36° 39.91'	121° 59.96'	121	10
B287	36° 39.26'	122° 00.47'	125	Grab
B296	36° 36.69'	122° 00.65'	117	49
B297	36° 44.56'	121° 49.11'	18	20
B299	36° 46.14'	121° 51.79'	79	46
B304	36° 44.28'	121° 51.13'	56	39
B305	36° 41.98'	121° 53.27'	86	54
B306	36° 42.81'	121° 54.83'	97	57
B324	36° 43.97'	121° 53.91'	92	54
B325	36° 43.42'	121° 54.10'	88	52
B329	36° 42.68'	121° 56.23'	105	49
B330	36° 41.79'	121° 55.37'	98	50
B331	36° 42.48'	121° 55.18'	95	57
B332	36° 42.11'	121° 54.27'	92	54
B333	36° 40.95'	121° 54.63'	92	43
B334	36° 40.49'	121° 53.05'	81	37
B335	36° 39.06'	121° 51.78'	57	30
B336	36° 40.66'	121° 50.67'	52	34
B337	36° 41.71'	121° 50.00'	43	35
B339	36° 42.41'	121° 49.49'	40	34
B342	36° 41.55'	121° 51.01'	62	35
B344	36° 41.41'	121° 52.29'	78	49
B346	36° 42.60'	121° 52.79'	82	49
B347	36° 42.90'	121° 52.50'	77	48
B350	36° 39.43'	121° 53.04'	75	36
B351	36° 44.76'	121° 54.60'	99	46
C291	36° 38.61'	121° 55.63'	41	Grab
C295	36° 36.64'	122° 00.66'	118	Grab

Table 2. Descriptive textural characteristics.

Station id.	Mean Grain Size	% Gravel	% Sand	% Silt	% Clay	% Mud
B147	4.35	0	67.45	23.88	8.67	32.55
B148	4.03	0	78.57	14.53	6.91	21.43
B149	2.29	0	90.46	5.04	4.49	9.54
B150	1.89	0	98.14	1.86	0	1.86
B151	3.66	0	86.07	8.67	5.26	13.93
B153	4.08	4.03	67.77	18.68	9.53	28.2
B154	6.48	0	4.19	76.4	19.41	95.81
B154	6.64	0	4.15	74	21.85	95.85
B157	4.84	0	55.26	33.11	11.63	44.74
B159	4.75	0	62.91	24.72	12.37	37.09
B159b	4.57	0	64.97	24.07	10.96	35.03
B160	5.41	0	39.13	42.21	18.66	60.87
B160b	5.5	0	39.11	41.71	19.18	60.89
B163	8.38	0	3.68	43.42	52.91	96.32
B163	5.72	0	12.93	71.29	15.78	87.07
B164f	7.33	0	26.19	31.17	42.64	73.81
B164sf	4.21	0	68.42	25.43	6.15	31.58
B165	2.89	4.91	88.03	5.76	1.3	7.06
B167	3.48	0	90.98	7.61	1.41	9.02
B281	3.4	0	89.43	6.13	4.44	10.57
B282	2.92	0	92.56	4.79	2.65	7.44
B283	2.14	9	81.24	5.01	4.75	9.76
B287g	2.49	14.59	69.14	7.52	8.74	16.26
B296	3.19	2.85	74.58	12.59	9.97	22.56
B297	2.63	0	98.25	0.7	1.05	1.75
B299	6.61	0	10.25	63.26	26.49	89.75
B304	4.97	0	43.73	45.15	11.11	56.27
B305	6.62	0	2.48	76.51	21.01	97.52
B306	6.8	0	1.55	76.59	21.85	98.45
B324	6.45	0	4.16	75.29	20.54	95.84
B324	6.46	0	4.19	75.34	20.47	95.81
B325	6.53	0	2.42	78.4	19.19	97.58
B325	6.55	0	2.43	78.07	19.49	97.57
B329	6.39	0	13.04	66.18	20.78	86.96
B329	6.31	0	15.35	64.69	19.96	84.65
B330	6.15	0	17.29	64.05	18.66	82.71
B330	6.04	0	18.04	64	17.97	81.96
B331	6.68	0	2.82	76.63	20.55	97.18
B331	6.75	0	2.86	76.31	20.83	97.14
B332	6.65	0	3.17	75.89	20.94	96.83
B332	6.63	0	3.15	76.23	20.62	96.85
B333	4.97	0	50.05	38.29	11.66	49.95
B333	4.94	0	50.11	38.25	11.63	49.89
B334	3.8	0	79.87	14.89	5.24	20.13
B334	3.79	0	79.88	14.85	5.28	20.12

Table 2. Descriptive textural characteristics (con't).

Station id.	Mean Grain Size	% Gravel	% Sand	% Silt	% Clay	% Mud
B335	3.47	0	89.08	8.7	2.23	10.92
B335	3.47	0	89.06	8.64	2.3	10.94
B336	3.24	0	90.57	6.96	2.47	9.43
B336	3.25	0	90.5	7.01	2.49	9.5
B337	3.65	0	80.33	16.41	3.26	19.67
B337	3.64	0	80.33	16.43	3.24	19.67
B339	4	0	71.74	24.54	3.72	28.26
B339	4.02	0	71.73	24.37	3.9	28.27
B342	5.08	0	26.22	64.11	9.67	73.78
B342	5.07	0	25.66	64.91	9.42	74.34
B344	5.13	0	28.19	61.02	10.79	71.81
B344	5.27	0	27.27	61.4	11.33	72.73
B346	6.13	0	4.7	78.75	16.54	95.3
B346	6.18	0	4.72	79.17	16.11	95.28
B346	6.18	0	4.58	79.24	16.18	95.42
B346	6.2	0	4.58	78.16	17.26	95.42
B347	6.32	0	5.99	74.25	19.76	94.01
B347	6.35	0	5.99	74.05	19.96	94.01
B347	6.3	0	7.28	72.97	19.75	92.72
B347	6.29	0	9.13	71.66	19.22	90.87
B350	3.6	0	87.94	8.63	3.42	12.06
B350	3.6	0	87.88	8.55	3.56	12.12
B351	6.53	0	15.98	60.63	23.39	84.02
B351	6.31	0	15.9	63.25	20.85	84.1
C291	1.06	0	99.99	0.01	0	0.01
C295	2.54	7.91	73.4	9.53	9.16	18.69

Table 3. Pecent organic carbon and calcium carbonate.

Station ID	% Organic C	% CaCO3
B147	0.44	0.69
B147r	-0.06	0.52
B148	0.34	0.56
B148r	-0.06	0.5
B149	0.51	2.5
B150	-0.01	43.6
B150r	-4.37	36.42
B151	0.31	0.22
B151r	0.32	0
B153	0.6	0.28
B153r	0.63	0
B154 tx1	0.84	0.98
B154 tx2	0.85	1
B157	0.77	0.53
B157r	-0.06	0.53
B159	0.55	0.4
B160	0.83	0.93
B163f	1.05	1.67
B163sf	0.49	0.71
B164f	0.61	1.32
B164sf	0.2	0.62
B165	0.06	0.69
B165r	-0.14	1.15
B167	0.03	0.29
B167r	0.06	0
B281	0.3	0.15
B282	0.07	37.57
B282r	-4.61	38.38
B283	0.48	2.28
B287g	0.33	5.78
B287gr	0.57	3.81
C291g	0.28	22.27
C295g	0.37	33.17
B296	0.75	38.7
B296r	5.46	0
B297	0.12	0.65
B297r	-0.09	0.79
B299	0.76	0.86
B304	0.4	0.55
B304r	-0.05	0.45
B305	1.04	0.77
B306	1.08	1.02
B306r	-0.13	1.07
B324	0.98	0.83
B325	0.98	0.92
B329	1.08	1.08

Table 3. Pecent organic carbon and calcium carbonate (con't).

Station ID	% Organic C	% CaCO3
B330	0.98	0.92
B331	1.12	1
B332	1.08	1
B333	0.66	0.92
B334	0.35	0.25
B335	0.22	0.17
B336	0.19	0.08
B337	0.19	0.17
B339	0.21	0.25
B342	0.43	0.33
B344	0.61	0.5
B346	0.89	0.67
B347	0.94	0.67
B348	0.19	0.08
B350	0.25	0.17
B351	1.27	1.17

APPENDIX A

GEOTEK Whole Core Logger
Physical Property Logs

MONTEREY BAY NATIONAL MARINE SANCTUARY

P2-95-MB

PHYSICAL PROPERTY LOGS - Fort Ord Study Area

B324 (0-54 cm)

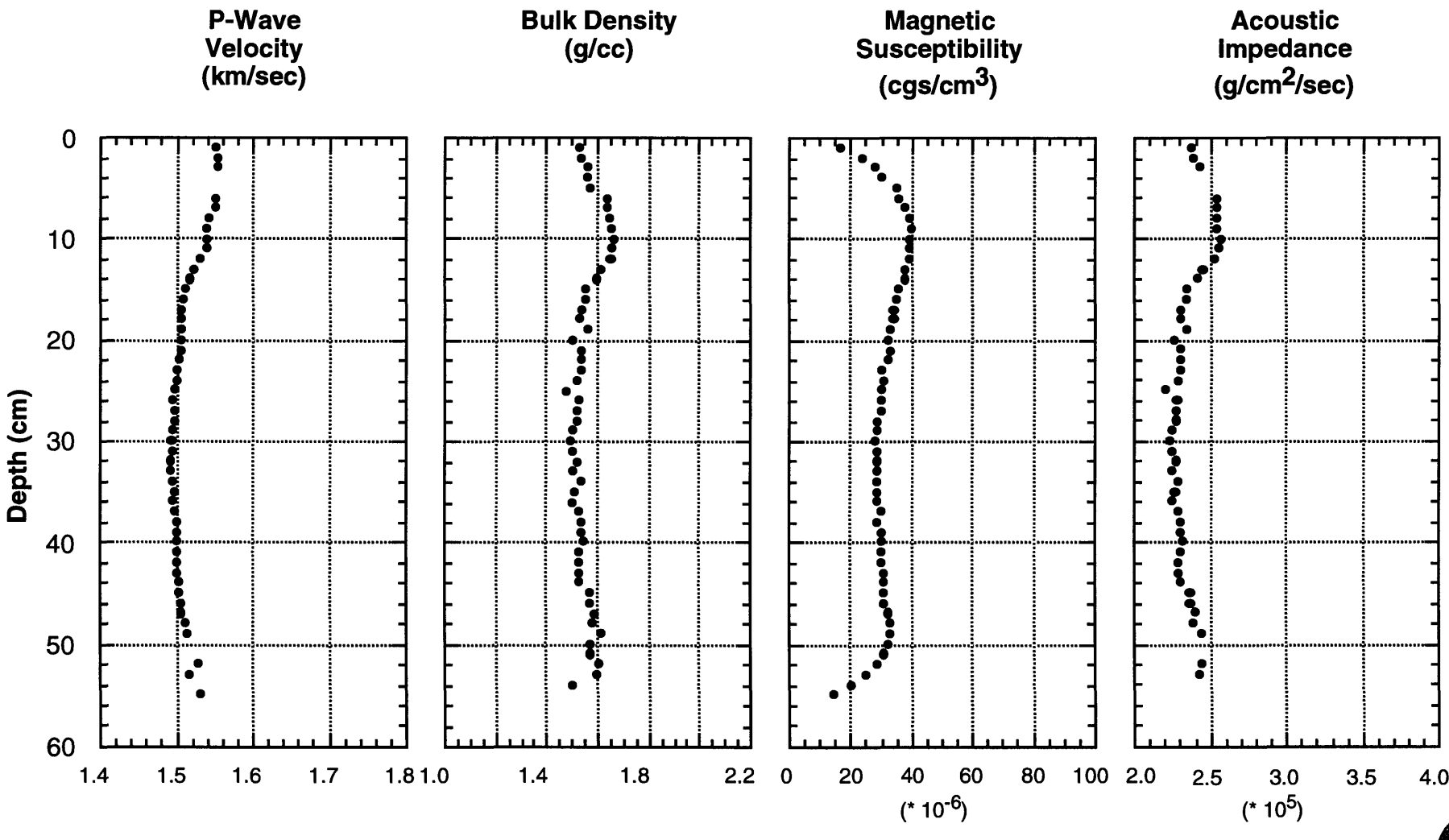

LAT: 36.7328° N
LON: 121.8985° W

Location: Center of mid-shelf mud belt
Depth: 92 meters

USGS

MONTEREY BAY NATIONAL MARINE SANCTUARY

P2-95-MB

PHYSICAL PROPERTY LOGS - Fort Ord Study Area

B325 (0-52 cm)

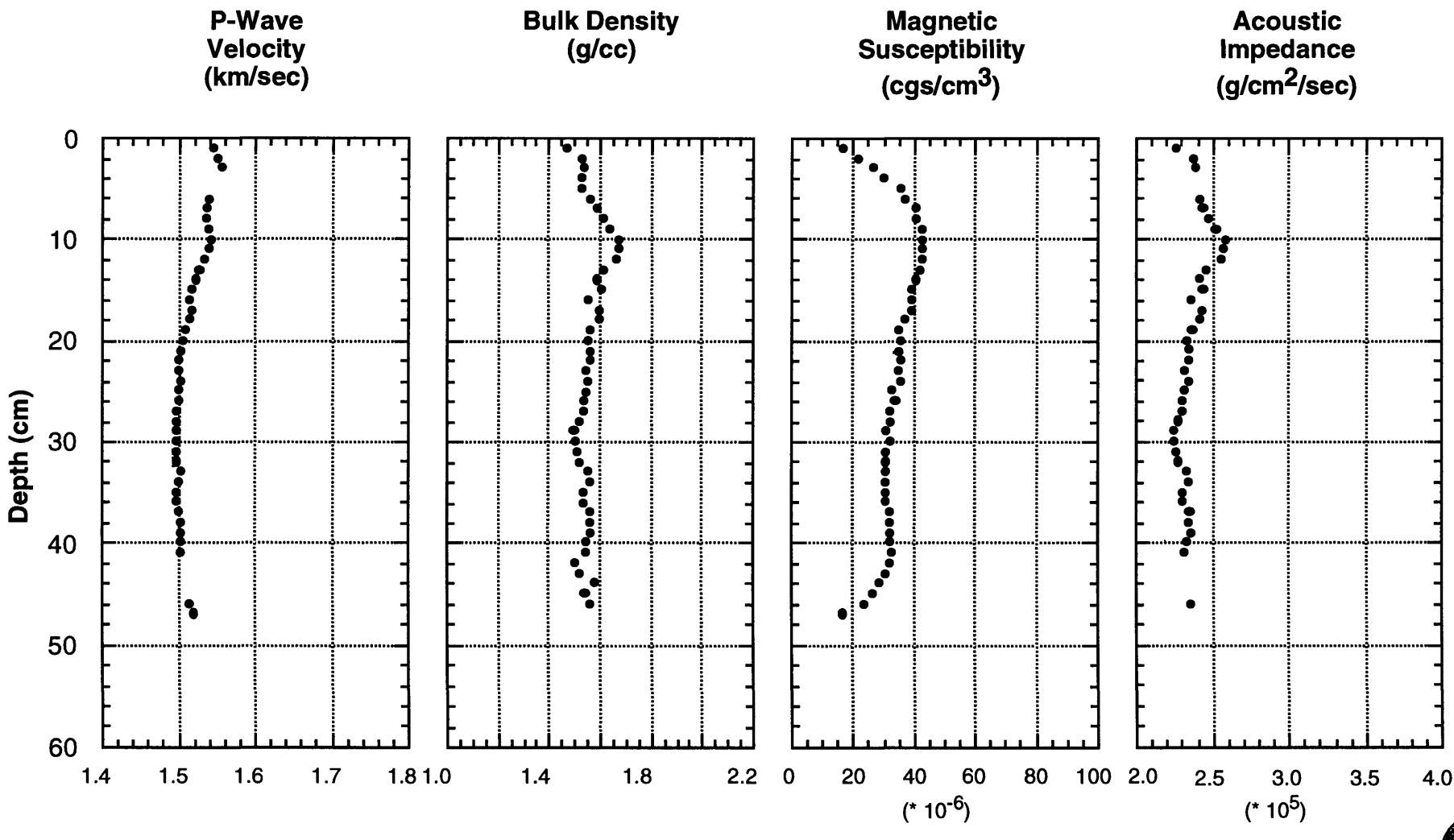

LAT: 36.7237° N
LON: 121.9017° W

Location: Center of mid-shelf mud belt
Depth: 88 meters

USGS

MONTEREY BAY NATIONAL MARINE SANCTUARY

P2-95-MB

PHYSICAL PROPERTY LOGS - Fort Ord Study Area

B329 (0-49 cm)

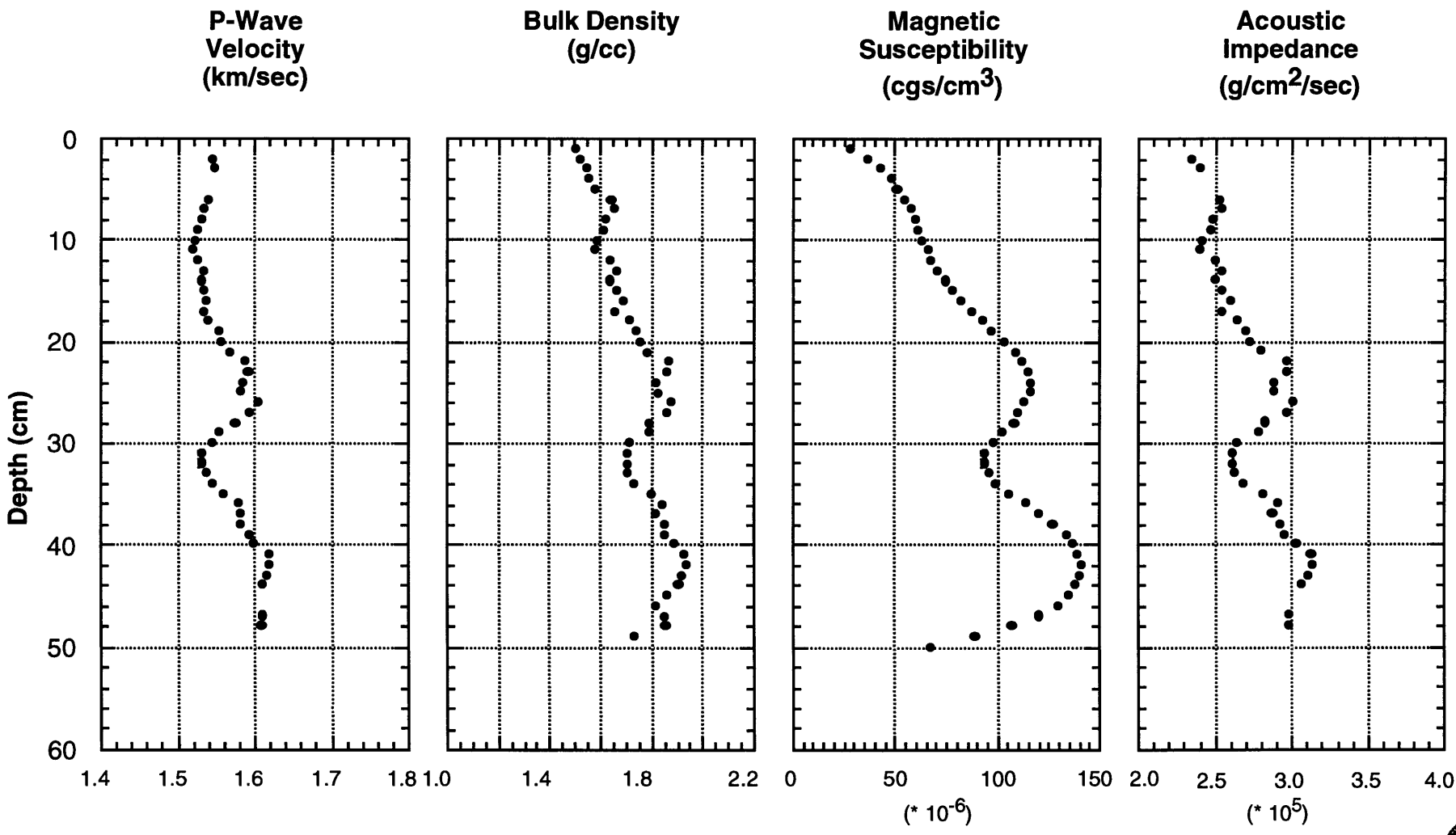

LAT: 36.7113° N
LON: 121.9372° W

Location: Western edge of mid-shelf mud belt
Depth: 105 meters

USGS

MONTEREY BAY NATIONAL MARINE SANCTUARY

P2-95-MB

PHYSICAL PROPERTY LOGS - Fort Ord Study Area

B330 (0-50 cm)

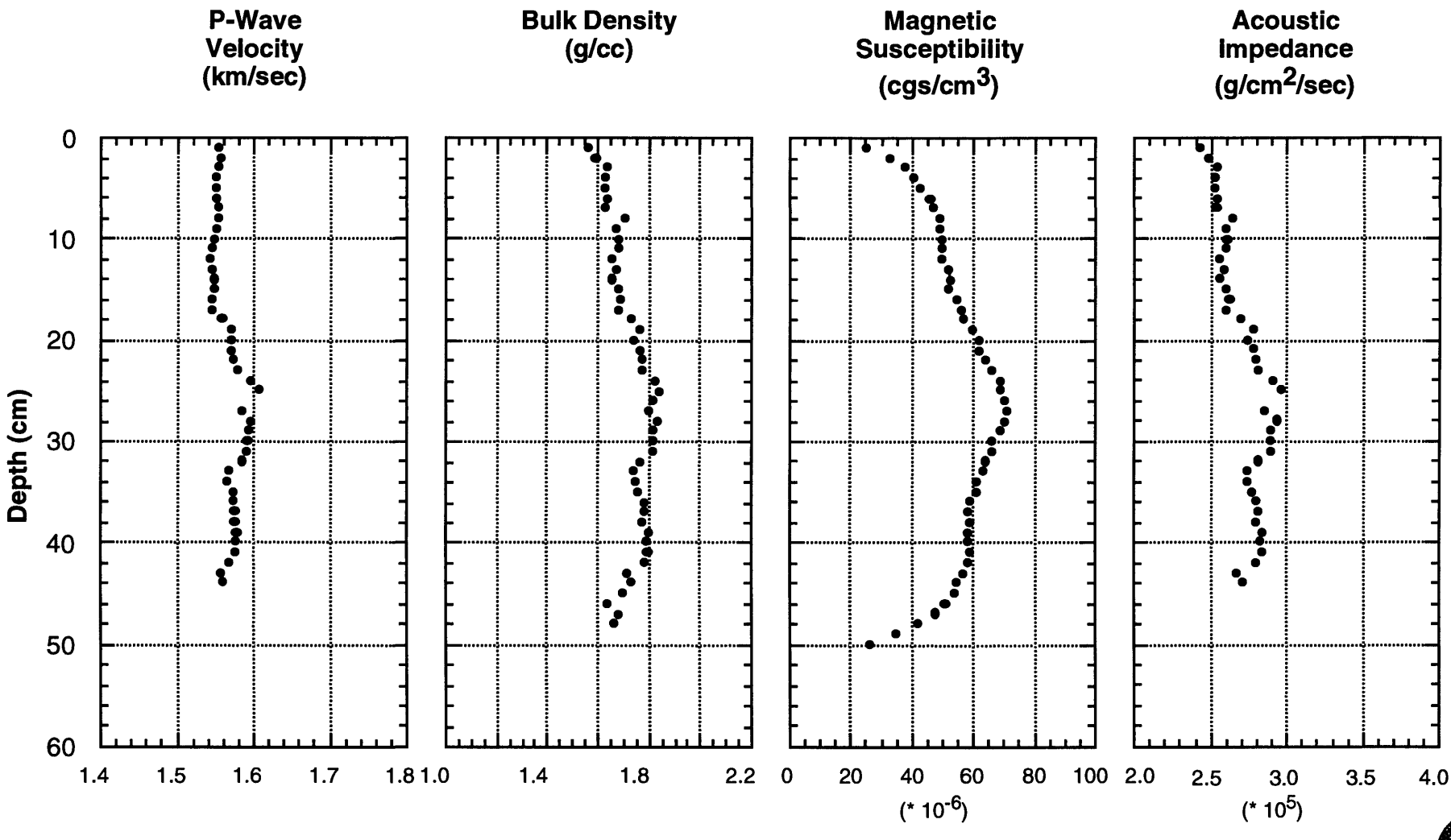

LAT: 36.6965° N **Location: Mid-shelf mud belt**

LON: 121.9228° W **Depth: 98 meters**

USGS

MONTEREY BAY NATIONAL MARINE SANCTUARY

P2-95-MB

PHYSICAL PROPERTY LOGS - Fort Ord Study Area

B331 (0-57 cm)

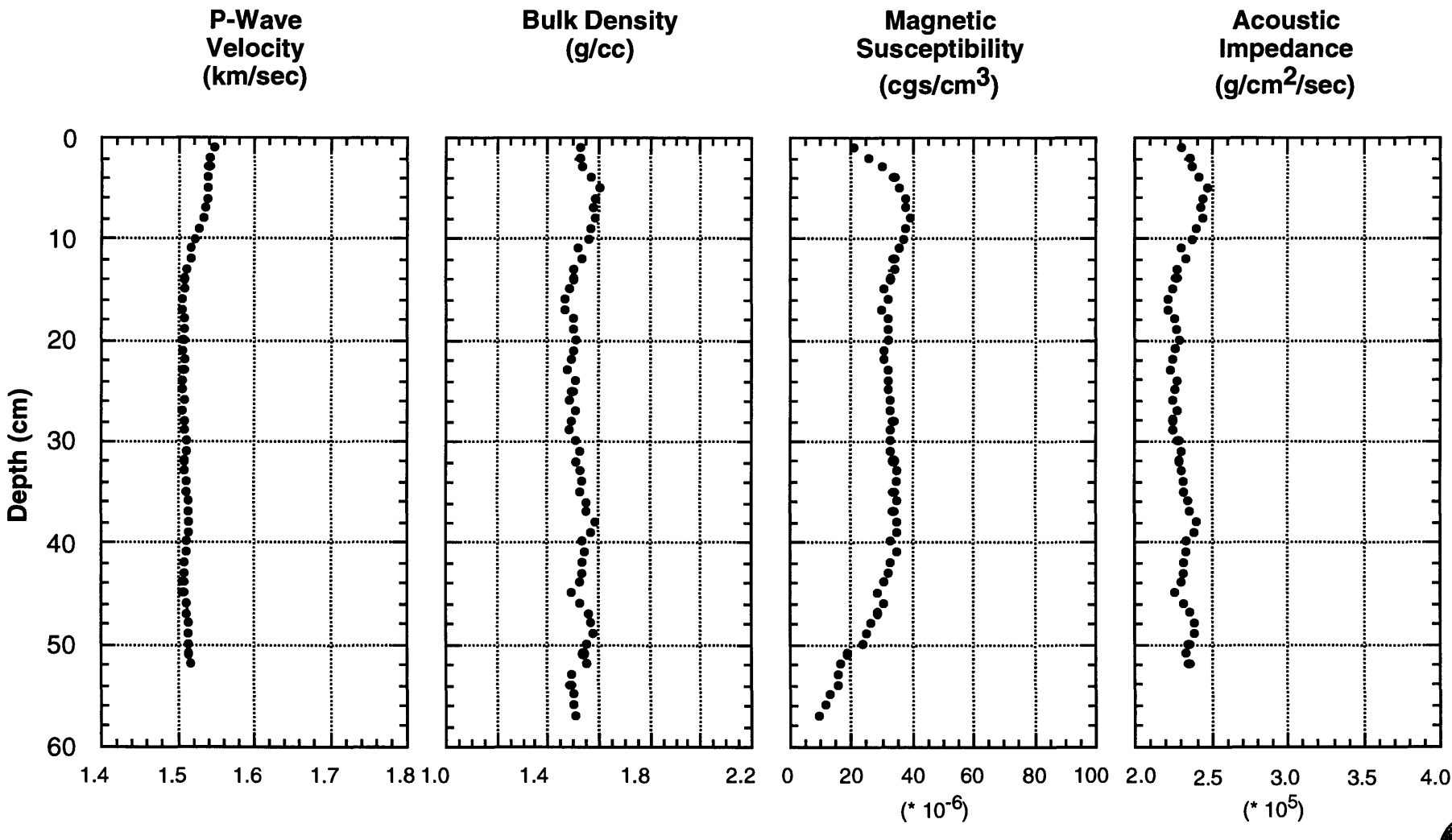

LAT: 36.7080° N
LON: 121.9197° W

Location: Center of mid-shelf mud belt
Depth: 95 meters

USGS

MONTEREY BAY NATIONAL MARINE SANCTUARY

P2-95-MB

PHYSICAL PROPERTY LOGS - Fort Ord Study Area

B332 (0-54 cm)

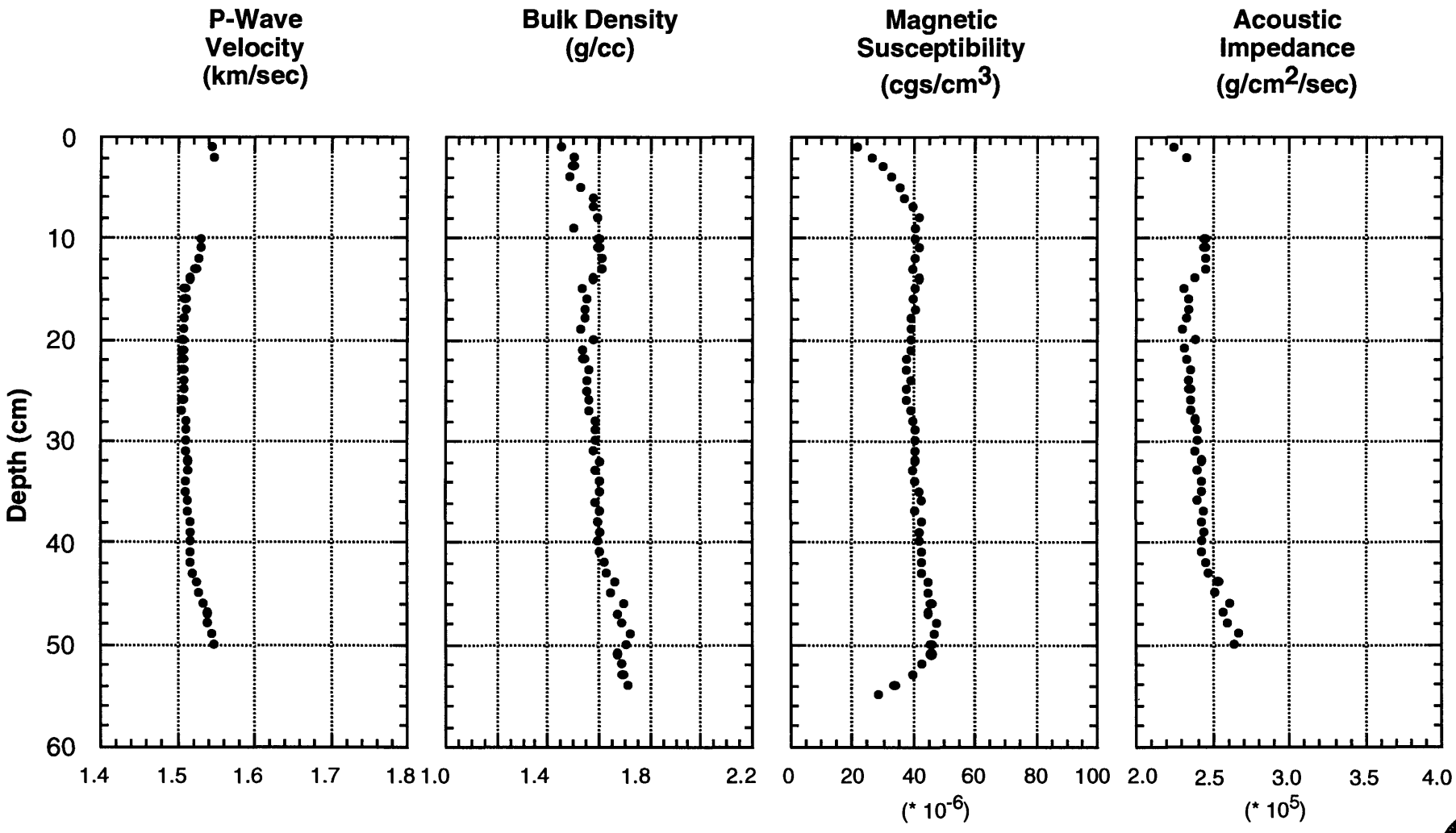

LAT: 36.7018° N **Location: Mid-shelf mud belt**

LON: 121.9045° W **Depth: 92 meters**

USGS

MONTEREY BAY NATIONAL MARINE SANCTUARY

P2-95-MB

PHYSICAL PROPERTY LOGS - Fort Ord Study Area

B333 (0-43 cm)

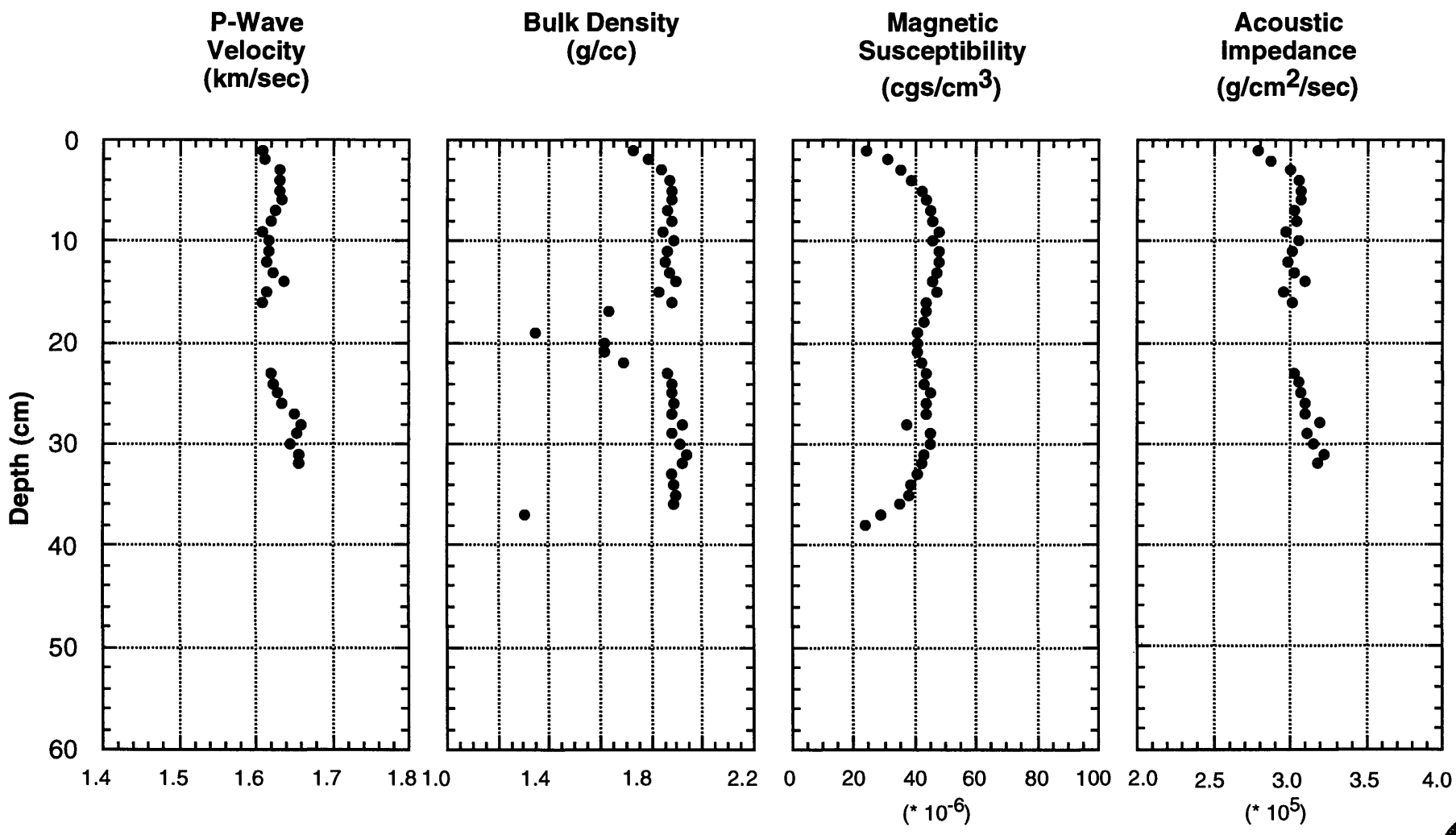

LAT: 36.6825° N
LON: 121.9105° W

Location: Southen edge of mid-shelf mud belt
Depth: 92 meters

USGS

MONTEREY BAY NATIONAL MARINE SANCTUARY

P2-95-MB

PHYSICAL PROPERTY LOGS - Fort Ord Study Area

B334 (0-37 cm)

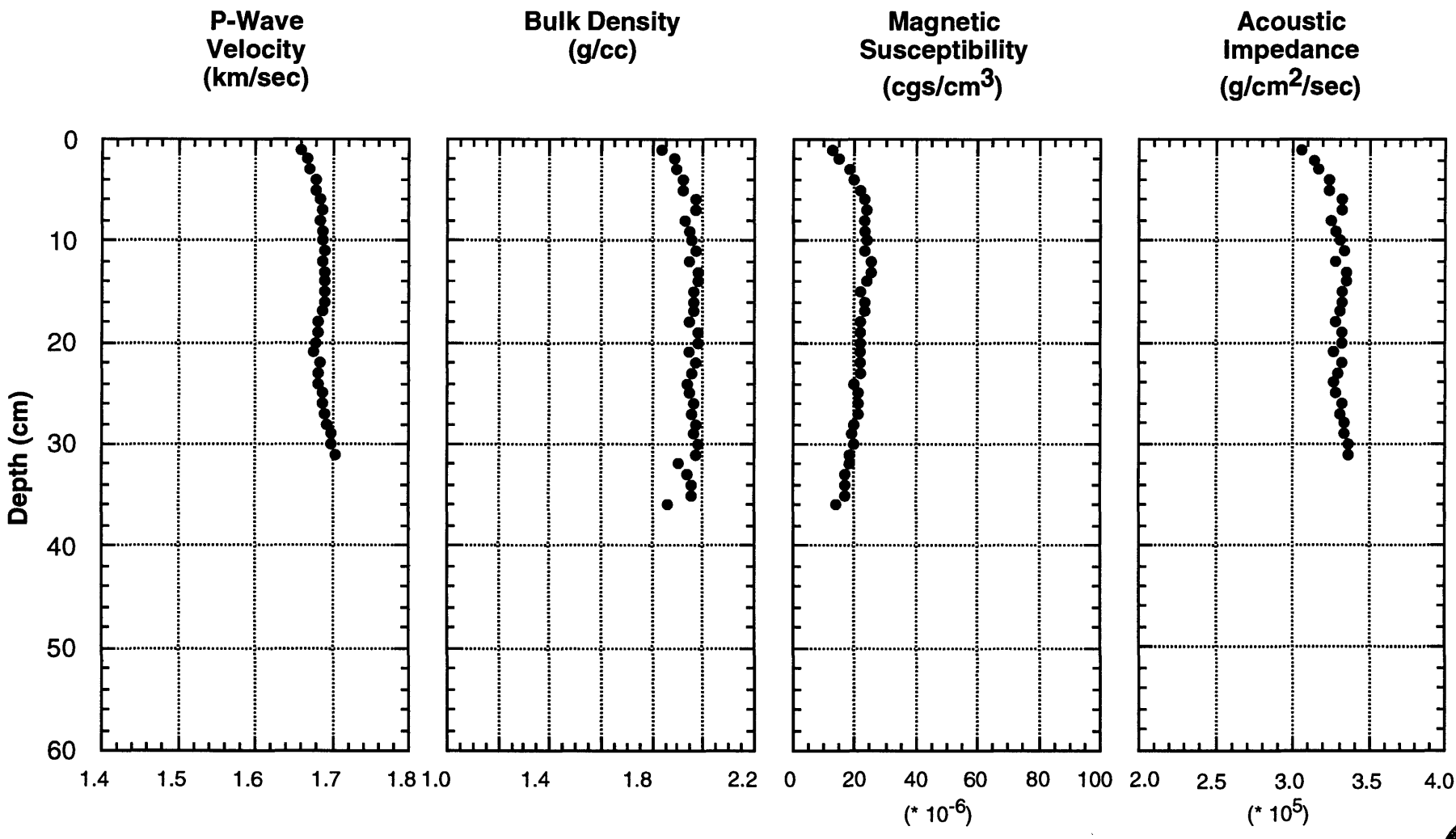

LAT: 36.6748° N
LON: 121.8842° W

Location: Eastern boundary of mid-shelf mud belt
Depth: 81 meters

USGS

MONTEREY BAY NATIONAL MARINE SANCTUARY

P2-95-MB

PHYSICAL PROPERTY LOGS - Fort Ord Study Area

B335 (0-30 cm)

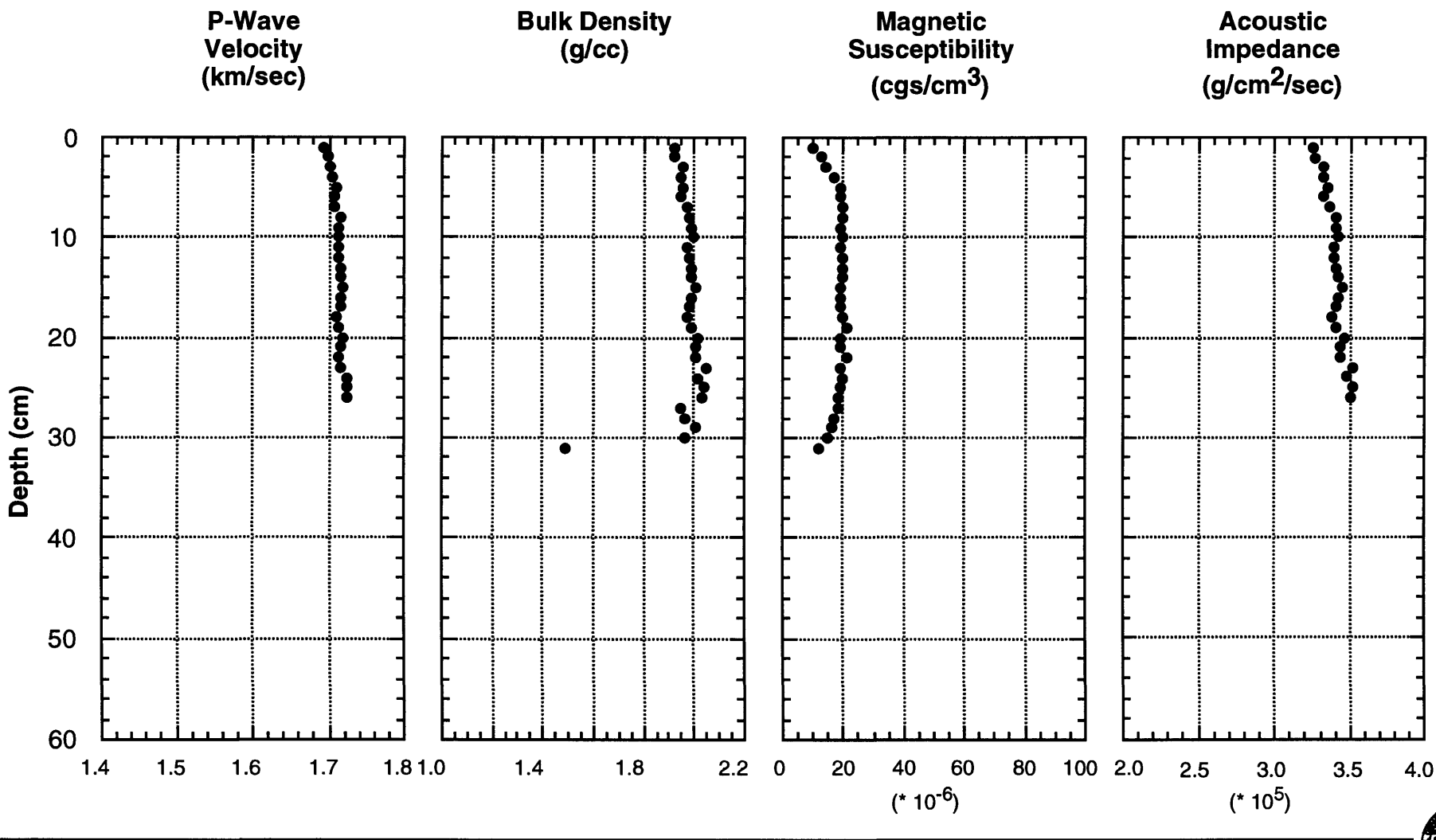

LAT: 36.6510° N
LON: 121.8630° W

Location: Nearshore sands offshore former Fort Ord
Depth: 57 meters

USGS

MONTEREY BAY NATIONAL MARINE SANCTUARY

P2-95-MB

PHYSICAL PROPERTY LOGS - Fort Ord Study Area

B336 (0-34 cm)

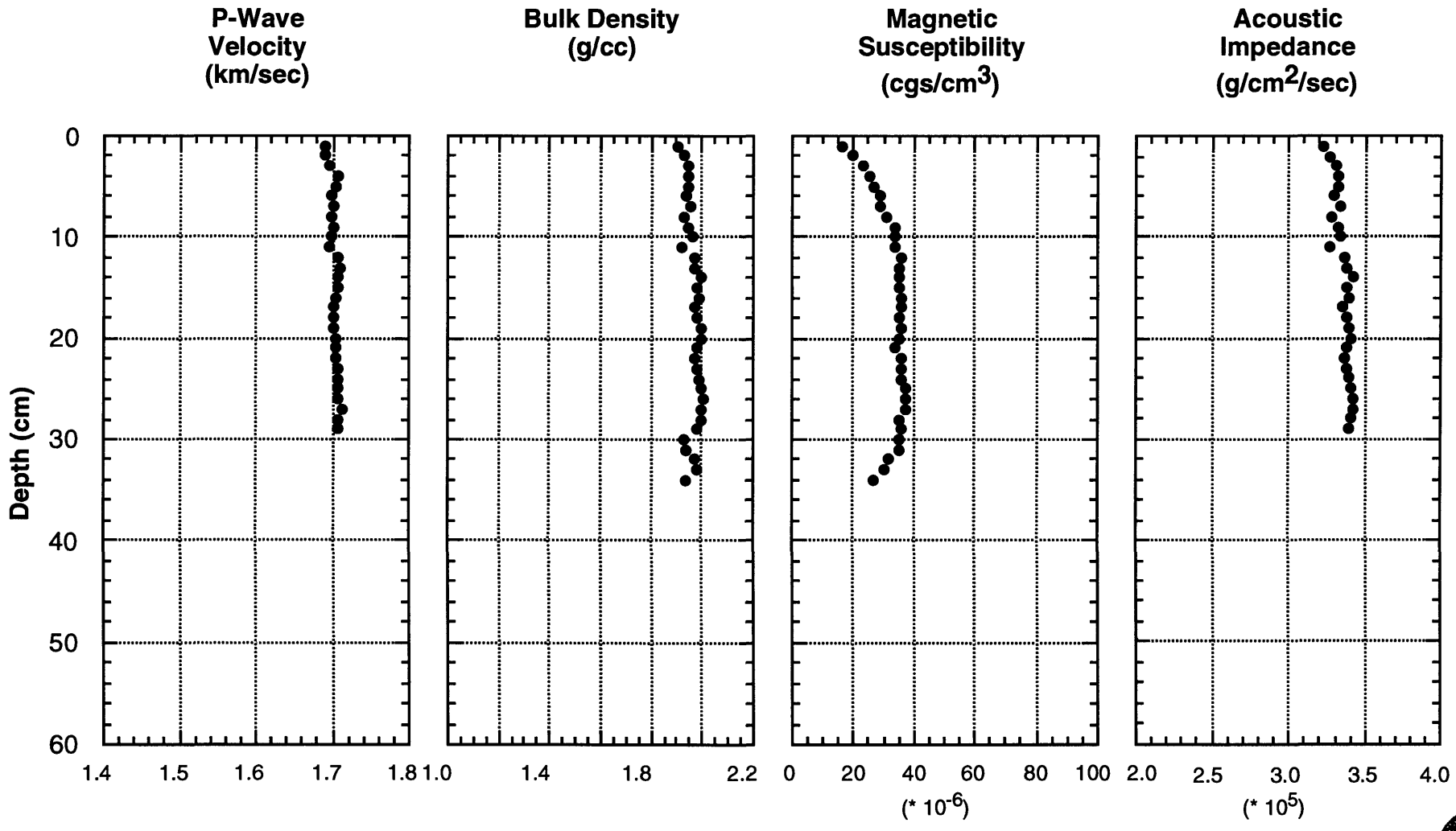

LAT: 36.6777° N
LON: 121.8445° W

Location: Nearshore sands offshore former Fort Ord
Depth: 52 meters

USGS

MONTEREY BAY NATIONAL MARINE SANCTUARY

P2-95-MB

PHYSICAL PROPERTY LOGS - Fort Ord Study Area

B337 (0-35 cm)

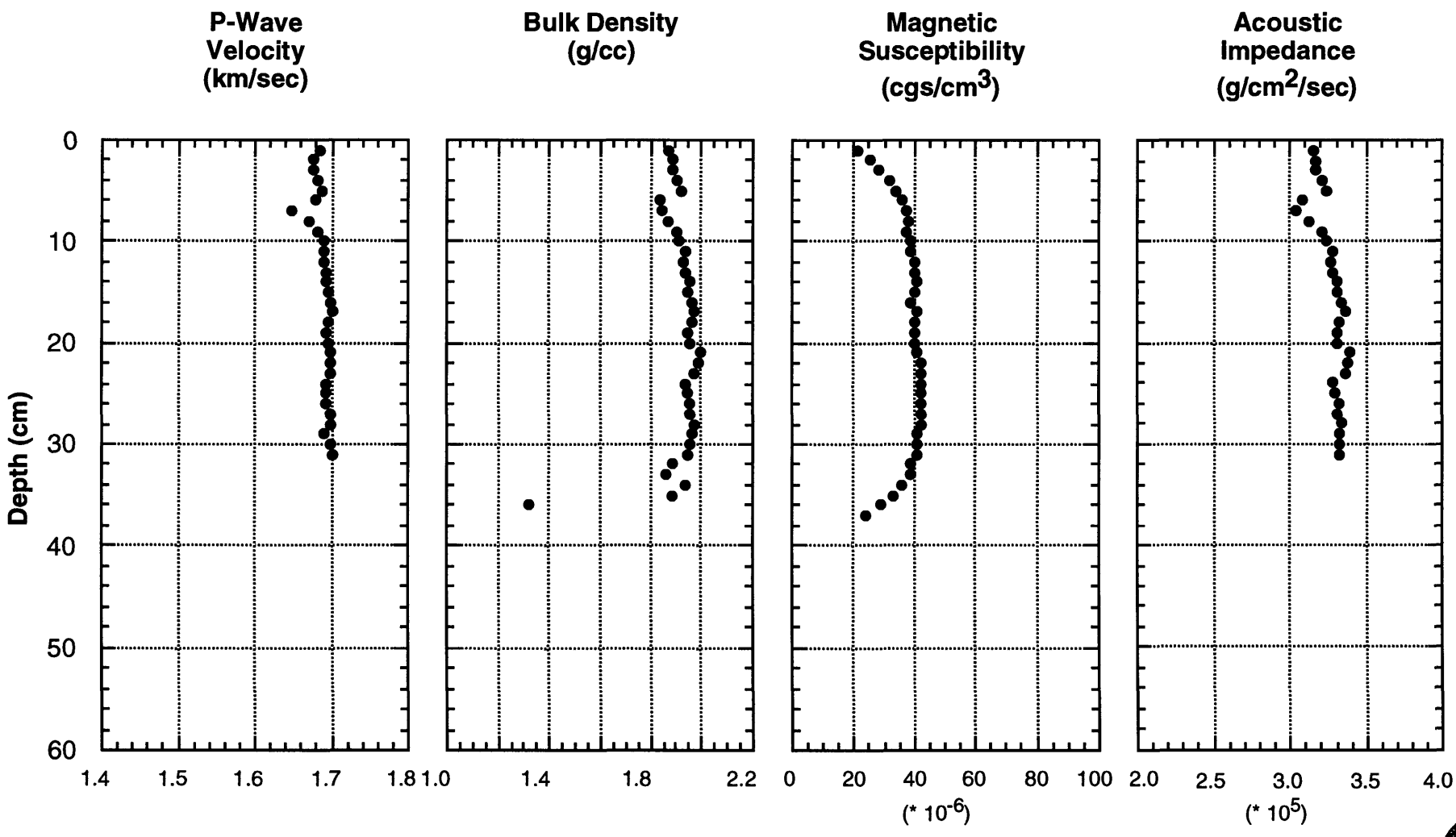

LAT: 36.6952° N
LON: 121.8333° W

Location: Nearshore sands offshore former Fort Ord
Depth: 43 meters

USGS

MONTEREY BAY NATIONAL MARINE SANCTUARY

P2-95-MB

PHYSICAL PROPERTY LOGS - Fort Ord Study Area

B339 (0-34 cm)

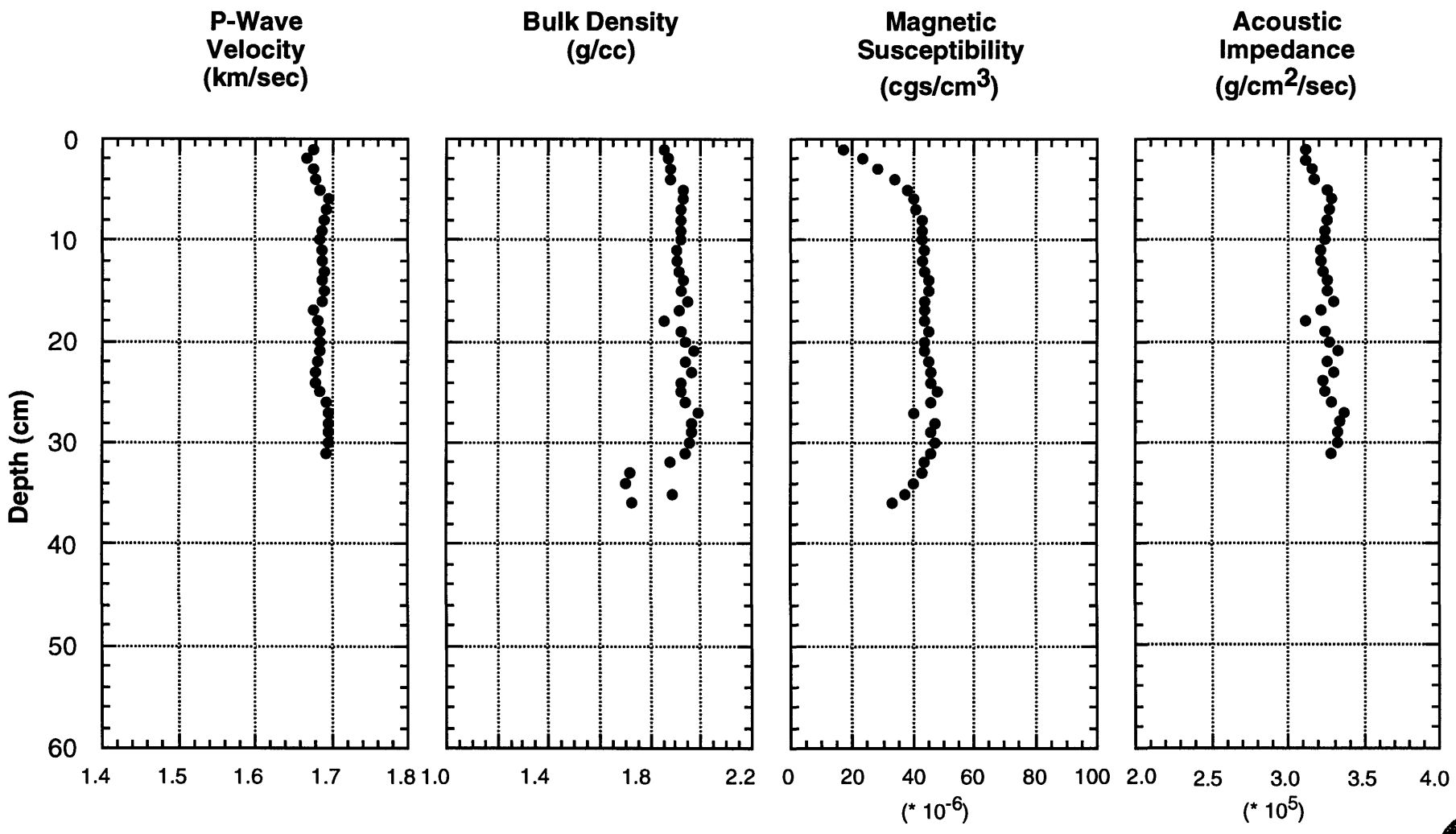

LAT: 36.7068° N
LON: 121.8248° W

Location: Nearshore sands south of Salinas River mouth
Depth: 40 meters

USGS

MONTEREY BAY NATIONAL MARINE SANCTUARY

P2-95-MB

PHYSICAL PROPERTY LOGS - Fort Ord Study Area

B342 (0-35 cm)

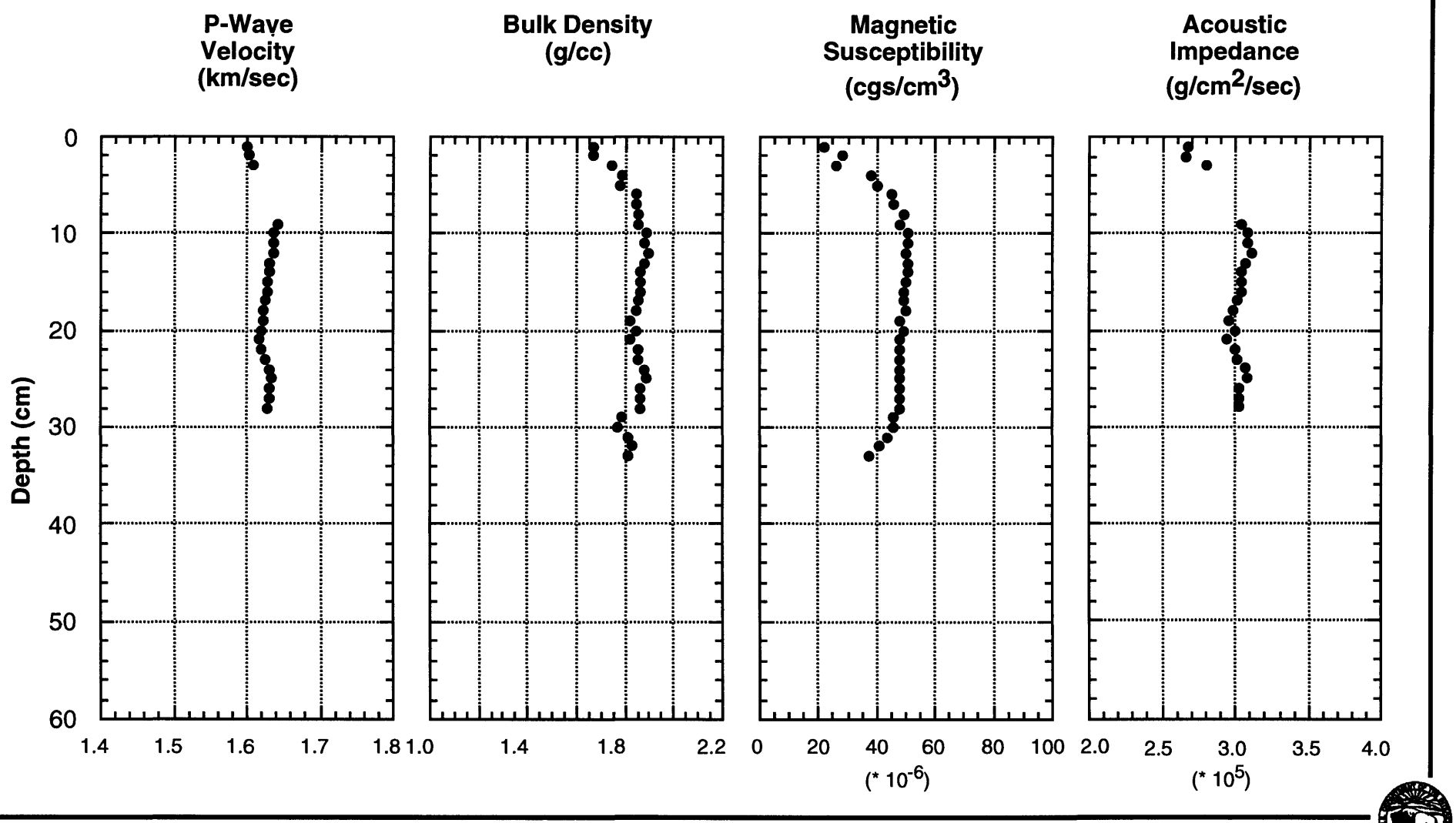

LAT: 36.6925° N
LON: 121.8502° W

Location: Eastern edge of mid-shelf mud belt
Depth: 62 meters

USGS

MONTEREY BAY NATIONAL MARINE SANCTUARY

P2-95-MB

PHYSICAL PROPERTY LOGS - Fort Ord Study Area

B344 (0-49 cm)

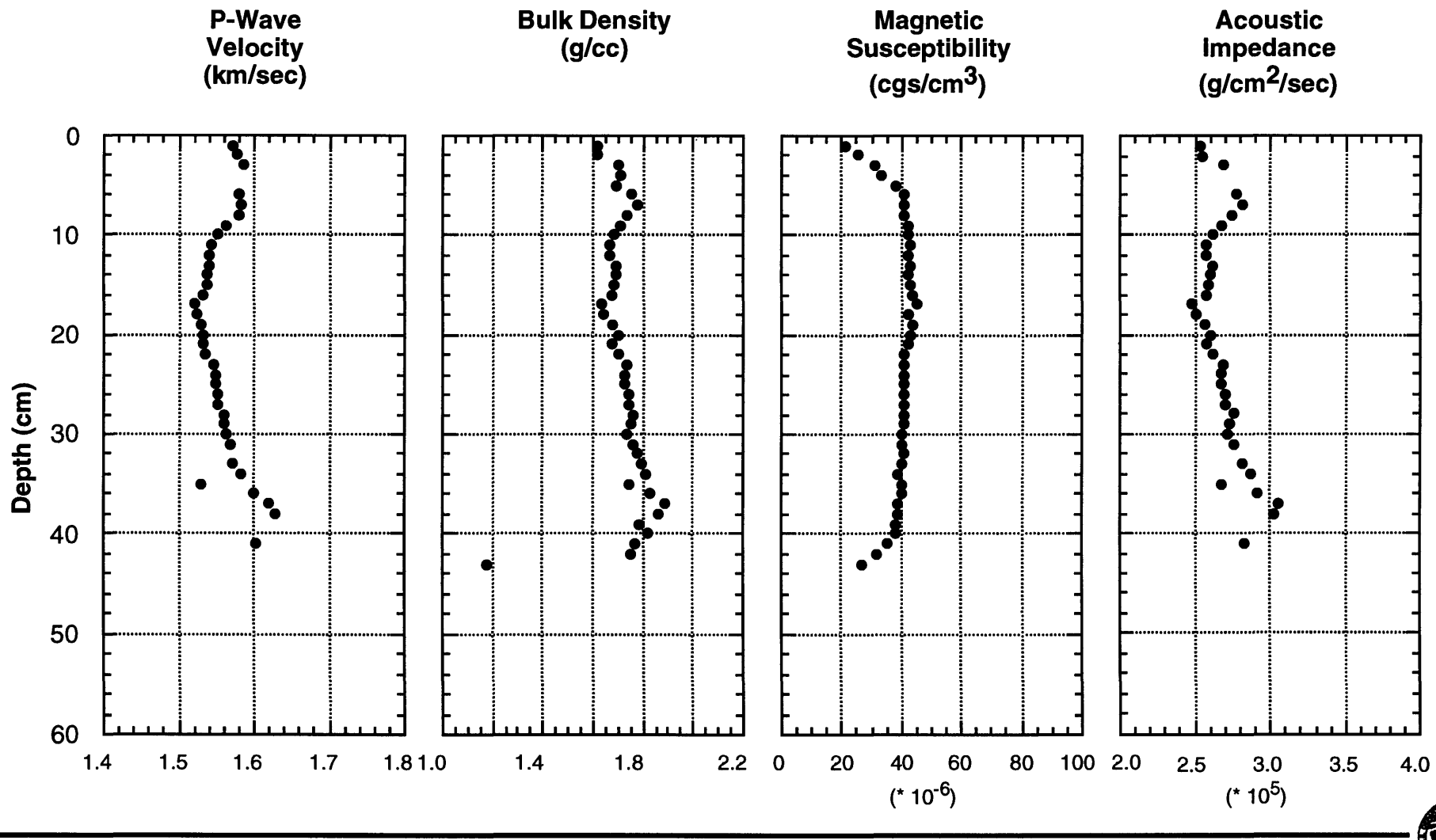

LAT: 36.6902° N
LON: 121.8715° W

Location: Eastern edge of mid-shelf mud belt
Depth: 78 meters

USGS

MONTEREY BAY NATIONAL MARINE SANCTUARY

P2-95-MB

PHYSICAL PROPERTY LOGS - Fort Ord Study Area

B346 (0-49 cm)

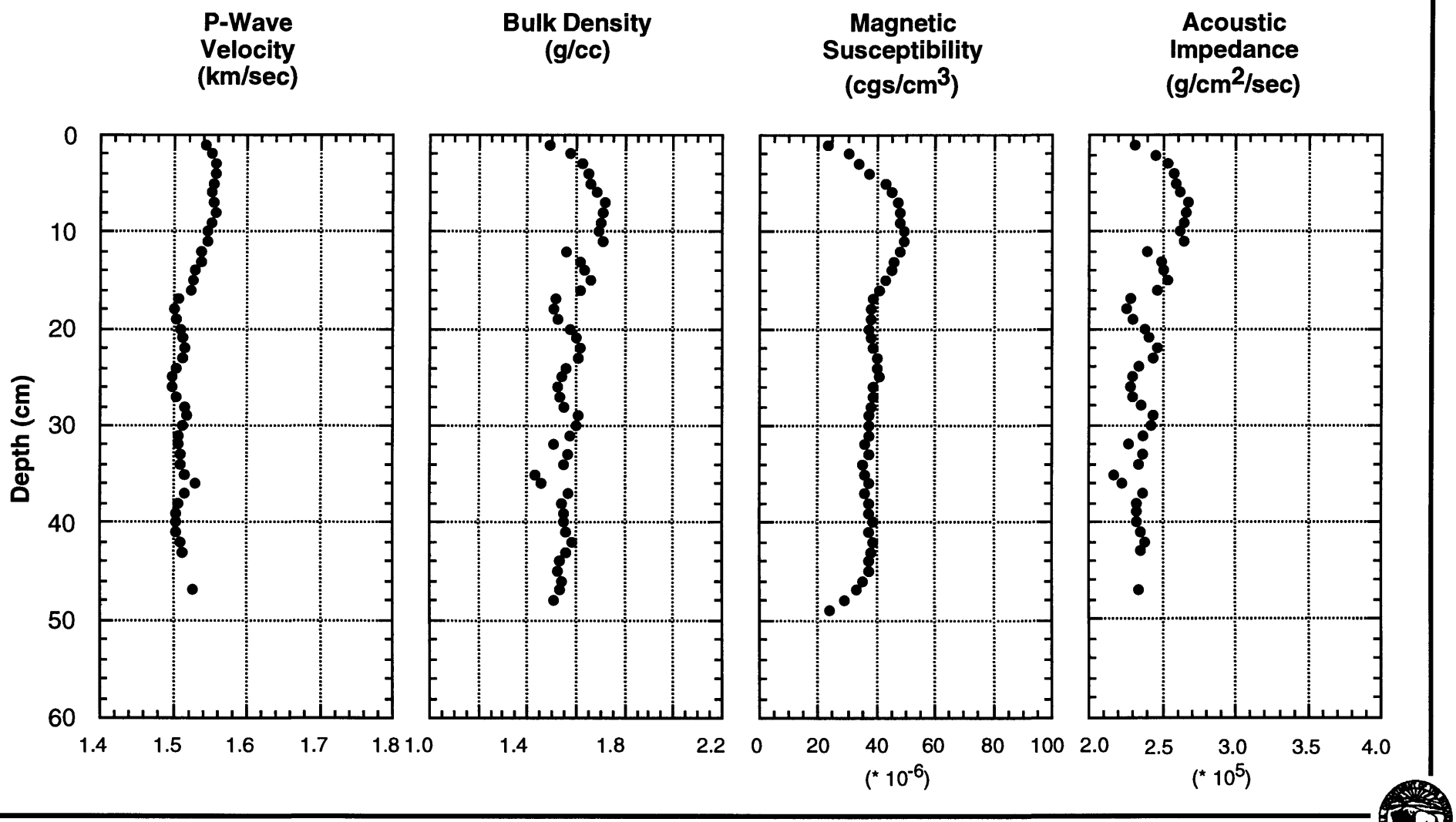

LAT: 36.7100° N **Location: Mid-shelf mud belt**

LON: 121.8798° W **Depth: 82 meters**

USGS

MONTEREY BAY NATIONAL MARINE SANCTUARY

P2-95-MB

PHYSICAL PROPERTY LOGS - Fort Ord Study Area

B347 (0-48 cm)

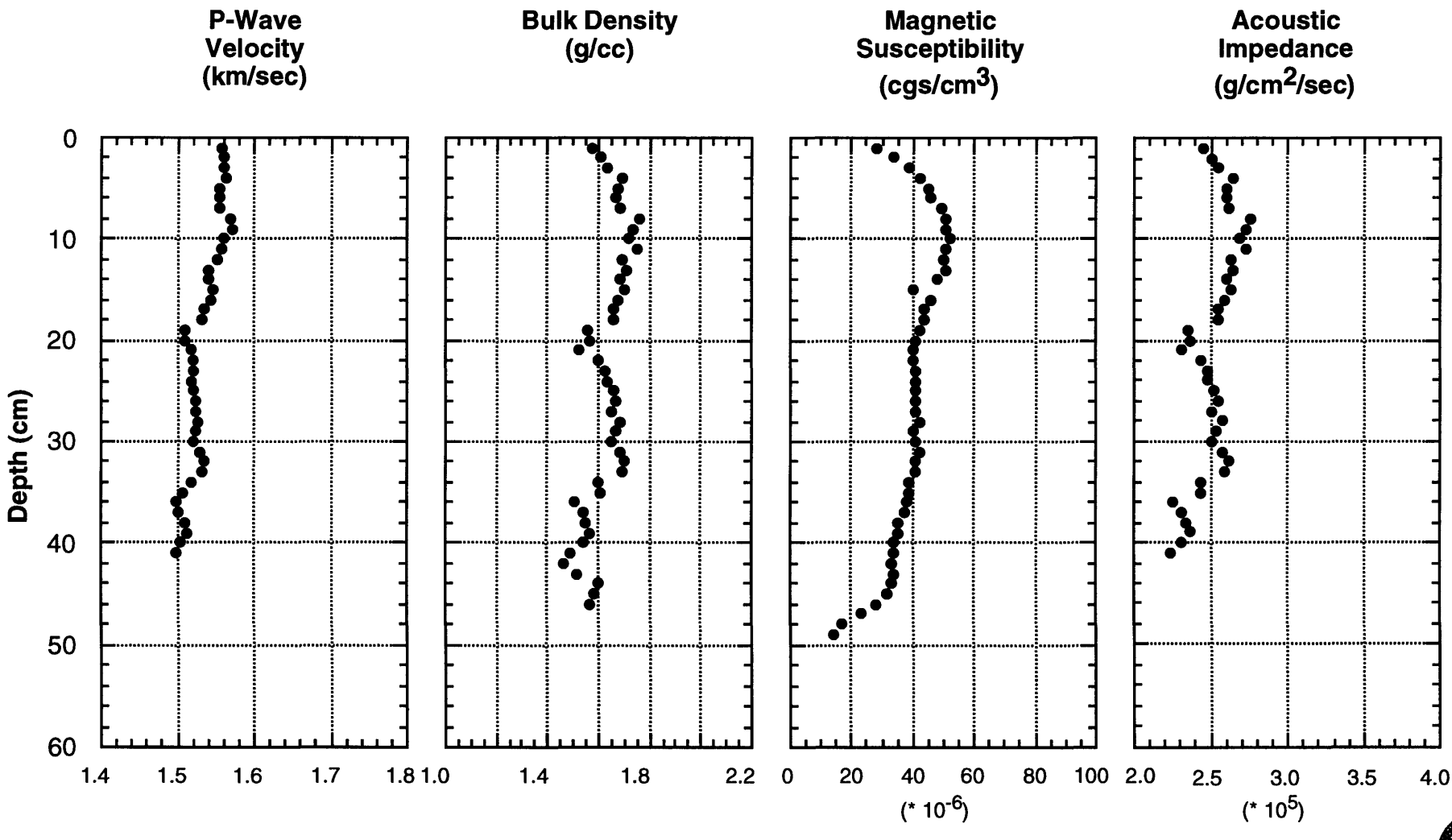

LAT: 36.7150° N
LON: 121.8750° W

Location: Mid-shelf mud belt
Depth: 77 meters

USGS

MONTEREY BAY NATIONAL MARINE SANCTUARY

P2-95-MB

PHYSICAL PROPERTY LOGS - Fort Ord Study Area

B350 (0-36 cm)

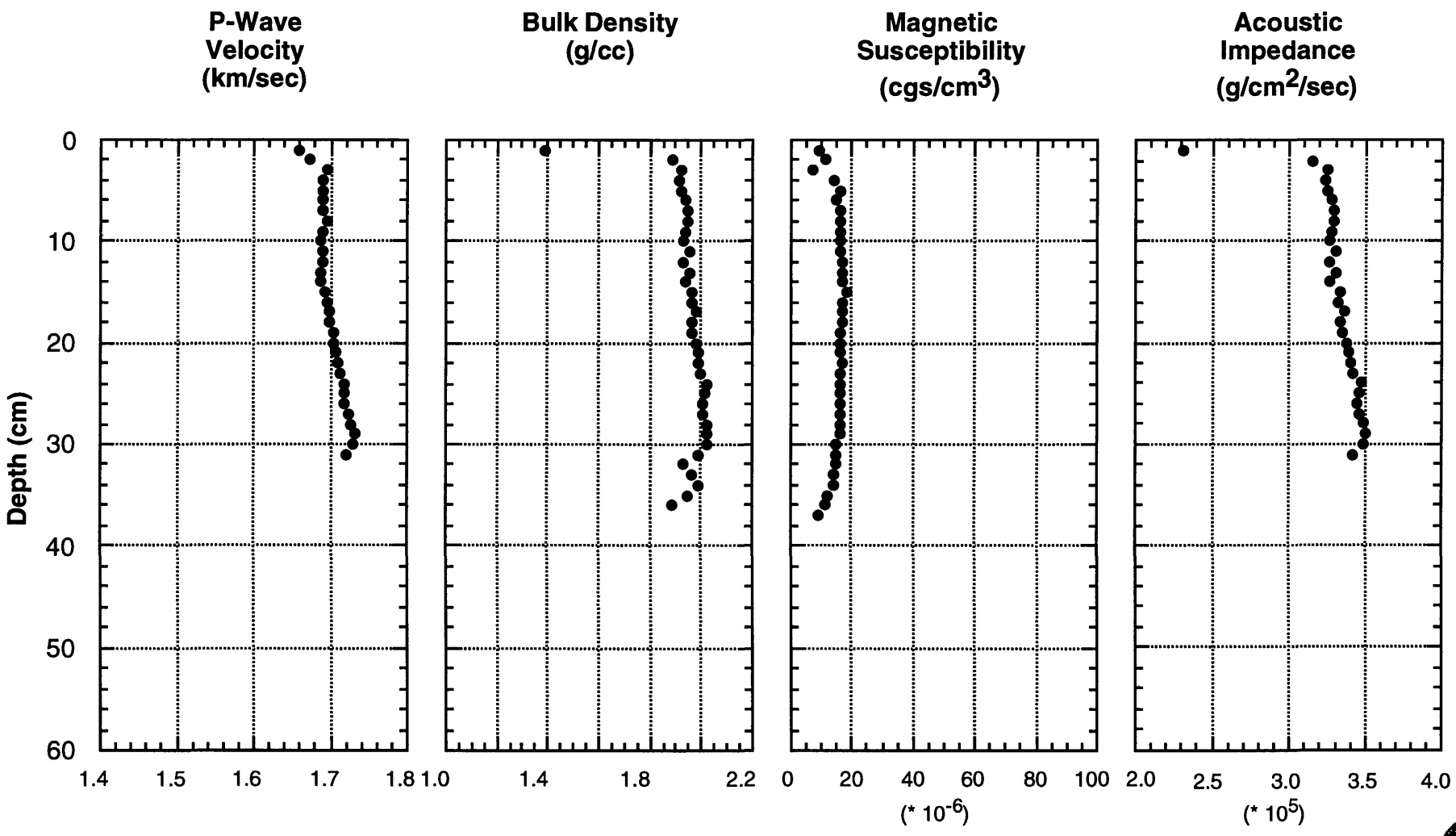

LAT: 36.6572° N
LON: 121.8840° W

Location: Nearshore sands offshore former Fort Ord
Depth: 75 meters

USGS

MONTEREY BAY NATIONAL MARINE SANCTUARY

P2-95-MB

PHYSICAL PROPERTY LOGS - Fort Ord Study Area

B351 (0-46 cm)

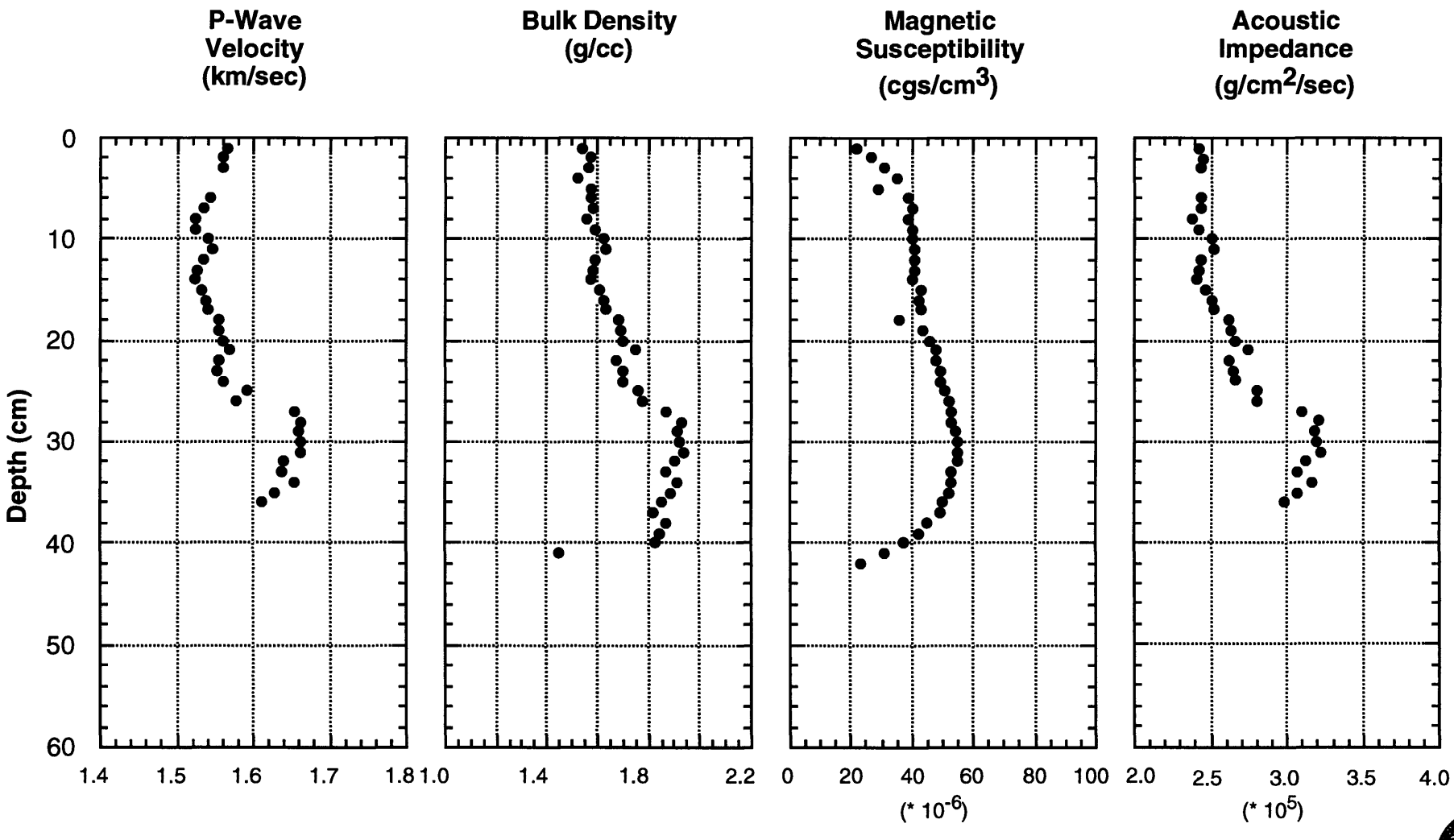

LAT: 36.7460° N
LON: 121.9100° W

Location: Mid-shelf mud belt near Monterey Canyon
Depth: 99 meters

USGS

Distribution and Concentration of Selected Contaminants in Monterey Bay Sediments

Mark Stephenson, Gary Ichikawa, Jon Goetzl, Kim Paulson and Mark Pranger
CA Department of Fish and Game, Moss Landing Marine Laboratories, Moss Landing CA 95039

Russell Fairey and Stewart Lamerdin
Moss Landing Marine Laboratories, Moss Landing CA 95039

Ronald Tjeerdema, John Newman, Johnathon Becker and Matthew Stoetling
University of California Santa Cruz, Santa Cruz, CA 95065

ABSTRACT

The presence/absence of contamination in sediments directly off the coast of Fort Ord, California was investigated in this study. Twenty sediment samples were collected in 1995 from Monterey Bay for this assessment. Lead concentrations ranged from 7.3 to 13.4 ppm and was highest in the two samples closest to Fort Ord but the identity of the source needs to be investigated further in order to distinguish lead from Fort Ord from lead smelter waste known to exist in Monterey Harbor. DDT concentrations ranged from non detected to 23.5 ppb and was highest offshore of the Salinas and Pajaro Rivers. PAHs and most metals were found in the fine grained sediments furthest offshore. A relatively small number of samples exceeded sediment quality guidelines (ERMs, ERLs, PELs, TELs). It is unlikely that the current DDT values reported from Monterey Bay are at levels that would cause an ecotoxicological effect.

INTRODUCTION

The US Army Corp of Engineers commissioned several studies offshore of Fort Ord in order to demonstrate the presence/absence of dump sites and/or contamination resulting from discharges from the base through storm drains, firing range activities, or base sewage disposal outfalls. This study was commissioned to investigate possible contamination of sediments near the area offshore of Fort Ord. The overall objectives of this study were to:

1. Determine the distribution of sediment contaminants in Monterey Bay
2. Evaluate the contaminant distribution to determine if there is an association between contaminants and Fort Ord activities

METHODS

Field and laboratory work was accomplished by staff of the San Jose State University Foundation at the Moss Landing Marine Laboratories, Moss Landing, CA (MLML). Trace metals analyses were performed by California Department of Fish and Game (CDFG) personnel at the trace metal facility at Moss Landing Marine Laboratories. Synthetic organic pesticides, polycyclic aromatic hydrocarbons (PAHs), and polychlorinated biphenyls (PCBs) were analyzed at the University of California at Santa Cruz's (UCSC) trace organics analytical facility located at Long Marine Laboratory.

Sampling Design

The samples were collected during two cruises on the RVs McArthur and Pt. Sur. The stations near Fort Ord were sampled in September 1995 (station numbers > B300, Figure 1) and the stations more distant from Fort Ord were sampled in April 1995 (station numbers < B300). The sampling stations were a subset of the stations collected for sedimentary characteristics by the U.S. Geological Survey (see also Edwards et al., this volume). Stations were selected based on the following criteria:

Figure 1. Station locations for Monterey Bay DOD sediment Study

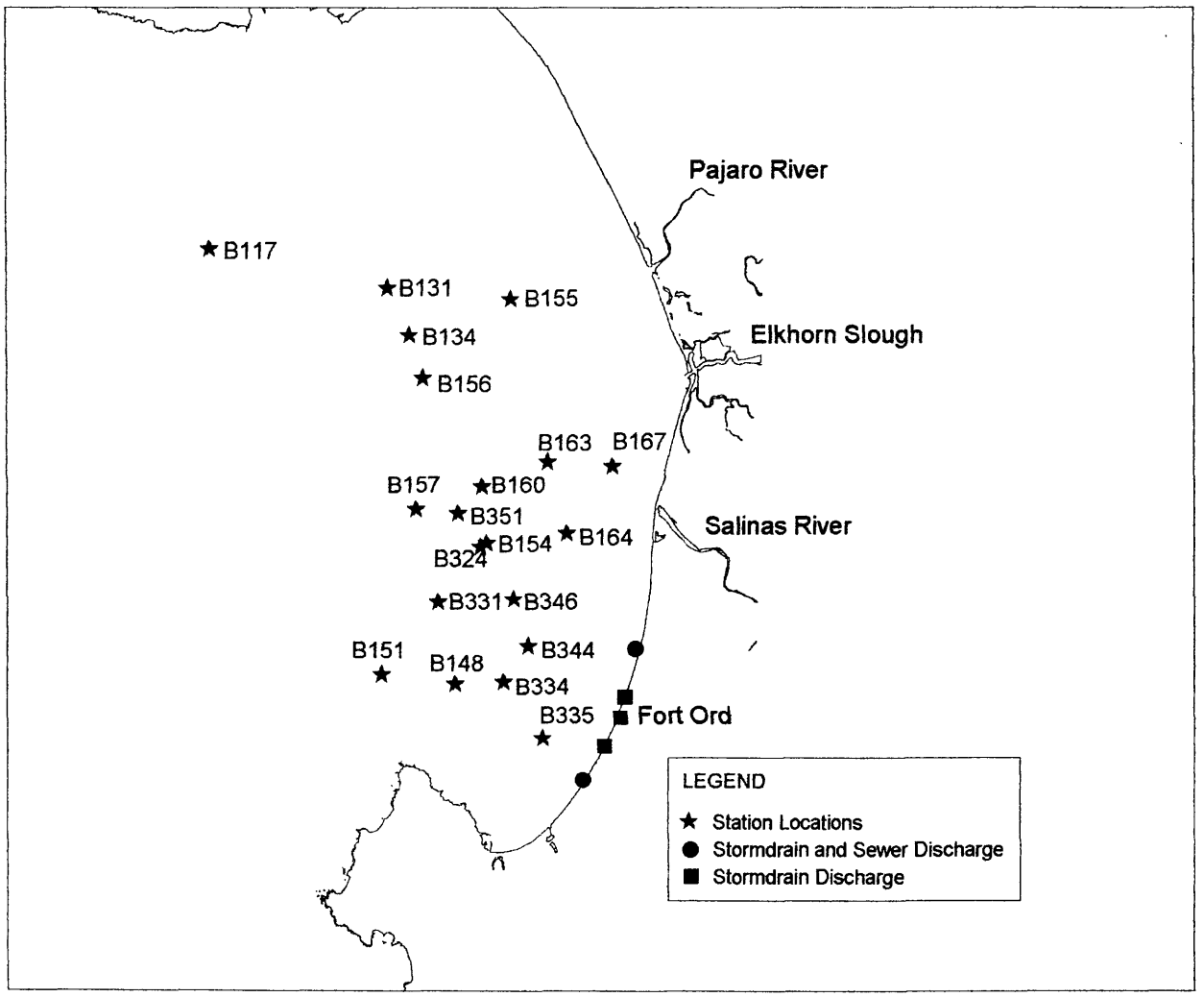

Ord); many of the sediments were to be collected offshore of Fort Ord; sediments were to be collected both in the southern and northern parts of the bay; and sediments were to be collected near the mouth of the Salinas River.

Sample Collection and Processing

Summary of Methods

Specific techniques used for collecting and processing samples are described in this section. Because collection of sediments influences the results of all subsequent laboratory and data analyses, it was important that samples be collected in a consistent and conventionally acceptable manner. Field and laboratory technicians were trained to conduct a wide variety of activities using standardized protocols to ensure comparability in sample collection among crews and across geographic areas. Sampling protocols in the field followed the accepted procedures of EPA's Environmental Monitoring and Assessment Program (EMAP), NOAA's National Status and Trends Program (NS&T), and American Society for Testing Materials (ASTM), and included methods to avoid cross-contamination; methods to avoid contamination by the sampling activities, crew, and vessel; collection of representative samples of the target surficial sediments; careful temperature control, homogenization and subsampling; and chain of custody procedures.

Cleaning Procedures

All sampling equipment (*i.e.*, cores, containers, container liners, scoops, etc.) was made from non-contaminating materials and was precleaned and packaged protectively prior to entering the field. Sample collection gear and samples were handled only by personnel wearing non-contaminating polyethylene gloves. All sample collection equipment (excluding the sediment grab) was cleaned using the following sequential process:

> Two-day soak and wash in Micro® detergent, three tap-water rinses, three deionized water rinses, a three-day soak in 10% HCl, three ASTM Type II Milli-Q® water rinses, air dry, three petroleum ether rinses, and air dry.

All cleaning, after the Micro® detergent step, was performed in a positive pressure "clean" room to prevent airborne contaminants from contacting sample collection equipment. Air supplied to the clean room was filtered.

Plastic containers (high density polyethylene, HDPE) for trace metal analysis media (sediment, archive sediment, and pore water) were cleaned by: a two-day Micro® detergent soak, three tap-water rinses, three deionized water rinses, a three-day soak in 10% HCl or HNO_3, three Type II Milli-Q® water rinses, and air dry.

Glass containers for total organic carbon (TOC), grain size or synthetic organic analysis media (sediment, archive sediment, pore water, and subsurface water) and additional teflon sheeting cap-liners were cleaned by: a two-day Micro® detergent soak, three tap-water rinses, three deionized water rinses, a three-day soak in 10% HCl or HNO_3, three Type II Milli-Q® water rinses, air dry, three petroleum ether rinses, and air dry.

Sediment Sample Collection

Samples were collected during two cruises (4/95 and 9/95) aboard the research vessels McArthur and Point Sur. All sampling locations (latitude & longitude), whether altered in the field or predetermined, were verified using a differential-corrected global positioning system (GPS) provided by the research vessel, and recorded in the field logbook. The method of sediment collection was a box core with a 20 by 30 centimeter stainless steel box provided by the United States Geological Survey. The core was deployed off the stern of each of the research vessels. After the filled box core was secured on deck, the research vessel was moved perpendicular to the current wind direction to ensure any exhaust form the ships engines was not contaminating the sediment sample. The following acceptability criteria were met prior to taking sediment samples:

1. Grab sampler was not over-filled (*i.e.*, the sediment surface was not pressed against the top of the box core).
2. Overlying water was present, indicating minimal leakage.
3. Overlying water was not excessively turbid, indicating minimal sample disturbance.
4. Sediment surface was relatively flat, indicating minimal sample disturbance.
5. Sediment sample was not washed out due to an obstruction in the box core.
6. Desired penetration depth was achieved.
7. Sample did not include excessive shell, organic or man-made debris.

If a sample did not meet all the above criteria, it was rejected and another sample was collected.

It was critical that sample contamination be avoided during sample collection. All sampling equipment (*i.e.*, cores, scoops, containers, etc.) was made of non-contaminating material and was cleaned appropriately before use. Field samplers were required to wear disposable polyethylene gloves at all times while processing samples. Before samples from the box core were taken, the overlying water was removed using a siphon hose, being careful to minimize disturbance or loss of fine-grained surficial sediment. Once overlying water was removed, the top two centimeters of surficial sediment was subsampled from the box core using a ten centimeter diameter polycarbonate core. Subsamples were extruded from the core with a precleaned plunger and "sliced" off using a precleaned polycarbonate spatula. Samples were placed in precleaned, prelabeled containers and stored at minus ten degrees celsius for the duration of the cruises. When subsampling surficial sediments, unrepresentative material (e.g., large stones or vegetative material) was removed from the sample in the field. Small rocks and other small foreign material remained in the sample. Determination of overall sample quality was determined by the chief scientist in the field and any removals were noted on the field data sheet. Field data sheets also included bottom depths, salinity, texture of the sediment, and general field observations.

Trace Metals Analysis of Sediments

Summary of Methods

Trace Metals analyses were conducted at the California Department of Fish and Game's (CDFG) Trace Metals Facility at Moss Landing, CA. These methods were modifications of those described by Evans and Hanson (1993) as well as those developed by the CDFG (California Department of Fish and Game,
1990).

Analytes and Detection Limits

Trace metals and their detection limits in sediments (µg/g, dry weight) are:

Aluminum	1.0	Antimony	0.1
Arsenic	0.1	Cadmium	0.01
Chromium	0.1	Copper	0.1
Iron	0.1	Lead	0.1
Manganese	0.05	Mercury	0.03
Nickel	0.1	Selenium	0.2
Silver	0.01	Tin	0.02
Tributyltin	0.013	Zinc	0.05

Sediment Digestion Procedures for all metals except for Se and As

One gram aliquot of sediment was placed in a pre-weighed Teflon vessel, and one ml concentrated 4:1 nitric:perchloric acid mixture was added. The vessel was capped and heated in a vented oven at 130^0 C for four hours. Three ml concentrated hydrofluoric acid were added to vessel, recapped and returned to oven overnight. Twenty ml of 2.5% boric acid were added to vessel and placed in oven for an additional 8 hours. Weights of vessel and solution were recorded, and solution was transferred to 30 ml polyethylene bottles.

Atomic Absorption Methods

Samples were analyzed by zeeman furnace atomic absorption (AA) on a Perkin-Elmer Zeeman 3030 Atomic Absorption Spectrophotometer, with an AS60 auto sampler, or a flame AA Perkin Elmer Model 2280. Samples, blanks, matrix modifiers, and standards were prepared using clean techniques inside a clean laboratory. ASTM Type II water and ultra clean chemicals were used for all standard preparations. All elements were analyzed with platforms for stabilization of temperatures. Matrix modifiers were used when components of the matrix interferes with adsorption. The matrix modifier was used for Sn, Sb and Pb. Continuing calibration check standards (CLC) were analyzed with each furnace sheet, and calibration curves were run with three concentrations after every 10 samples. Mercury was analyzed by flameless AA. Selenium and As were analyzed by hydride generation. Blanks and standard reference materials, MESS1, PACS, BCSS1 or 1646 were analyzed with each set of samples for sediments. All contaminants in standard reference materials analyzed as part of this study were within the published acceptable ranges.

Trace Organic Analysis of Sediments (PCBs, Pesticides, and PAHs)

Summary of Methods

Trace organics analysis was conducted at the Toxicology Lab of the Institute of Marine Sciences, UC Santa Cruz. Analytical sets of 12 samples were scheduled such that extraction and analysis will occur within a 40 day window. The methods employed by the UCSC-Trace Organic Facility were modifications of those described by Sloan *et al.* (1993).

Analytes and Detection Limits

Organochlorine pesticides analyzed and their abbreviations (in parenthesis) and detection limits (MDL) in sediment, ng/g dry weight are:

Pesticide	MDL
Aldrin	0.5
cis-Chlordane (CCHLOR)	0.5
trans-Chlordane (TCHLOR)	0.5
alpha-Chlordene (ACDEN)	0.5
gamma-Chlordene (GCDEN)	0.5
Chlorpyrifos (CLPYR)	1.0
Dacthal (DACTH)	0.2
o,p'-DDD (OPDDD)	1.0
p,p'-DDD (PPDDD)	0.4
o,p'-DDE (OPDDE)	1.0
p,p'-DDE (PPDDE)	1.0
p,p'-DDMS (PPDDMS)	3.0
p,p'-DDMU (PPDDMU)	2.0
o,p'-DDT (OPDDT)	1.0
p,p'-DDT (PPDDT)	1.0
p,p'-Dichlorobenzophenone (DICLB)	3.0
Dieldrin	0.5
Endosulfan I (ENDO_1)	0.5

Endosulfan II (ENDO_2)	1.0
Endosulfan sulfate (ESO4)	2.0
Endrin	2.0
Ethion	2.0
alpha-HCH (HCHA)	0.2
beta-HCH (HCHB)	1.0
gamma-HCH (HCHG)	0.2
delta-HCH (HCHD)	0.5
Heptachlor	0.5
Heptachlor Epoxide (HE)	0.5
Hexachlorobenzene (HCB)	0.2
Methoxychlor (METHOXY)	1.5
Mirex	0.5
cis-Nonachlor (CNONA)	0.5
trans-Nonachlor (TNONA)	0.5
Oxadiazon (OXAD)	2.0
Oxychlordane (OCDAN)	0.5
Toxaphene (TOXAPH)	10

PCB congeners analyzed in sediment, ng/g dry weight are:

NIST Congeners:

PCB Congener 8 (PCB8)	PCB Congener 128 (PCB128)
PCB Congener 18 (PCB18)	PCB Congener 138 (PCB138)
PCB Congener 28 (PCB28)	PCB Congener 153 (PCB153)
PCB Congener 44 (PCB44)	PCB Congener 170 (PCB170)
PCB Congener 52 (PCB52)	PCB Congener 180 (PCB180)
PCB Congener 66 (PCB66)	PCB Congener 187 (PCB187)
PCB Congener 87 (PCB87)	PCB Congener 195 (PCB195)
PCB Congener 101 (PCB101)	PCB Congener 206 (PCB206)
PCB Congener 105 (PCB105)	PCB Congener 209 (PCB209)
PCB Congener 118 (PCB118)	

All individual PCB Congener detection limits were 1 ng/g dry weight. Abreviations are given in parenthesis.

PAHs analyzed in sediment, ng/g dry weight are:

Polycyclic Aromatic Hydrocarbons

Naphthalene (NPH)
2-Methylnaphthalene (MNP2)
1-Methylnaphthalene (MNP1)
Biphenyl (BPH)
2,6-Dimethylnaphthalene (DMN)
Acenaphthylene (ACY)
Acenaphthene (ACE)
2,3,5-Trimethylnaphthalene (TMN)
Fluorene (FLU)
Phenanthrene (PHN)
Anthracene (ANT)

1-Methylphenanthrene (MPH1)
Fluoranthrene (FLA)
Pyrene (PYR)
Benz[a]anthracene (BAA)
Chrysene (CHR)
Benzo[b]fluoranthrene (BBF)
Benzo[k]fluoranthrene (BKF)
Benzo[e]pyrene (BEP)
Benzo[a]pyrene (BAP)
Perylene (PER)
Indo[1,2,3-cd]pyrene (IND)
Dibenz[a,h]anthracene (DBA)
Benzo[ghi]perylene (BGP)

All individual PAH detection limits were 5 ng/g dry weight. Abreviations are given in parenthesis.

Extraction and Analysis

Samples were removed from the freezer and allowed to thaw. A 10 gram sample of sediment was removed for chemical analysis and an independent 10 gram aliquot was removed for dry weight determinations. The dry weight sample was placed into a pre-weighed aluminum pan and dried at 110°C for 24 hours. The dried sample was reweighed to determine the sample's percent moisture. The analytical sample was extracted 3 times with methylene chloride in a 250-mL amber Boston round bottle on a modified rock tumbler. Prior to rolling, sodium sulfate, copper, and extraction surrogates were added to the bottle. Sodium sulfate dehydrates the sample allowing for efficient sediment extraction. Copper, which was activated with hydrochloric acid, complexes free sulfur in the sediment.

After combining the three extraction aliquots, the extract was divided into two portions, one for chlorinated hydrocarbon (CH) analysis and the other for polycyclic aromatic hydrocarbon (PAH) analysis.

The CH portion was eluted through a silica/alumina column, separating the analytes into two fractions. Fraction 1 (F1) was eluted with 1% methylene chloride in pentane and contains > 90% of p,p'-DDE and < 10% of p,p'-DDT. Fraction 2 (F2) analytes were eluted with 100% methylene chloride. The two fractions were exchanged into hexane and concentrated to 500 µL using a combination of rotary evaporation, controlled boiling on tube heaters, and dry nitrogen blow downs.

F1 and F2 fractions were analyzed on Hewlett-Packard 5890 Series gas chromatographs utilizing capillary columns and electron capture detection (GC/ECD). A single 2 µl splitless injection was directed onto two 60m x 0.25mm i.d. columns of different polarity (DB-17 & DB-5; J&W Scientific) using a glass Y-splitter to provide a two dimensional confirmation of each analyte. Analytes were quantified using internal standard methodologies. The extract's PAH portion was eluted through a silica/alumina column with methylene chloride. It then underwent additional cleanup using size-exclusion high performance liquid chromatography (HPLC/SEC). The collected PAH fraction was exchanged into hexane and concentrated to 250 µL in the same manner as the CH fractions.

Quality Assurance/Quality Control

Summary of Methods

Summaries of quality assurance and quality control procedures are described in the California State Water Resources Control Board's Bay Protection and Toxic Cleanup Program Quality Assurance Project Plan (QAPP) (Stephenson et al. 1994). This document describes procedures within the program which ensure data quality and integrity. Quality assurance procedures follow

those of the NS&T Program to ensure comparability with other NOAA survey areas nationwide. In addition, individual laboratories prepare quality assurance evaluations of each discrete set of samples analyzed and authorized by task order.

Sediment Quality Guidelines

There have been several recent studies associating pollutant concentrations with biological responses (Long and Morgan, 1990; MacDonald et al. 1996). These studies provide guidance for evaluating the degree to which sediment chemical pollutants levels are responsible for effects observed in a toxicity test. Reported values are based on individual chemical pollutants within sediments. Therefore, their application may be confounded when dealing with: biological effects which could be attributed to a synergistic effect of low levels of multiple chemicals, unrecognized chemicals, or physical parameters in the sediment which were not measured.

The National Status and Trends Program has used chemical and toxicological evidence from a number of modeling, field and laboratory studies to determine the ranges of chemical concentrations which are rarely, sometimes, or usually associated with toxicity (Long *et al.*, 1995). Evaluation of available data (Long *et al.*, 1995) has led to identification of three ranges in concentration for each chemical:

1) Minimal Effects Range: The range in concentration over which toxic effects are rarely observed:

2) Possible Effects Range: The range in concentrations over which toxic effects are occasionally observed;

3) Probable-Effects Range: The range in chemical concentrations over which toxic effects are frequently or always observed.

Two slightly different methods were used to determine these chemical ranges. One method developed by NOAA (Long *et al.*, 1995) used chemical data which were associated with a toxic biological effect. These data were used to determine the lower 10th percentile of ranked data where the chemical level was associated with an effect (Effects Range-Low, or ERL). Sediment samples in which all chemical concentrations were below the 25 ERL values were not expected to be toxic. The Effects Range-Median (ERM) reflects the 50th percentile of ranked data and represents the level above which effects are expected to occur. Effects are expected to occur occasionally when chemical concentrations fall between the ERL and ERM. The probability of toxicity was expected to increase with the number and degree of exceedances of the ERM values.

Another method identifies three ranges using chemical concentration data associated with both toxic biological effects and no observed effects (MacDonald et al. 1996). The ranges are identified as TEL (Threshold Effects Level) and the PEL (Probable Effects Level). TEL values were derived by taking the geometric mean of the 50th percentile of the "no effects" data and the 15th percentile of the "effects" data. The PEL values were derived by taking the geometric mean of the 85th percentile of the "no effects" data and the 50th percentile of the "effects" data. Although different percentiles were used for these two methods, they are in close agreement, usually within a factor of 2. Neither of these methods is advocated over the use of the other in this report. Instead, both are used.

A cautionary note should be included; the degree of confidence which MacDonald et al. (1996) and Long et al. (1995) had in their respective guidelines varied considerably among the different chemicals. For example, they express low confidence in the values derived for nickel, mercury, DDTs, chlordane, dieldrin, and endrin. They also express low confidence in values derived for chromium. When more data becomes available regarding these chemicals and their potential effects, the guidelines may be revised, probably upward for some substances.

Figure 2. PPDDE concentration (ng/g, dry weight) in sediments from the Monterey Bay area.

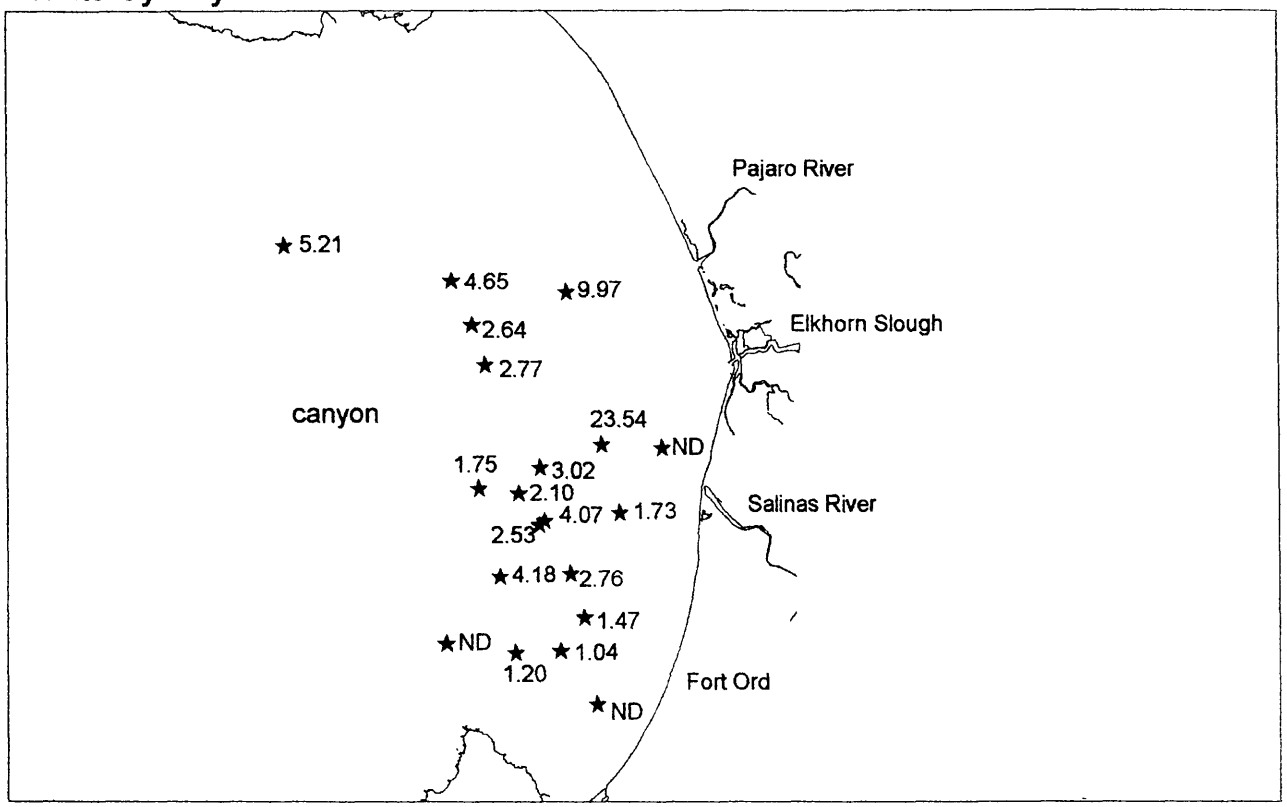

Figure 3. TOC normalized PPDDE concentration (ng/g, organic carbon weight) in sediments from the Monterey Bay area.

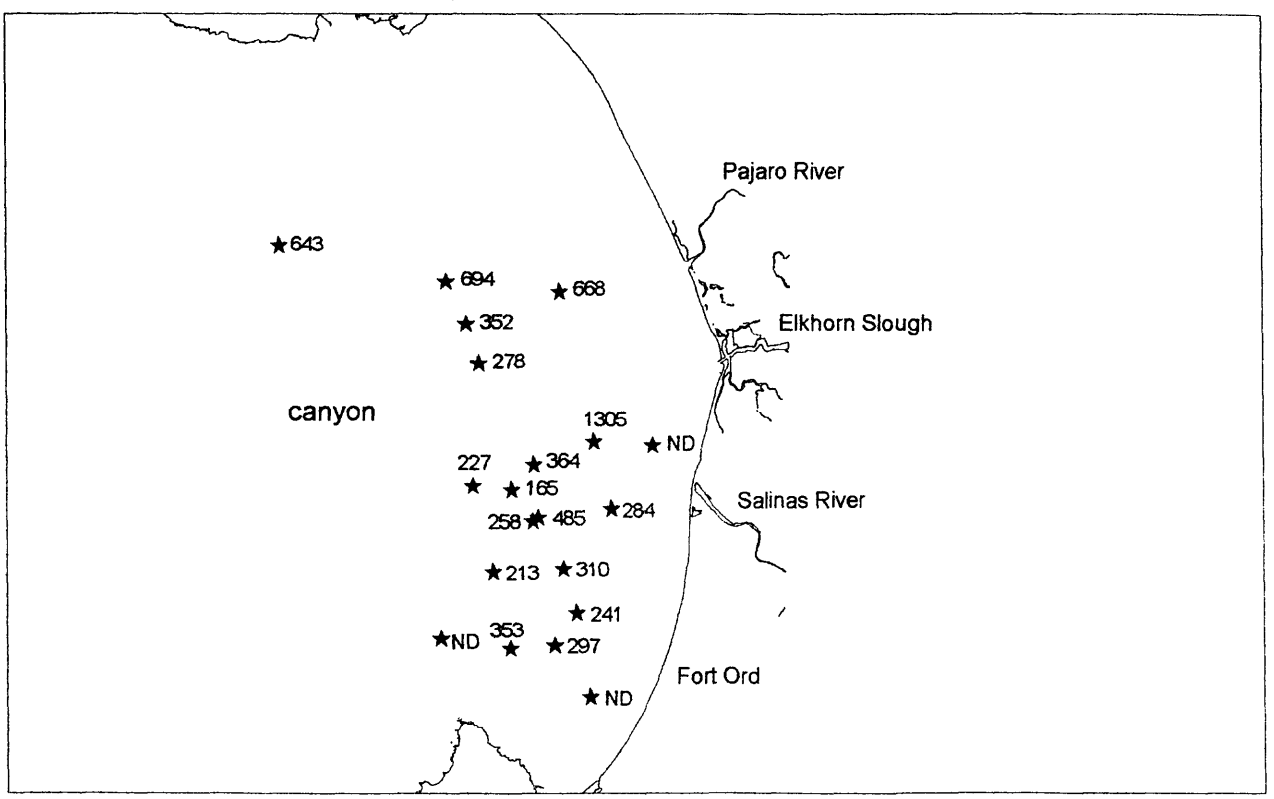

Figure 4. Total PAH concentrations (ng/g, dry weight) in sediments from the Monterey Bay area.

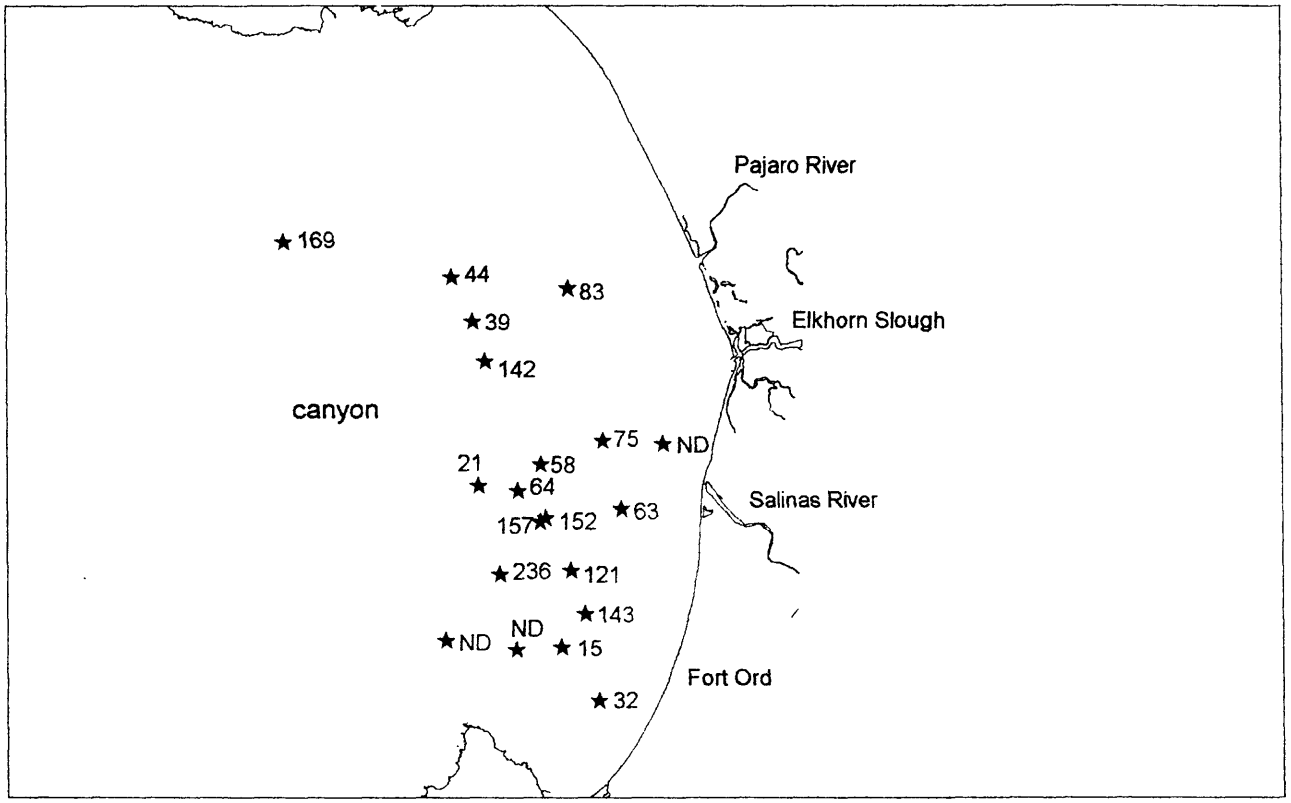

Figure 5. TOC normalized PAH concentration (ng/g, organic carbon weight) in sediments from the Monterey Bay area.

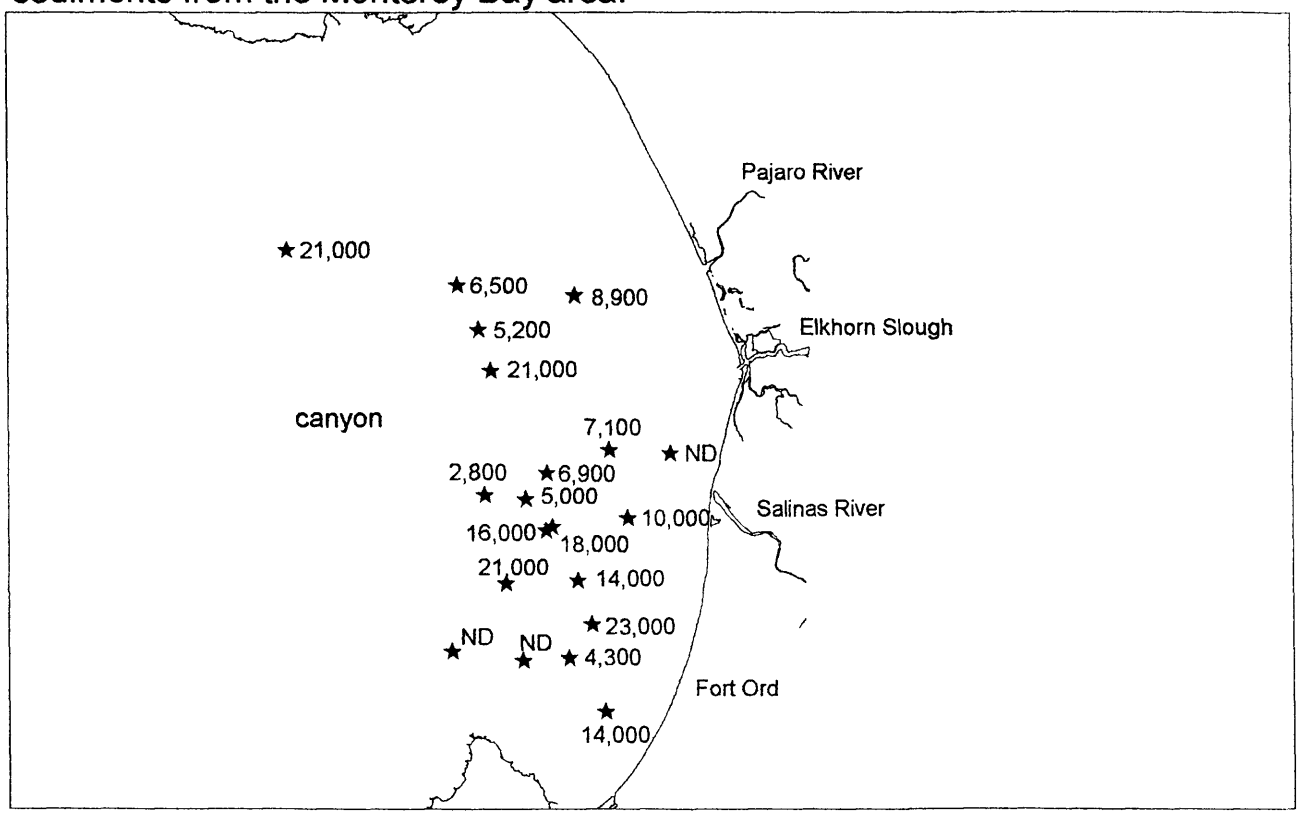

Figure 6. Lead concentration (ug/g, dry weight) in sediments from the Monterey Bay.

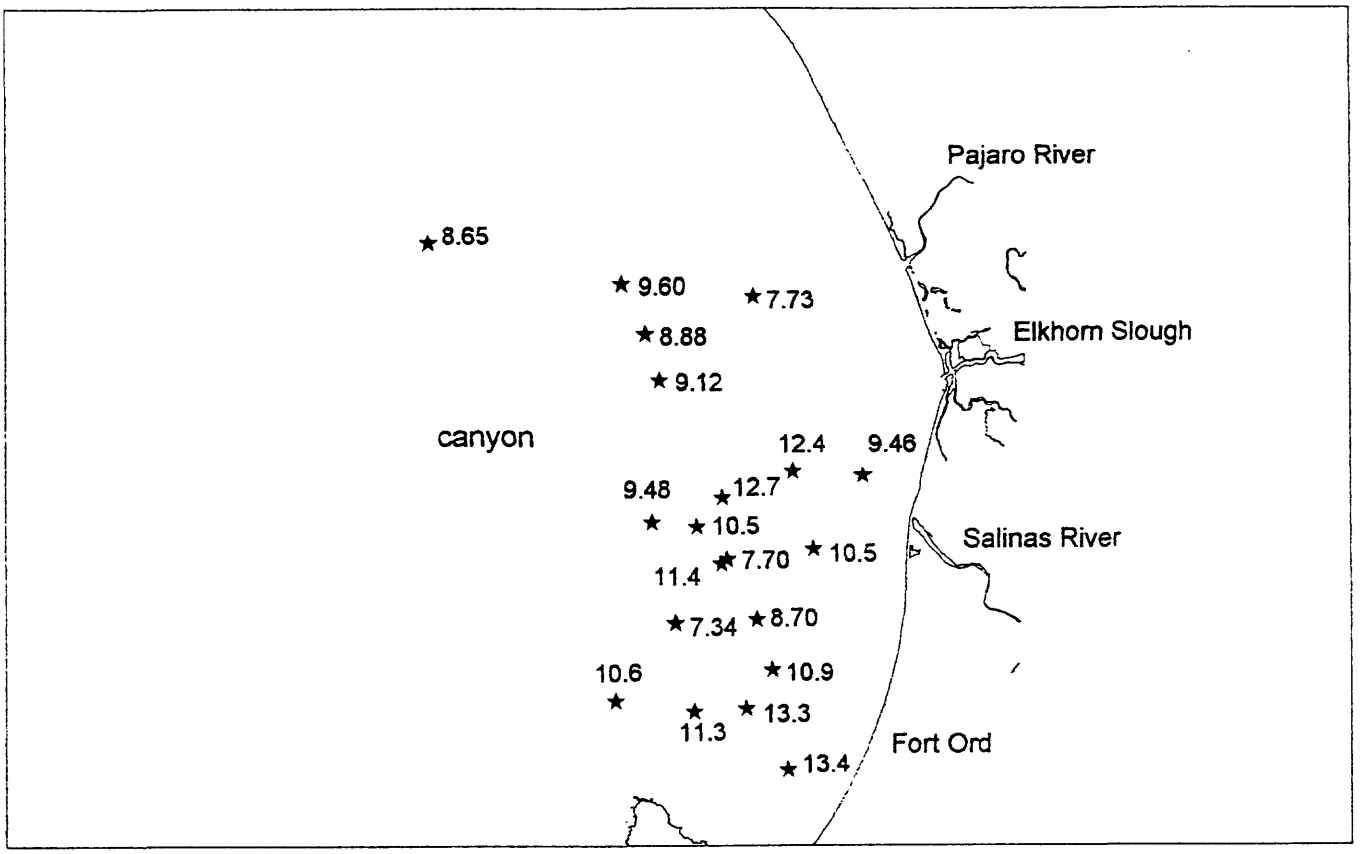

Figure 7. TOC normalized lead concentration (ug/g, organic carbon weight) in sediment from the Monterey Bay area.

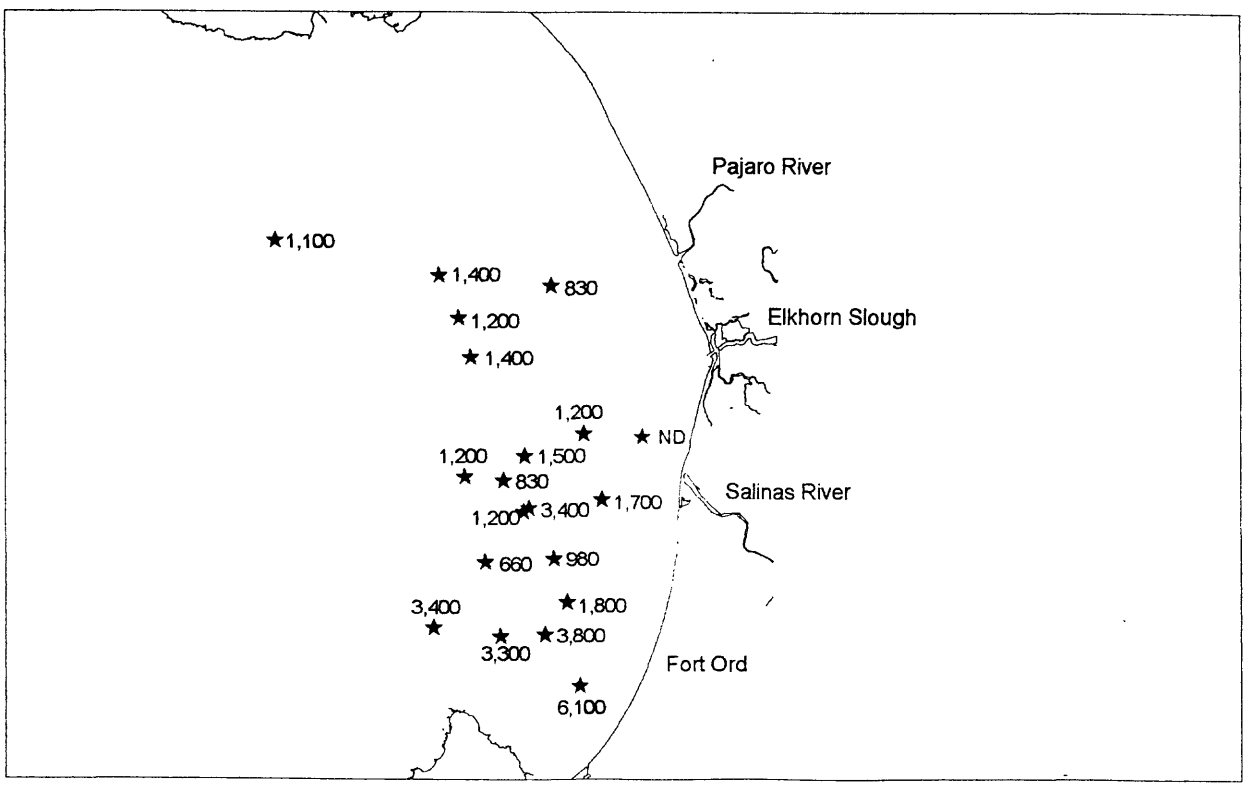

Figure 8. Grain Size normalized lead concentration (ug/g, fines) in sediment from the Monterey Bay area.

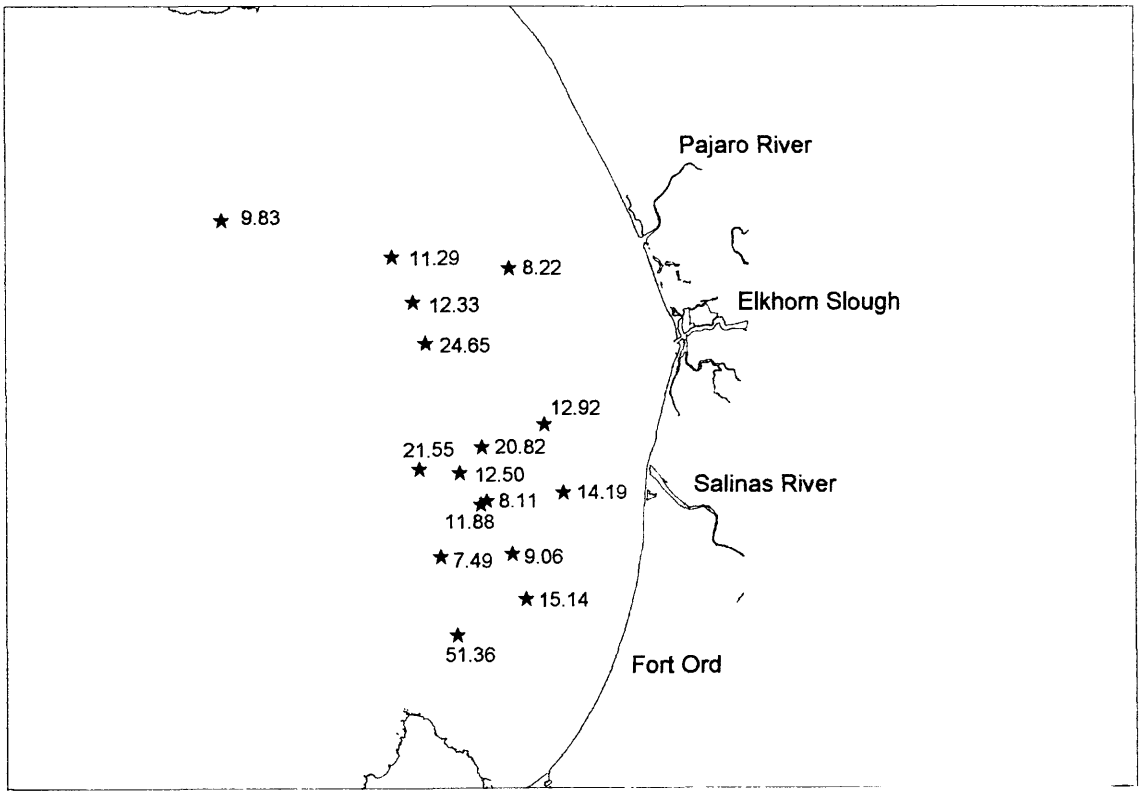

Figure 9. Grain Size normalized zinc concentration (ug/g, fines) in sediment from the Monterey Bay area.

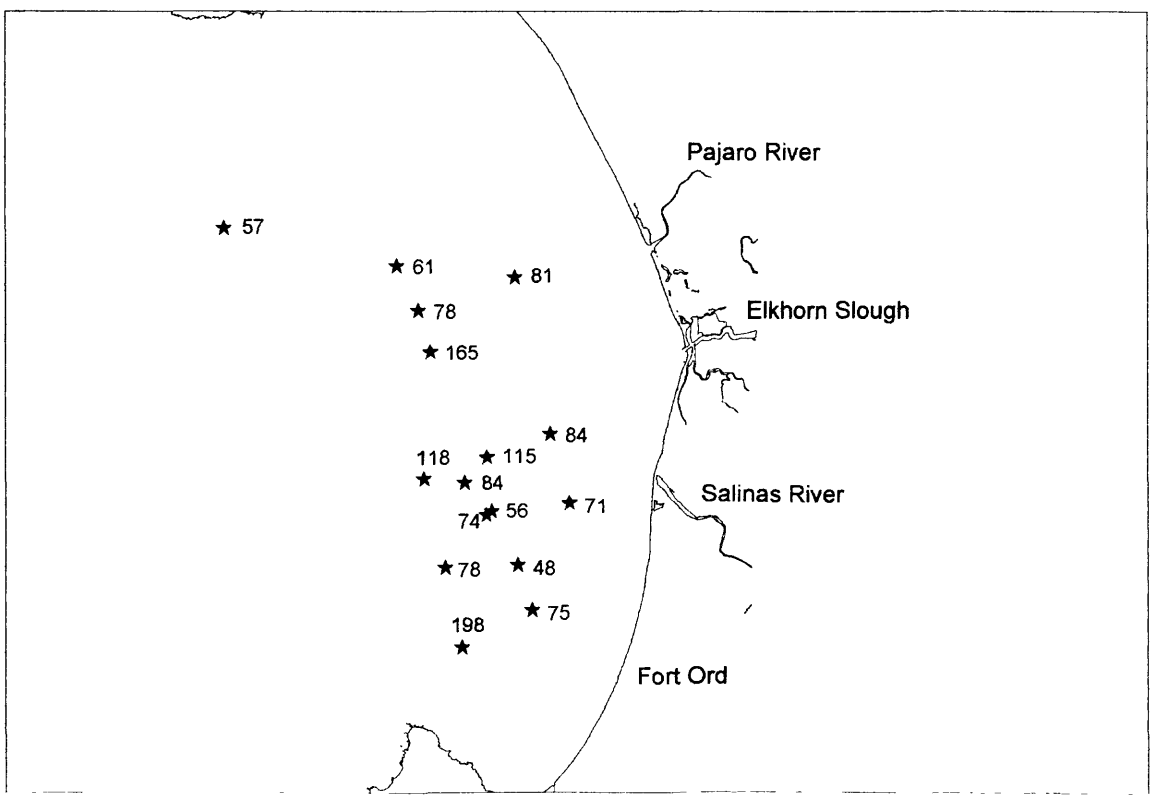

Figure 10. Grain Size normalized chromium concentration (ug/g, fines) in sediment from the Monterey Bay area.

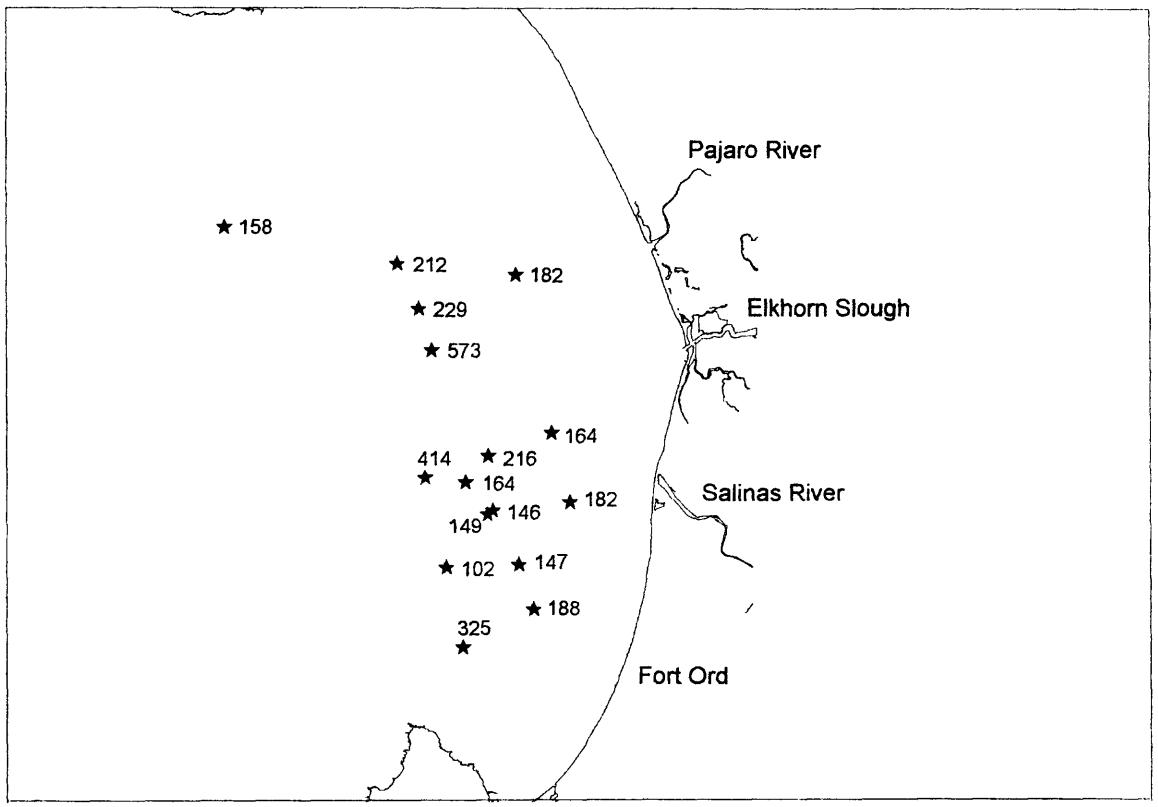

Figure 11. Grain Size normalized cadmium concentration (ug/g, fines) in sediment from the Monterey Bay area.

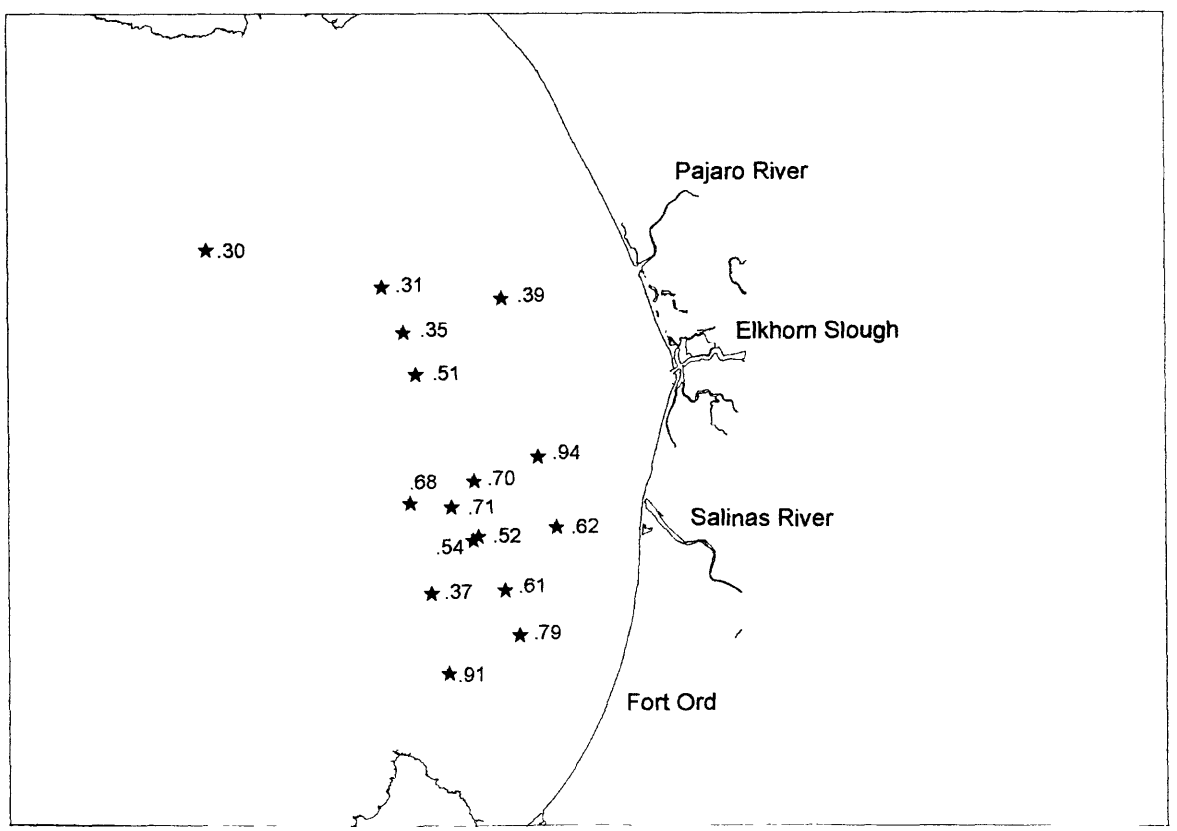

RESULTS AND DISCUSSION

Distribution of Chemical Pollutants

PCB's in the sediments measured "not detected" at all stations (Table 1). Dacthal and dieldrin were found at a few stations at or near the detection limits (Table 2). DDT and a it's metabolites were found at virtually every station (Table 2). DDE was the principle metabolite in the samples and its distribution is plotted in Figure 2 and ranged from <1 to 23 ppb. Concentrations were highest near the mouth of the Salinas River (station B163) however the closest station to the mouth (B167) did not have any DDE. This can be explained because it was over 90 percent sand and was the shallowest station (30m) in this study. DDT is usually found in fine grain sediments that are high in organic matter. When DDE is normalize to TOC (Table 2 and Figure 3) to correct for variable sand concentrations the pattern is similar to that of the unnormalized data. This is an indication that even in the organic fraction of the sediments the contaminants show the same trends as the whole sediment with sand and fines. Station B163 just off the mouth of the Salinas River is highest in concentration and the next highest are stations in the northern part of the bay at three stations offshore of the Pajaro River. In general the concentrations offshore of Fort Ord are lower than those to the north indicating the source of DDT and its metabolites is not near the Fort. A more probable explanation is that the DDT and its metabolites are coming from agriculture fields and are deposited in the bay during storms through the Salinas and Pajaro Rivers. It also appears that currents do not transport the DDT from the Salinas River south towards Fort Ord.

PAHs and PAHs normalized to TOC in sediments show that the distribution is correlated with TOC and fine grain size which are generally more prevelant offshore (Table 4). In contrast to DDE the stations highest in concentration were not close to Fort Ord, the Salinas, or Pajaro Rivers (Table 3, Figures 4 and 5).

The metals showed a different pattern from the pesticides. Both the normalized and TOC unnormalized lead data indicate the two samples with the highest concentrations of lead were the two closest to Fort Ord (Table 5, Figures 6 and 7). Lead normalized to grain size showed the highest value near Fort Ord and Monterey Harbor (Figure 8). The metals were normalized to TOC in the case of lead, and fine grain size in the case of lead, cadmium, chromium, and cadmium. The normalization allowed for comparisons that correct for the variable amounts of sand in the sample. A metal normalized to fine grain size or TOC allows the concentrations to be presented as if all the metals were found in the fine grains or TOC only. The fine grain size normalization formula is ug element divided by the dry weight of the combined silt and clay fractions (fines fraction < 63u). Several stations were not plotted in the grain size normalized graphs because the concentrations of fines in the samples was less than 20% and would lead to errors because of the lack of accuracy in determning fines at low concentrations (see NOAA, 1991 and Daskalakis and O'Connor, 1994 for discussion of normalization of metals to correct for sand). The metals were not normalized to aluminum as has been done by some other researchers because none of the elements correlated with it. Possibilities for the high lead in south bay include lead from smelter waste in Monterey Harbor, lead from Fort Ord in the form of bullets, atmospheric lead, and discarded fishing leads. Lead is not correlated with other metals (Table 4).

The other metals do not have a similar distribution as lead (Tables 4 and 5) and can be lumped in the following intercorrelated groups: copper, mercury, nickel, selenium silver, tin, zinc; arsenic, chromium and iron; and cadmium . Most of them (copper, mercury, nickel, selenium, silver, tin and zinc) are correlated with TOC (Table 4) and are found in higher concentrations offshore but when normalized to grain size there is no apparent relationship to sources (see Figure 9 where zinc is plotted as an example of this group). Chromium, arsenic, and iron also show no apparent relationship to sources when normalized to grain size (see Figure 10 where chromium is plotted as an example of this group). Cadmium also shows no apparent relationship to sources when normalized to fine grain size (Figure 11).

Most of the levels of metals and organics in sediments from this study are low when compared to PELs, TELs, ERMs and ERLs (Long et al. 1995, Mac Donald et al. 1996) (Table 6). Nickel is higher than ERMs and PELs and chromium is higher than ERLs and TELs for the majority of stations but this is common in Northern California and is probably related to crustal abundances of these metals in northern California as these metals have been found to be high in San Francisco Bay, Tomales Bay and Humboldt Bay by the California Bay Protection and Toxic Cleanup Program (Fairey, personnel communication). These levels are in the range of background levels found in Northern California (NOAA, 1987). Copper and arsenic are higher than the TELs at a few stations. DDE levels are higher than the published ERL values but less than the ERM values found in Long et al. (1995). Long et al. (1995) and Mac Donald et al. (1996) have both expressed low confidence in their respective guidelines for DDT and its metabolites. Recent research on DDT contamination by Swartz et al. (1994) demonstrates DDT concentrations much higher than ERM or PEL values may be required before toxicological effects are apparent. Toxic effects to amphipods in bioassays were observed at levels above 300,000 ng/g TOC normalized while abundance of amphipods in field surveys occurred above 100,000 ng/g TOC normalized. The highest value found in this study is almost 3 orders of magnitude lower than these new recommended numbers from Swartz et al. (1994). The use of ERMs and PELs is controversial in the scientific community to evaluate sediment contamination. They are based on relatively crude measures of toxicity and do not account for bioavailability influences. The Environmental Protection Agency does not accept these values as sediment quality criteria. Despite the controversy over use of these guidelines almost all the samples were lower than the ERMs and PELs and it seems improbable that the current DDT, PAH, or metal values reported from Monterey Bay are at levels that would cause an ecotoxicological effect based on these guidelines.

Another method of set of guidelines is provided by the NS&T program. The NS&T program collected data from almost 300 coastal and estuarine sites throughout the United States from 1984 to 1989. They determined the "high" concentrations as those exceeding the mean plus one standard deviation of the lognormal distribution (NOAA, 1991). One unique feature of these guidelines is that they correct for sand content by normalizing the data by the amount of fine grained sediment in the sample. The data from this study and the guidelines given in Table 6 show that nickel and to a lesser extent chromium (and one station for arsenic) are the only elements that are "high" by these guidelines. As mentioned above these elements have been shown to be high in almost all the Northern California Bays and are thought to be natural in origin.

CONCLUSIONS

1. Lead is higher in sediments from the two stations closest to Fort Ord and Monterey Harbor. Possible sources include Fort Ord, the atmosphere, lead in Monterey Harbor, and fishing leads.
2. DDT distribution is probably related to discharges from the Pajaro and Salinas Rivers.
3. PAHs and most metals other than lead are higher in sediments with high TOC and are found in the highest concentrations in deeper waters with no apparent relation to Fort Ord or river discharges.
4. PCB's and most pesticides analyzed were near or below detection limits.
5. Almost all the levels of metals and organics are low when compared to the most generally accepted sediment quality guidelines, the ERMs, PELs, ERLs, and TELs (Long et al. 1995, MacDonald 1994) and the NS&T guidelines (NOAA 1991). It is improbable that the current DDT and metal values reported from outer Monterey Bay are at levels that would cause an ecotoxicological effect.

RECOMMENDATIONS

An additional study should be commisioned to determine the source of lead in south Monterey Bay. The lead could be coming from the lead slag deposits that exist in the Monterey

Harbor, the lead bullets from the days when the firing ranges were active at Fort Ord, or from discarded fishing leads. Additional stations would have to be collected between Fort Ord and the Harbor and the sediments should be analyzed for lead and lead isotopes.

ACKNOWLEDGEMENTS

The collection of the sediment samples from this study was funded by the Monterey Bay National Marine Sanctuary. Analysis of the sediments was funded by the U.S. Army.

REFERENCES

California Department of Fish and Game, 1990, Water Pollution Control Laboratory Standard Operating Procedure for Determination of Selenium in Biological Tissue, Sediment, and Water.

Daskalas, K., T. O'Connor, 1994, Inventory of Chemical Concentrations in Coastal and Estuarine Sediments: NOAA Technical Memorandum NOS ORCA 76.

Evans, D. and P. Hanson, 1993, Analytical methods for trace elements in sediments by atomic absorption spectrophotometry, *In* Sampling and Analytical Methods of the National Status and Trends Program National Benthic Surveillance and Mussel Watch Project 1984-1992: vol. 3. Lauenstein, G. and A. Cantillo (eds.), NOAA Tech. Mem. NOS ORCA 71, 53-81.

Long, E.R., D.L. MacDonald, S.L. Smith and F.D. Calder, 1995, Incidence of Adverse Biological Effects Within Ranges of Chemical Concentration in Marine and Estuarine Sediments: *Environmental Management.*, 19 (1): 81-97.

Mac Donald, D.D., R. S. Carr, F.D. Calder, E.R. Long and C.G. Ingersoll, 1996, Development and Evaluation of Sediment Quality Guidelines for Florida coastal waters: *Ecotox*, 5: 253-278.

NOAA, 1987, A summary of Selected Data on Chemical Contaminants in Sediments Collected During 1984, 1985,1986, and 1987: NOAA Technical Memorandum NOS OMA 44.

NOAA, 1991. A summary of Selected Data on Chemical Contaminants in Sediments from the National Status and Trends Program: NOAA Technical Memorandum NOS OMA 59.

Sloan, C.A., N.G. Adams, R.W. Pearce, D.W. Brown, and S.L. Chan, 1993, Northwest Fisheries Science Center Organic Analytical Procedures. In Sampling and Analytical Methods of The National Status and Trends Program National Benthic Surveillance and Mussel Watch Projects 1984-1992 - Volume VI, Comprehensive descriptions of the trace organic analytical methods, G.G. Lauenstein and A.Y. Cantillo (Eds): NOAA Technical Memorandum NOS ORCA 71, p 53-97.

Stephenson, M. M. Puckett, N. Morgan, and M. Reid, 1994, Bay Protection and Toxic Cleanup Program: Quality Assurance Project Plan: Bay Protection and Toxic Cleanup Program, State Water Resources Control Board, Sacramento,CA.

Swartz, R.C., F.A. Cole, J.O. Lamberson, S.P. Ferraro, D.W. Schults, W.A. DeBen, H.Lee II, and R.J. Ozretich, 1994, Sediment Toxicity, Contamination and Amphipod Abundance at a DDT- and Dieldrin- Contaminated Site in San Francisco Bay: *Environ. Tox. And Chem.*, 13 6: 949-962.

TABLE 1A: PCBS--SEDIMENT DRY WEIGHT DATA IN ng/g

STATION NUMBER (IDORG)	DATE	PCB5	PCB8	PCB15	PCB18	PCB27	PCB28	PCB29	PCB31	PCB44	PCB49	PCB52	PCB66	PCB70	PCB74	PCB87	PCB95
B117	4/8/95	ND	ND	NA	ND	ND	ND	ND	ND	ND	ND	ND	ND	ND	ND	ND	ND
B131	4/9/95	ND	ND	NA	ND	ND	ND	ND	ND	ND	ND	ND	ND	ND	ND	ND	ND
B134	4/9/95	ND	ND	NA	ND	ND	ND	ND	ND	ND	ND	ND	ND	ND	ND	ND	ND
B148	4/10/95	ND	ND	NA	ND	ND	ND	ND	ND	ND	ND	ND	ND	ND	ND	ND	ND
B151	4/10/95	ND	ND	NA	ND	ND	ND	ND	ND	ND	ND	ND	ND	ND	ND	ND	ND
B154	4/10/95	ND	ND	NA	ND	ND	ND	ND	ND	ND	ND	ND	ND	ND	ND	ND	ND
B155	4/11/95	ND	ND	NA	ND	ND	ND	ND	ND	ND	ND	ND	ND	ND	ND	ND	ND
B156	4/11/95	ND	ND	NA	ND	ND	ND	ND	ND	ND	ND	ND	ND	ND	ND	ND	ND
B157	4/11/95	ND	ND	NA	ND	ND	ND	ND	ND	ND	ND	ND	ND	ND	ND	ND	ND
B160	4/11/95	ND	ND	NA	ND	ND	ND	ND	ND	ND	ND	ND	ND	ND	ND	ND	ND
B163	4/11/95	ND	ND	NA	ND	ND	ND	ND	ND	ND	ND	ND	ND	ND	ND	ND	ND
B164	4/11/95	ND	ND	NA	ND	ND	ND	ND	ND	ND	ND	ND	ND	ND	ND	ND	ND
B167	4/11/95	ND	ND	NA	ND	ND	ND	ND	ND	ND	ND	ND	ND	ND	ND	ND	ND
B324	9/11/95	ND	ND	NA	ND	ND	ND	ND	ND	ND	ND	ND	ND	ND	ND	ND	ND
B331	9/11/95	ND	ND	NA	ND	ND	ND	ND	ND	ND	ND	ND	ND	ND	ND	ND	ND
B334	9/12/95	ND	ND	NA	ND	ND	ND	ND	ND	ND	ND	ND	ND	ND	ND	ND	ND
B335	9/12/95	ND	ND	NA	ND	ND	ND	ND	ND	ND	ND	ND	ND	ND	ND	ND	ND
B344	9/12/95	ND	ND	NA	ND	ND	ND	ND	ND	ND	ND	ND	ND	ND	ND	ND	ND
B346	9/12/95	ND	ND	NA	ND	ND	ND	ND	ND	ND	ND	ND	ND	ND	ND	ND	ND
B351	9/12/95	ND	ND	NA	ND	ND	ND	ND	ND	ND	ND	ND	ND	ND	ND	ND	ND

NOT DETECTED = ND NOT ANALYZED = NA

TABLE 1B: PCBS--SEDIMENT DRY WEIGHT DATA IN ng/g

STATION NUMBER (IDORG)	DATE	PCB97	PCB99	PCB101	PCB105	PCB110	PCB118	PCB128	PCB132	PCB137	PCB138	PCB149	PCB151	PCB153	PCB156	PCB157	PCB158
B117	4/8/95	ND	ND	ND	ND	ND	ND	ND	ND	ND	ND	ND	ND	ND	ND	ND	ND
B131	4/9/95	ND	ND	ND	ND	ND	ND	ND	ND	ND	ND	ND	ND	ND	ND	ND	ND
B134	4/9/95	ND	ND	ND	ND	ND	ND	ND	ND	ND	ND	ND	ND	ND	ND	ND	ND
B148	4/10/95	ND	ND	ND	ND	ND	ND	ND	ND	ND	ND	ND	ND	ND	ND	ND	ND
B151	4/10/95	ND	ND	ND	ND	ND	ND	ND	ND	ND	ND	ND	ND	ND	ND	ND	ND
B154	4/10/95	ND	ND	ND	ND	ND	ND	ND	ND	ND	ND	ND	ND	ND	ND	ND	ND
B155	4/11/95	ND	ND	ND	ND	ND	ND	ND	ND	ND	ND	ND	ND	ND	ND	ND	ND
B156	4/11/95	ND	ND	ND	ND	ND	ND	ND	ND	ND	ND	ND	ND	ND	ND	ND	ND
B157	4/11/95	ND	ND	ND	ND	ND	ND	ND	ND	ND	ND	ND	ND	ND	ND	ND	ND
B160	4/11/95	ND	ND	ND	ND	ND	ND	ND	ND	ND	ND	ND	ND	ND	ND	ND	ND
B163	4/11/95	ND	ND	ND	ND	ND	ND	ND	ND	ND	ND	ND	ND	ND	ND	ND	ND
B164	4/11/95	ND	ND	ND	ND	ND	ND	ND	ND	ND	ND	ND	ND	ND	ND	ND	ND
B167	4/11/95	ND	ND	ND	ND	ND	ND	ND	ND	ND	ND	ND	ND	ND	ND	ND	ND
B324	9/11/95	ND	ND	ND	ND	ND	ND	ND	ND	ND	ND	ND	ND	ND	ND	ND	ND
B331	9/11/95	ND	ND	ND	ND	ND	ND	ND	ND	ND	ND	ND	ND	ND	ND	ND	ND
B334	9/12/95	ND	ND	ND	ND	ND	ND	ND	ND	ND	ND	ND	ND	ND	ND	ND	ND
B335	9/12/95	ND	ND	ND	ND	ND	ND	ND	ND	ND	ND	ND	ND	ND	ND	ND	ND
B344	9/12/95	ND	ND	ND	ND	ND	ND	ND	ND	ND	ND	ND	ND	ND	ND	ND	ND
B346	9/12/95	ND	ND	ND	ND	ND	ND	ND	ND	ND	ND	ND	ND	ND	ND	ND	ND
B351	9/12/95	ND	ND	ND	ND	ND	ND	ND	ND	ND	ND	ND	ND	ND	ND	ND	ND

NOT DETECTED = ND NOT ANALYZED = NA

TABLE 1C: PCBS SEDIMENT DRY WEIGHT DATA IN ng/g

STATION NUMBER (IDORG)	DATE	PCB170	PCB174	PCB177	PCB180	PCB183	PCB187	PCB189	PCB194	PCB195	PCB201	PCB203	PCB206	PCB209	ARO1248	ARO1254	ARO1260	ARO5460	PESBATCH
B117	4/6/95	ND	ND	ND	ND	ND	ND	ND	ND	ND	ND	ND	ND	ND	ND	ND	ND	ND	95.0
B131	4/9/95	ND	ND	ND	ND	ND	ND	ND	ND	ND	ND	ND	ND	ND	ND	ND	ND	ND	95.1
B134	4/9/95	ND	ND	ND	ND	ND	ND	ND	ND	ND	ND	ND	ND	ND	ND	ND	ND	ND	95.0
B148	4/10/95	ND	ND	ND	ND	ND	ND	ND	ND	ND	ND	ND	ND	ND	ND	ND	ND	ND	95.1
B151	4/10/95	ND	ND	ND	ND	ND	ND	ND	ND	ND	ND	ND	ND	ND	ND	ND	ND	ND	95 0
B154	4/10/95	ND	ND	ND	ND	ND	ND	ND	ND	ND	ND	ND	ND	ND	ND	ND	ND	ND	95 1
B155	4/11/95	ND	ND	ND	ND	ND	ND	ND	ND	ND	ND	ND	ND	ND	ND	ND	ND	ND	95.0
B156	4/11/95	ND	ND	ND	ND	ND	ND	ND	ND	ND	ND	ND	ND	ND	ND	ND	ND	ND	95.0
B157	4/11/95	ND	ND	ND	ND	ND	ND	ND	ND	ND	ND	ND	ND	ND	ND	ND	ND	ND	95 0
B160	4/11/95	ND	ND	ND	ND	ND	ND	ND	ND	ND	ND	ND	ND	ND	ND	ND	ND	ND	95.0
B163	4/11/95	ND	ND	ND	ND	ND	ND	ND	ND	ND	ND	ND	ND	ND	ND	ND	ND	ND	95.0
B164	4/11/95	ND	ND	ND	ND	ND	ND	ND	ND	ND	ND	ND	ND	ND	ND	ND	ND	ND	95.1
B167	4/11/95	ND	ND	ND	ND	ND	ND	ND	ND	ND	ND	ND	ND	ND	ND	ND	ND	ND	95 0
B324	9/11/95	ND	ND	ND	ND	ND	ND	ND	ND	ND	ND	ND	ND	ND	ND	ND	ND	ND	95.0
B331	9/11/95	ND	ND	ND	ND	ND	ND	ND	ND	ND	ND	ND	ND	ND	ND	ND	ND	ND	95 0
B334	9/12/95	ND	ND	ND	ND	ND	ND	ND	ND	ND	ND	ND	ND	ND	ND	ND	ND	ND	95.0
B335	9/12/95	ND	ND	ND	ND	ND	ND	ND	ND	ND	ND	ND	ND	ND	ND	ND	ND	ND	95.0
B344	9/12/95	ND	ND	ND	ND	ND	ND	ND	ND	ND	ND	ND	ND	ND	ND	ND	ND	ND	95.0
B346	9/12/95	ND	ND	ND	ND	ND	ND	ND	ND	ND	ND	ND	ND	ND	ND	ND	ND	ND	95.0
B351	9/12/95	ND	ND	ND	ND	ND	ND	ND	ND	ND	ND	ND	ND	ND	ND	ND	ND	ND	95.0

NOT DETECTED = ND NOT ANALYZED = NA

TABLE 2A: PESTICIDES--SEDIMENT DRY WEIGHT DATA IN ng/g

STATION NUMBER (IDORG)	DATE	ALDRIN	CCHLOR	TCHLOR	ACDEN	GCDEN	CLPYR	DACTH	OPDDD	PPDDD	OPDDE	PPDDE	TOC DDE	PPDDMS
B117	4/8/95	ND	ND	ND	ND	ND	ND	ND	ND	2.0	ND	5.2	643	ND
B131	4/9/95	ND	ND	ND	ND	ND	ND	0.2	ND	0.8	ND	4.7	694	ND
B134	4/9/95	ND	ND	ND	ND	ND	ND	ND	ND	0.7	ND	2.6	352	ND
B148	4/10/95	ND	ND	ND	ND	ND	ND	ND	ND	ND	ND	1.2	353	ND
B151	4/10/95	ND	ND	ND	ND	ND	ND	ND	ND	ND	ND	ND	ND	ND
B154	4/10/95	ND	ND	ND	ND	ND	ND	ND	ND	0.6	ND	4.1	485	ND
B155	4/11/95	ND	ND	ND	ND	ND	ND	2.1	ND	2.7	ND	10.0	668	ND
B156	4/11/95	ND	ND	ND	ND	ND	ND	ND	ND	ND	ND	2.8	278	ND
B157	4/11/95	ND	ND	ND	ND	ND	ND	ND	ND	0.4	ND	1.8	227	ND
B160	4/11/95	ND	ND	ND	ND	ND	ND	ND	ND	0.7	ND	3.0	364	ND
B163	4/11/95	ND	ND	ND	ND	ND	ND	6.3	ND	3.8	ND	23.5	1305	ND
B164	4/11/95	ND	ND	ND	ND	ND	ND	0.5	ND	ND	ND	1.7	284	ND
B167	4/11/95	ND	ND	ND	ND	ND	ND	ND	ND	ND	ND	ND	ND	ND
B324	9/11/95	ND	ND	ND	ND	ND	ND	ND	ND	0.9	ND	2.5	258	ND
B331	9/11/95	ND	ND	ND	ND	ND	ND	ND	ND	1.7	ND	4.2	213	ND
B334	9/12/95	ND	ND	ND	ND	ND	ND	ND	ND	ND	ND	1.0	297	ND
B335	9/12/95	ND	ND	ND	ND	ND	ND	ND	ND	ND	ND	ND	ND	ND
B344	9/12/95	ND	ND	ND	ND	ND	ND	ND	ND	ND	ND	1.5	241	ND
B346	9/12/95	ND	ND	ND	ND	ND	ND	ND	ND	0.7	ND	2.8	310	ND
B351	9/12/95	ND	ND	ND	ND	ND	ND	ND	ND	0.5	ND	2.1	165	ND

NOT DETECTED = ND NOT ANALYZED = NA TOC DDE = DDE NORMALIZED TO TOC

TABLE 2B: PESTICIDES--SEDIMENT DRY WEIGHT DATA IN ng/g

STATION NUMBER (IDORG)	DATE	PPDDMU	OPDDT	PPDDT	DICLB	DIELDRIN	ENDO_I	ENDO_II	ESO4	ENDRIN	HCHA	HCHB	HCHG	HCHD
B117	4/8/95	ND	ND	ND	ND	ND	ND	ND	ND	ND	ND	ND	ND	ND
B131	4/9/95	ND	ND	ND	ND	ND	ND	ND	ND	ND	ND	ND	ND	ND
B134	4/9/95	ND	ND	ND	ND	ND	ND	ND	ND	ND	ND	ND	ND	ND
B148	4/10/95	ND	ND	ND	ND	ND	ND	ND	ND	ND	ND	ND	ND	ND
B151	4/10/95	ND	ND	ND	ND	ND	ND	ND	ND	ND	ND	ND	ND	ND
B154	4/10/95	ND	ND	ND	ND	ND	ND	ND	ND	ND	ND	ND	ND	ND
B155	4/11/95	ND	2.5	4.4	ND	ND	ND	ND	ND	ND	ND	ND	ND	ND
B156	4/11/95	ND	ND	ND	ND	ND	ND	ND	ND	ND	ND	ND	ND	ND
B157	4/11/95	ND	ND	ND	ND	ND	ND	ND	ND	ND	ND	ND	ND	ND
B160	4/11/95	ND	ND	ND	ND	ND	ND	ND	ND	ND	ND	ND	ND	ND
B163	4/11/95	ND	7.1	16.8	ND	1.4	ND	ND	ND	ND	ND	ND	ND	ND
B164	4/11/95	ND	ND	ND	ND	ND	ND	ND	ND	ND	ND	ND	ND	ND
B167	4/11/95	ND	ND	ND	ND	ND	ND	ND	ND	ND	ND	ND	ND	ND
B324	9/11/95	ND	ND	ND	ND	ND	ND	ND	ND	ND	ND	ND	ND	ND
B331	9/11/95	ND	ND	ND	ND	ND	ND	ND	ND	ND	ND	ND	ND	ND
B334	9/12/95	ND	ND	ND	ND	ND	ND	ND	ND	ND	ND	ND	ND	ND
B335	9/12/95	ND	ND	ND	ND	ND	ND	ND	ND	ND	ND	ND	ND	ND
B344	9/12/95	ND	ND	ND	ND	ND	ND	ND	ND	ND	ND	ND	ND	ND
B346	9/12/95	ND	ND	ND	ND	ND	ND	ND	ND	ND	ND	ND	ND	ND
B351	9/12/95	ND	ND	ND	ND	ND	ND	ND	ND	ND	ND	ND	ND	ND

NOT DETECTED = ND NOT ANALYZED = NA

TABLE 2C: PESTICIDES--SEDIMENT DRY WEIGHT DATA IN ng/g

STATION NUMBER (IDORG)	DATE	HEPTACHLOR	HE	HCB	METHOXY	MIREX	CNONA	TNONA	OXAD	OCDAN	TOXAPH
B117	4/8/95	ND	ND	ND	ND	ND	ND	ND	ND	ND	ND
B131	4/9/95	ND	ND	ND	ND	ND	ND	ND	ND	ND	ND
B134	4/9/95	ND	ND	ND	ND	ND	ND	ND	ND	ND	ND
B148	4/10/95	ND	ND	ND	ND	ND	ND	ND	ND	ND	ND
B151	4/10/95	ND	ND	ND	ND	ND	ND	ND	ND	ND	ND
B154	4/10/95	ND	ND	ND	ND	ND	ND	ND	ND	ND	ND
B155	4/11/95	ND	ND	ND	ND	ND	ND	ND	ND	ND	ND
B156	4/11/95	ND	ND	ND	ND	ND	ND	ND	ND	ND	ND
B157	4/11/95	ND	ND	ND	ND	ND	ND	ND	ND	ND	ND
B160	4/11/95	ND	ND	ND	ND	ND	ND	ND	ND	ND	ND
B163	4/11/95	ND	ND	ND	ND	ND	ND	ND	ND	ND	ND
B164	4/11/95	ND	ND	ND	ND	ND	ND	ND	ND	ND	ND
B167	4/11/95	ND	ND	ND	ND	ND	ND	ND	ND	ND	ND
B324	9/11/95	ND	ND	ND	ND	ND	ND	ND	ND	ND	ND
B331	9/11/95	ND	ND	ND	ND	ND	ND	ND	ND	ND	ND
B334	9/12/95	ND	ND	ND	ND	ND	ND	ND	ND	ND	ND
B335	9/12/95	ND	ND	ND	ND	ND	ND	ND	ND	ND	ND
B344	9/12/95	ND	ND	ND	ND	ND	ND	ND	ND	ND	ND
B346	9/12/95	ND	ND	ND	ND	ND	ND	ND	ND	ND	ND
B351	9/12/95	ND	ND	ND	ND	ND	ND	ND	ND	ND	ND

NOT DETECTED = ND

NOT ANALYZED = NA

Table 3A: PAHS--Sediment dry Weight Data in ng/g

PAHBATCH	STATION NUMBER (IDORG)	DATE	ACY	ACE	ANT	BAA	BAP	BBF	BKF	BGP	BEP	BPH	CHR	COR
95.030	B117	4/8/95	ND	ND	ND	9.0	8.7	11.2	ND	7.7	7.5	ND	11.2	5.9
95.070	B131	4/9/95	ND	ND	ND	ND	ND	5.5	ND	ND	ND	ND	ND	ND
95.030	B134	4/9/95	ND	ND	ND	ND	ND	5.7	ND	ND	ND	ND	ND	ND
95.070	B148	4/10/95	ND	ND	ND	ND	ND	ND	ND	ND	ND	ND	ND	ND
95.030	B151	4/10/95	ND	ND	ND	ND	ND	ND	ND	ND	ND	ND	ND	ND
95.070	B154	4/10/95	ND	ND	ND	9.8	9.5	12.8	ND	7.4	7.3	ND	7.9	ND
95.040	B155	4/11/95	ND	ND	ND	ND	5.4	6.3	ND	6.4	ND	ND	ND	6.1
95.040	B156	4/11/95	ND	ND	ND	7.5	8.6	13.8	ND	7.0	6.8	ND	8.5	ND
95.030	B157	4/11/95	ND	ND	ND	ND	ND	ND	ND	ND	ND	ND	ND	ND
95.030	B160	4/11/95	ND	ND	ND	ND	ND	5.7	ND	ND	ND	ND	ND	ND
95.040	B163	4/11/95	ND	ND	ND	ND	ND	ND	ND	ND	ND	ND	ND	ND
95.070	B164	4/11/95	ND	ND	ND	ND	ND	6.6	ND	ND	7.7	7.8	ND	ND
95.030	B167	4/11/95	ND	ND	ND	ND	ND	ND	ND	ND	ND	ND	ND	ND
95.030	B324	9/11/95	ND	ND	ND	8.9	9.1	13.0	ND	8.5	8.5	ND	10.7	ND
95.040	B331	9/11/95	ND	ND	ND	12.0	17.2	17.5	6.5	12.4	11.4	ND	13.8	6.1
95.030	B334	9/12/95	ND	ND	ND	ND	ND	ND	ND	ND	ND	ND	ND	ND
95.040	B335	9/12/95	ND	ND	ND	ND	ND	ND	ND	ND	ND	ND	ND	ND
95.030	B344	9/12/95	ND	ND	ND	11.1	10.5	13.5	5.2	8.1	8.6	ND	12.4	ND
95.030	B346	9/12/95	ND	ND	ND	7.1	7.0	9.1	ND	7.1	6.9	ND	10.2	ND
95.030	B351	9/12/95	ND	ND	ND	ND	ND	6.6	ND	ND	ND	ND	ND	ND

NOT DETECTED = ND NOT ANALYZED = NA

Table 3B: PAHS--Sediment dry Weight Data in ng/g

STATION NUMBER (IDORG)	DATE	DBA	DBT	DMN	FLA	FLU	IND	MNP1	MNP2	MPH1	NPH	PHN	PER	PYR	TMN	TRY	Sum PAHs	TOC PAHs
B117	4/8/95	ND	ND	ND	22.5	ND	6.2	6.9	7.6	5.7	ND	21.6	13.1	24.4	ND	ND	169	20884
B131	4/9/95	ND	ND	ND	7.8	ND	ND	ND	5.4	ND	ND	9.1	6.6	9.4	ND	ND	44	6539
B134	4/9/95	ND	ND	ND	8.4	ND	ND	ND	ND	ND	ND	8.7	7.3	8.7	ND	ND	39	5159
B148	4/10/95	ND	ND	ND	ND	ND	ND	ND	ND	ND	ND	ND	ND	ND	ND	ND	ND	ND
B151	4/10/95	ND	ND	ND	ND	ND	ND	ND	ND	ND	ND	ND	ND	ND	ND	ND	ND	ND
B154	4/10/95	ND	ND	ND	20.4	ND	6.3	5.7	7.9	ND	6.7	22.2	6.2	21.9	ND	ND	152	18086
B155	4/11/95	ND	ND	ND	8.9	ND	ND	5.9	6.8	ND	11.4	7.8	7.7	10.1	ND	ND	83	8890
B156	4/11/95	ND	ND	ND	23.9	ND	6.5	ND	ND	ND	8.2	12.9	19.3	19.1	ND	ND	142	21197
B157	4/11/95	ND	ND	ND	7.0	ND	ND	ND	ND	ND	ND	6.6	ND	7.7	ND	ND	21	2761
B160	4/11/95	ND	ND	ND	8.3	ND	ND	5.6	6.5	ND	5.3	10.0	7.0	9.1	ND	ND	58	6928
B163	4/11/95	ND	ND	ND	5.4	ND	ND	13.5	14.0	ND	17.0	11.5	8.2	5.3	ND	ND	75	7130
B164	4/11/95	ND	ND	ND	9.1	ND	ND	ND	6.3	ND	5.6	11.9	ND	7.9	ND	ND	63	10310
B167	4/11/95	ND	ND	ND	ND	ND	ND	ND	ND	ND	ND	ND	ND	ND	ND	ND	7	ND
B324	9/11/95	ND	ND	ND	21.5	ND	6.7	6.6	8.5	ND	8.9	16.1	7.5	22.4	ND	ND	157	16009
B331	9/11/95	ND	ND	ND	27.4	ND	8.7	7.9	8.4	5.7	13.2	23.1	10.9	33.5	ND	ND	236	21048
B334	9/12/95	ND	ND	ND	7.1	ND	ND	ND	ND	ND	ND	ND	ND	8.0	ND	ND	15	4309
B335	9/12/95	ND	ND	ND	9.2	ND	ND	ND	ND	ND	5.1	7.7	ND	9.5	ND	ND	32	14336
B344	9/12/95	ND	ND	ND	23.5	ND	7.2	ND	ND	ND	5.2	13.1	ND	24.3	ND	ND	143	23384
B346	9/12/95	ND	ND	ND	17.3	ND	5.4	5.4	6.3	ND	ND	14.1	5.6	19.9	ND	ND	121	13643
B351	9/12/95	ND	ND	ND	9.1	ND	ND	5.8	7.1	ND	5.7	11.6	7.0	10.8	ND	ND	64	5020

NOT DETECTED = ND NOT ANALYZED = NA SUM PAH = SUM OF ALL PAH COMPOUNDS TOC PAH = SUM PAHS NORMALIZED TO TOC

TABLE 4--CORRELATIONS BETWEEN CONTAMINANTS

	TOC	Aluminum	Arsenic	Cadmium	Chromium	Copper	Iron	Lead	TOC LEAD	Manganese
TOC	1.000									
Aluminum	-0.313	1.000								
Arsenic	0.313	-0.449	1.000							
Cadmium	0.475	-0.291	-0.089	1.000						
Chromium	0.184	-0.387	0.634	-0.096	1.000					
Copper	0.778	-0.477	0.368	0.317	0.509	1.000				
Iron	0.235	-0.384	0.916	-0.267	0.630	0.261	1.000			
Lead	-0.341	-0.087	-0.210	0.335	-0.370	-0.418	-0.257	1.000		
TOC LEAD	-0.631	0.188	-0.308	-0.210	0.096	-0.442	-0.228	0.041	1.000	
Manganese	0.329	-0.224	0.057	0.178	0.508	0.663	0.076	-0.265	0.087	1.000
Mercury	0.711	-0.294	0.414	0.158	0.432	0.888	0.318	-0.526	-0.506	0.431
Nickel	0.767	-0.503	0.330	0.510	0.459	0.933	0.234	-0.290	-0.430	0.674
Selenium	0.864	-0.246	0.511	0.305	0.118	0.603	0.460	-0.180	-0.795	0.114
Silver	0.838	-0.310	0.124	0.529	0.191	0.810	0.022	-0.344	-0.371	0.507
Tin	0.811	-0.243	0.058	0.638	0.146	0.637	-0.064	-0.258	-0.361	0.324
Zinc	0.833	-0.440	0.419	0.363	0.275	0.734	0.303	-0.263	-0.395	0.491
DDE	0.541	-0.468	0.271	0.558	0.267	0.742	0.118	-0.053	-0.307	0.673
TOC DDE	0.450	-0.419	0.273	0.436	0.254	0.722	0.114	-0.043	-0.353	0.506
Sum PAHs	0.603	-0.020	0.313	0.227	0.038	0.311	0.258	-0.490	-0.362	-0.099
TOC PAHs	0.046	0.064	0.215	0.094	0.162	-0.083	0.170	-0.354	0.259	-0.220
% FINES	0.869	-0.265	0.176	0.485	0.184	0.836	0.059	-0.458	-0.530	0.415

	Mercury	Nickel	Selenium	Silver	Tin	Zinc	DDE	TOC DDE	Sum PAHs	TOC PAHs	% FINES
	1.000										
Mercury	0.431	1.000									
Nickel	0.674	0.796	1.000								
Selenium	0.114	0.653	0.600	1.000							
Silver	0.507	0.741	0.863	0.649	1.000						
Tin	0.324	0.615	0.734	0.590	0.879	1.000					
Zinc	0.491	0.569	0.723	0.714	0.801	0.672	1.000				
DDE	0.573	0.610	0.735	0.465	0.648	0.426	0.606	1.000			
TOC DDE	0.506	0.628	0.695	0.435	0.578	0.316	0.502	0.961	1.000		
Sum PAHs	-0.099	0.452	0.371	0.603	0.632	0.617	0.486	0.223	0.165	1.000	
TOC PAHs	-0.220	0.043	0.003	0.016	0.234	0.264	0.045	-0.051	-0.108	0.731	1.000
% FINES	0.415	0.799	0.865	0.682	0.934	0.853	0.704	0.605	0.564	0.680	0.233

Critical Value for correlation coefficient is .561 for P,.01: values > .561 in bold

TABLE 5: SEDIMENT RESULTS FOR METALS ON A DRY WEIGHT BASIS AND LEAD ON A TOC BASIS (UG/G)

IDORG	DATE	TOC	Aluminum	Arsenic	Cadmium	Chromium	Copper	Iron	Lead	TOC LEAD	Manganese	Mercury	Nickel	Selenium	Silver	Tin	Zinc
B117	4/9/95	0 81	76700	6.33	0 26	139	14.6	43500	8.65	1068	235	0.0959	67.6	0.19	0.090	1.02	50.2
B131	4/10/95	0.67	93300	7.09	0.26	180	19.4	43700	9.60	1433	352	0.129	99.2	0.18	0.096	1.04	51.9
B131-D	4/10/95	0.67	81700	7.33	0.28	160	17.9	45000	10.6	1582	1060	0.0959	86.1	0.18	0.10	1.12	77.4
B134	4/10/95	075	84400	6.74	0 25	165	17.8	43600	8.88	1184	318	0.107	96.2	0.17	0 089	1.00	56.2
B148	4/11/95	0 34	89500	3.91	0.20	71 6	6.55	28100	11.3	3324	191	0.0402	34.1	0 13	0 051	0.58	43 6
B151	4/11/95	0 31	82300	4.53	0.15	121	6.97	39100	10.6	3419	286	0 0311	36.5	0 12	0 043	0 73	44 9
B154	4/11/95	0 84	62500	6.02	0 49	139	15.8	39800	7.70	917	247	0 102	94.6	0 18	0 106	1.19	53 6
B155	4/12/95	0 93	59500	8.35	0.37	171	20.8	33800	7.73	831	294	0.122	94.0	0.15	0 100	1 25	75 9
B156	4/12/95	0 67	69000	16 3	0.19	212	11.4	105000	9.12	1361	213	0.0789	64.6	0 22	0 057	0.80	61.2
B157	4/12/95	0 77	81400	5.57	0 30	182	12.7	43000	9.48	1231	307	0.0739	64.4	0 17	0 072	1.02	51 9
B160	4/12/95	0 83	55700	8.01	0.43	132	14.0	43300	12.7	1530	258	0 0878	78.4	0 22	0.098	1.27	69 9
B163	4/12/95	1.05	61300	7.71	0.90	157	20.4	40600	12 4	1181	401	0 0986	127	0 22	0 121	1.31	80 8
B164	4/12/95	0 61	79000	5.90	0.46	135	12.1	29800	10.5	1721	316	0.0419	83.7	0.13	0 077	0.99	52.5
B167	4/12/95	ND	87900	3.56	0.26	171	6.51	25900	9.46	ND	321	0.0214	37.5	<.10	0.059	0.81	39.6
B167-D	4/12/95	ND	90800	3.81	0.34	169	6.98	27000	11.0	ND	316	0.0236	46.8	<.10	0.061	0.84	41.9
B324	9/12/95	0 98	65600	5.97	0.52	143	15.1	44100	11.4	1163	279	0.0835	103	0 19	0 119	1 46	71 1
B331	9/12/95	1 12	114000	5.56	0.36	99.5	12.2	31000	7.34	655	267	0 0907	64.4	0 24	0 116	1 37	76.8
B334	9/13/95	0 35	94700	4.11	0 43	118	6.53	16500	13.3	3800	183	0.0391	36 3	0 12	0.052	0.85	36 2
B335	9/13/95	0 22	90100	4.93	0.48	95.2	3 36	25600	13.4	6091	144	0.0278	17.7	0 10	0 037	0.68	25.3
B344	9/13/95	0 61	87000	4.95	0 57	135	9.24	21800	10.9	1787	197	0.0495	64.4	0 16	0 090	1 32	53.7
B346	9/13/95	0.89	87200	5.85	0.59	141	14.4	34000	8.70	978	266	0 117	93.1	0.18	0 094	1.55	46 0
B351	9/13/95	1 27	76600	6.00	0.60	138	16.1	38800	10.5	827	262	0.0677	83 9	0.22	0 093	1 32	70 5

D after station number indicates a duplicate analysis
Not detected = ND Not analyzed = NA

Table 6- Comparison of Sediment Screening Levels
Developed by NOAA and the State of Florida

SUBSTANCE	State of Florida (1) TEL	State of Florida (1) PEL	NOAA (2) ERL	NOAA (2) ERM
Organics (ug/kg- dry weight)				
Total PCBs	21.550	188.79	22.70	180.0
PAHs				
Acenaphthene	6.710	88.90	16.00	500.0
Acenaphthylene	5.870	127.89	44.00	640.0
Anthracene	46.850	245.00	85.30	1100.0
Fluorene	21.170	144.35	19.00	540.0
2-methylnaphthalene	20.210	201.28	70.00	670.0
Naphthalene	34.570	390.64	160.00	2100.0
Phenanthrene	86.680	543.53	240.00	1500.0
Total LMW-PAHs	311.700	1442.00	552.00	3160.0
Benz(a)anthracene	74.830	692.53	261.00	1600.0
Benzo(a)pyrene	88.810	763.22	430.00	1600.0
Chrysene	107.710	845.98	384.00	2800.0
Dibenz(a,h)anthracene	6.220	134.61	63.40	260.0
Fluoranthene	112.820	1493.54	600.00	5100.0
Pyrene	152.660	1397.60	665.00	2600.0
Total HMW-PAHs	655.340	6676.14	1700.00	9600.0
Total PAHs	1684.060	16770.54	4022.00	44792.0
Pesticides				
p,p'-DDE	2.070	374.17	2.20	27.0
p,p'-DDT	1.190	4.77		
Total DDT	3.890	51.70	1.58	46.1
Lindane	0.320	0.99		
Chlordane	2.260	4.79	0.50	6.0
Dieldrin	0.715	4.30	0.02	8.0
Endrin			0.02	45.0
Metals (mg/kg- dry weight)				
Arsenic	7.240	41.60	8.20	70.0
Antimony			2.00	2.5
Cadmium	0.676	4.21	1.20	9.6
Chromium	52.300	160.40	81.00	370.0
Copper	18.700	108.20	34.00	270.0
Lead	30.240	112.18	46.70	218.0
Mercury	0.130	0.70	0.15	0.7
Nickel	15.900	42.80	20.90	51.6
Silver	0.733	1.77	1.00	3.7
Zinc	124.000	271.00	150.00	410.0

(1) D.D. MacDonald, 1994

(2) Long et al., 1995

TABLE 7. CONTAMINANTS NORMALIZED TO GRAIN SIZE AND A COMPARISON TO NOAA STATUS AND TRENDS HIGH VALUES

STATION NUMBER (IDORG)	TOC	% fines	Aluminum/GS	Arsenic/GS	Cadmium/GS	Chromium/GS	Copper/GS	Iron/GS	Lead/GS	Manganese/GS	Mercury/GS	Nickel/GS	Selenium/GS	Silver/GS	Tin/GS	Zinc/GS	DDE/GS	SUM PAHs/GS
B117	0.81	88	87169	7.19	0.30	156	17	49432	10	267	0.11	77	77	0.10	1.16	57	5.92	192
B131	0.67	85	109765	8.34	0.31	212	23	51412	11	414	0.15	117	117	0.11	1.22	61	5.47	62
B134	0.75	72	117222	9.36	0.35	229	25	60556	12	442	0.15	134	134	0.12	1.39	78	3.67	64
B148	0.34	22	408818	17.77	0.91	325	30	127727	51	868	0.18	155	155	0.23	2.64	198	5.45	-36
B154	0.84	95	65789	6.34	0.52	146	17	41895	8	260	0.11	100	100	0.11	1.25	56	4.28	160
B155	0.93	94	63298	8.88	0.39	182	22	35967	8	313	0.13	100	100	0.11	1.33	81	10.61	88
B156	0.67	37	186486	44.05	0.51	573	31	283784	25	576	0.21	175	175	0.16	2.16	185	7.49	384
B157	0.77	44	185000	12.66	0.68	414	29	97727	22	698	0.17	146	146	0.16	2.32	118	3.98	48
B160	0.83	61	91311	13.13	0.70	216	23	70984	21	423	0.14	129	129	0.16	2.08	115	4.95	94
B163	1.06	96	63854	8.03	0.94	164	21	42292	13	418	0.10	132	132	0.13	1.36	84	24.48	78
B164	0.61	74	106757	7.97	0.62	182	16	40270	14	427	0.06	113	113	0.10	1.34	71	2.34	85
B324	0.98	96	68333	6.22	0.54	149	16	45938	12	291	0.09	107	107	0.12	1.52	74	2.64	163
B331	1.12	98	116327	5.67	0.37	102	12	31633	7	272	0.09	66	66	0.12	1.40	78	4.26	241
B344	0.61	72	120833	6.88	0.79	188	13	30278	15	274	0.07	89	89	0.13	1.83	75	2.04	198
B346	0.89	96	90833	6.09	0.61	147	15	36417	9	277	0.12	97	97	0.10	1.61	48	2.88	126
B361	1.27	84	91190	7.14	0.71	164	19	46190	13	312	0.08	100	100	0.11	1.57	84	2.50	76
NOAA STATUS AND TRENDS HIGH VALUES[1]				24	1.2	230	84	NA	89	NA	0.49	69	NA	1.2	8.5	270	37	3880

VALUES IN UG/G FINES ON A DRY WEIGHT BASIS
FINES = AMOUNT OF CLAY PLUS AMOUNT OF SILT IN SAMPLE
METAL /GS INDICATES THE METAL IS NORMALIZED TO GRAIN SIZE BY DIVIDING THE AMOUNT OF METAL BY THE DRY WEIGHT OF THE FINE GRAIN SEDIMENTS (FINES)
SAMPLES WITH LESS THAN 20% FINES NOT IN TABLE

Frequency and Determination of External Lesions in Dover Sole (*Microstomus pacificus*) and English Sole (*Pleuronectes vetulus*) in Monterey Bay, CA

Korie Ann Johnson and Gregor M. Cailliet
Moss Landing Marine Laboratories, Moss Landing, CA 95039

Mark Stephenson
California Department of Fish and Game, Moss Landing Marine Laboratories, Moss Landing, CA 95039

George Gardner
US Environmental Protection Agency, National Health and Environmental Effects Research Laboratory, Naragansett, RI 02882

ABSTRACT

Tumor-like lesions were observed on Dover and English sole in Monterey Bay, CA during a 1994 field survey conducted to develop information on population dynamics. The lesions, focal areas of raised epithelium, in these important groundfish raised concern about a possible relationship with anthropogenic contaminants emanating from the FORZ, the Pajaro River, and/or the Salinas River. As a result, monitoring activities were conducted to develop information on the distribution of these tumor-like lesions. Dover sole lesions were histologically diagnosed as X-cell pseudotumors, and English sole lesions as trematode cercaria infestations. At these Monterey Bay locations, we determined the mean percent of Dover sole affected with X-cell tumors to be 7.4, 7.7 and 6.9, and the mean percent of English sole with trematodiasis to be 10.7, 12.3 and 17.6, respectively. The occurrence of external lesions on flatfishes in Monterey Bay is not significantly elevated above normal baseline levels for southern California. This study has not demonstrated a relationship between past military activities associated with FORZ and the occurrence of external lesions on fishes in Monterey Bay.

INTRODUCTION

The occurrence of anomalous and diseased fishes along the coast of the North Pacific has been documented since the early 1950's (Young, 1964, Levings, 1967, Misitano, 1971, Mearns and Sherwood, 1974, Mearns and Sherwood, 1976, Sherwood and Mearns, 1976, Stich et al., 1976, Wellings et al., 1976, Compana, 1983, Cross, 1986). The cause of these abnormalities can range from a number of natural processes, including metabolic disorders, viruses, bacteria, fungi or other pathogenic organisms, to man-induced or anthropogenic influences, such as chemical or thermal contaminants (Sindermann, 1979, Cailliet et al., 1986, Harshbarger et al., 1993). Environmental contamination, a serious problem in urbanized areas, can have both direct and indirect effects on fishes (Sindermann, 1979). Examples of direct effects include cancerous tumors and birth defects. Indirect effects are much harder to detect and include weakening of the animals defense mechanisms, making them more susceptible to infection.

Flatfishes, in particular, are prone to diseases and abnormalities because of their benthic habitats and sedentary lifestyle (Stich and Acton, 1976). Juvenile and adult flatfish have a wide geographic distribution, absence of extensive migration patterns, and are commonly found in polluted waters, making them particularly susceptible to pollution-induced diseases. Tumors, in particular, have been reported on at least 10 species of flatfish between Alaska and California including starry flounder (*Platichthys stellatus*), sand sole (*Psettichthys melanostictus*), flathead sole (*Hippoglossoides classodon*), Dover sole (*Microstomus pacificus*) and English sole

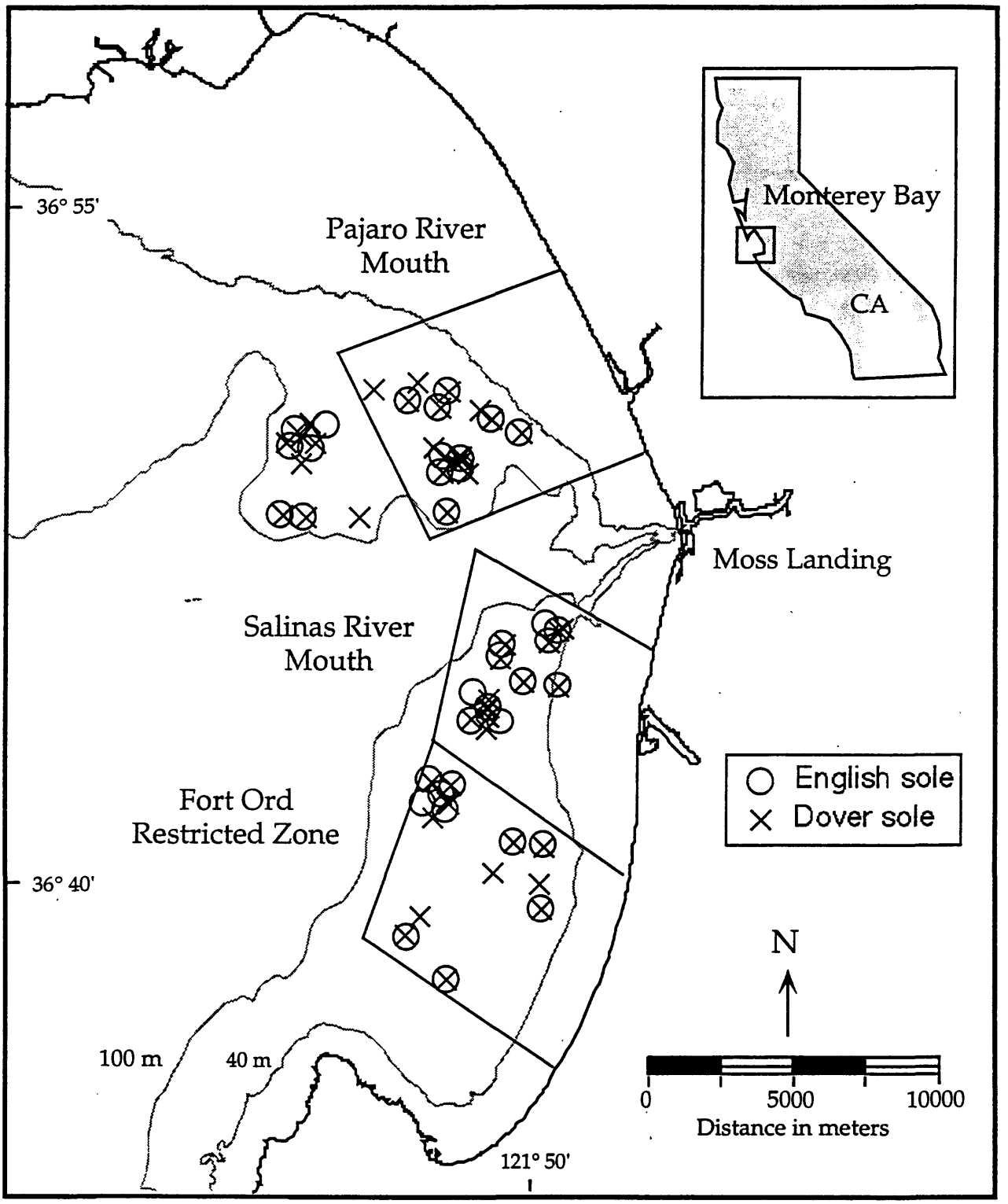

Figure 1. Map of individual trawl tows for English and Dover sole within each of the sampling areas (FORZ, Salinas River mouth and Pajaro River mouth) in Monterey Bay, CA.

(*Pleuronectes vetulus*; McArn and Wellings, 1971, Miller and Wellings, 1971, Mearns and Sherwood, 1974). In a pilot study conducted in Monterey Bay, CA, external lesions were found on both Dover sole, *Microstomus pacificus*, and English sole, *Pleuronectes vetulus*. The occurrence of external lesions on fishes in Monterey Bay had not previously been documented.

Monterey Bay is located along the central California coast between 36.5° N and 37° N (Figure 1). The bay is symmetrical in shape measuring 37 km long and covering approximately 550 km^2. Approximately 80% of the Bay is shallower than 100 m and most of this area is soft bottom habitat (Breaker and Broenkow, 1994).

There are several possible sources of contaminants in Monterey Bay. Environmental hazards may exist offshore of the former Fort Ord Restricted Zone (FORZ; Figure 1) resulting from decades of military use. Military activities included storm water discharge, sewage treatment outfalls, ocean disposal of military waste, munitions use, and amphibious beach landings (Harding Lawson Associates, 1994). In addition, two wastewater treatment plants are currently located along Monterey Bay with outfalls emptying into bay waters.

Monterey Bay water quality is also influenced by surrounding agricultural areas. A number of pesticides and fertilizers are used in these areas. Runoff from agricultural fields drain into the Salinas and Pajaro Rivers. Although both rivers have low rain-induced flow from May through October or November of each year, heavy rains in winter and early spring cause major flood conditions that wash contaminated water and sediments directly into Monterey Bay. These inputs and activities may have adverse affects on the soft-bottom ichthyofaunal community.

English sole and Dover sole are important ecological and economic species in Monterey Bay. Both English and Dover sole have pelagic eggs and extended larval stages before metamorphosis and recruitment to nearshore benthic habitats (Hagerman, 1952, Eshmeyer et al., 1983, Markle et al., 1992). Dover sole spawn in deep water from December to February. Settlement occurs the following January through April. During the planktonic stages, eggs and larvae are vulnerable to the southward flowing California Current System and may be transported over long distances. English sole spawning occurs between January and March. Eggs are pelagic but sink several hours before hatching. Young are pelagic for 6-10 weeks before settling out to shallow, intertidal areas such as estuaries and bays. Adults of both Dover and English sole are harvested by commercial trawlers as part of the groundfish fishery. In 1994 alone, Dover sole landings in the Monterey area totaled 1,010,770 lbs worth $275,638 in exvessel price. English sole landings for 1994 totaled 133,341 lbs worth $49,845 in exvessel price.

OBJECTIVES

The purposes of this study were to (1) examine species composition and percentage of benthic fishes with external lesions or abnormalities; (2) determine spatial distribution of Dover and English sole with external lesions in relation to the former FORZ, the Pajaro River and Salinas River mouths; and (3) use histopathology to determine type and possible cause of lesions.

METHODS

Collections

Three sampling areas were designated within Monterey Bay, CA, each approximately the same size and shape (Figure 1). Sediments within the three areas are described as soft bottoms ranging from sandy mud to silt and clay. Samples were taken between 40-100 m within each sampling area. Additional samples were also taken outside of these three areas in the northern half of the bay to provide further information on spatial distribution.

The R/V Ed Ricketts was used to conduct trawl sampling of fishes on soft bottoms within each study area. The primary gear used was an otter trawl with a bridle length of 22.9 m, a mouth width of 8.3 m, a body mesh size of 3.8 cm, and a cod-end mesh size of 1.0 cm. A 4:1 wire ratio was used for all tows to ensure that the trawl was consistently fishing on the bottom. The duration of each trawl tow was approximately 20 minutes. Latitude and longitude of the vessel, as determined from LORAN C, were recorded at the beginning and end of each trawl in order to

estimate distance traveled. Sampling began in August 1995 and continued weekly, as weather permitted, through January 1996.

All flatfish were examined for the presence of external lesions. Dover sole and English sole were separated from the catch, designated as tumorous or non-tumorous and measured to the nearest mm standard length. Samples of tumored fishes were brought back to the lab and preserved in Dietrich's Fixative for histopathology.

Histopathology

Pathological evaluations were made on both English sole and Dover sole using liver, spleen and muscle tissue. Tissue from preserved fishes was embedded in paraffin, sectioned at 6 microns, and stained with Harris' hematoxylin and eosin.

RESULTS

Species composition of the trawl samples from Monterey Bay remained relatively stable throughout the sampling period. Samples were dominated by several species of flatfish, especially Pacific sanddabs (*Citharichthys sordidus*), Dover sole (*Microstomus pacificus*) and English sole (*Pleuronectes vetulus*). External lesions were only observed on Dover sole and English sole.

Dover and English sole with external lesions were found throughout the bay. A total of 2,606 Dover sole was sampled, 6.3 % of which had external lesions (Table 1). Percentage of Dover sole with external lesions within individual trawl tows ranged from 0-50.0 %. A total of 1085 English sole was sampled, 9.9 % of which had external lesions, with percentages within individual trawl tows ranging from 0-69.2%.

Table 1. Summary of sample sizes and percent of sole with external lesions for both Dover and English sole in each of the three sampling areas in Monterey Bay: FORZ, Salinas River and Pajaro River.

	Dover sole				English sole			
	# tows	# fish	overall %	mean % / tow	# tows	#fish	overall %	mean % / tow
FORZ	14	858	7.3	7.4 ± 1.6	10	373	9.4	10.7 ± 3.7
Salinas River	14	282	8.9	6.9 ± 1.8	10	239	13.4	17.6 ± 8.0
Pajaro River	23	954	6.3	7.7 ± 2.3	13	297	9.4	12.3 ± 4.5

The outward appearance of the lesions differed between species. Lesions on Dover sole were larger in size reaching up to approximately 20 mm, varied from white to red in color, and often had a cauliflower-like appearance. The majority of Dover sole had only one lesion, but two lesions were found on several individuals. In English sole, lesions were smooth and reddish in color. Most of the English sole with external lesions had multiple nodules, approximately 1 mm in size, covering the blind side of the fish. Larger lesions, measuring 1-5 mm in size, were also evident at the base of the fins and between fin rays.

The proportion of fish with external lesions was not different among the three sampling areas for either Dover sole or English sole (Figure 2). Within each area, however, a higher percentage of English sole were affected than Dover sole. For Dover sole the mean percent fish per tow with external lesions was 6.9±14.8 off the Salinas River, 7.4±1.6 off FORZ, and 7.7±2.3 off the Pajaro River. For English sole the mean percent of fish per tow with external lesions was 10.7±3.7 off FORZ, 12.3±4.5 off the Pajaro River and 17.6±8.0 off the Salinas River.

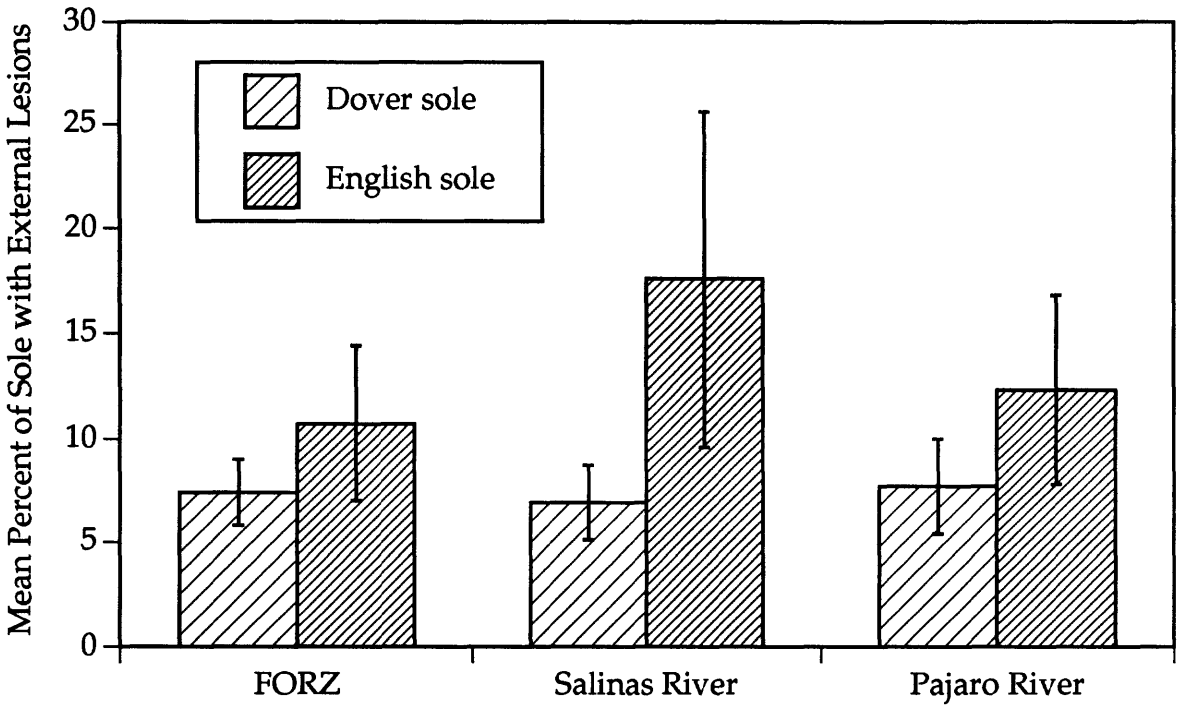

Figure 2. Percent of Dover and English sole affected with external lesions within each of the three sampling areas: FORZ, Salinas River mouth and Pajaro River mouth. Values represent mean percent per trawl. Error bars denote standard error.

Patterns of external lesions with size differed between Dover and English sole. Ninety-eight percent of the Dover sole sampled ranged from 60-140 mm. Fish within the entire size range were affected by lesions. No clear trend between fish size ad occurrence of external lesions was evident. (Figure 3).

English sole were a little larger than Dover sole, with 96% ranging from 80-220 mm standard length. The percentage of English sole affected by external lesions increased with increasing size (Figure 4). Nineteen percent of English sole greater than 100 mm exhibited external lesions, while only 2% of those less than or equal to 100 mm had external lesions.

Histopathological results concluded that external lesions on the Dover sole were X-cell pseudotumors. X-cells are infections of parasitic amebae resembling *Hartmanella.* They have a large nucleoli composed of fine granules and numerous, small clumps of chromatin, and are surrounded by thin epidermal cell processes.

Lesions on the English sole were raised epithelia due to larval forms of endo-parasites. The parasites were characteristic of Platyhelminthes worms from the Class Trematodes and Order Digenea, and were found in the subdermal epithelial layer, musculature and liver. Infestation by this parasite is known as trematodiasis or helminthiasis.

Spleen tissue sections in the English sole samples showed increasing macrophage area and number with increasing prevalence of trematodiasis. No tumors or other significant lesions were identified in the liver tissue samples.

DISCUSSION

Dover and English sole were the only two species caught in our samples that had external lesions. Occurrence of external lesions and abnormalities has been cited for these two species in previous studies (Wellings et al., 1976, Mearns and Sherwood, 1974, Cross, 1986). Pacific sanddabs were the most abundant species in this study and none were observed to have external lesions. Previous studies have shown that in most cases only one or two species in an area have tumors, even though other potentially vulnerable species are present in the same or greater abundance (Wellings et al., 1976). At present it is unknown why the species composition of tumored fishes changes between regional location, when similar species are available throughout the eastern Pacific nearshore areas.

The widespread occurrence of Dover sole and English sole with lesions in Monterey Bay makes it impossible to pinpoint affects from specific sources of contaminants. More extensive sampling is needed which extends outside of the bay to determine if the lesions are concentrated within the bay or abundant throughout the central coast.

The numbers of external lesion-bearing fishes in Monterey Bay were similar to findings in previous studies. Mearns and Sherwood (1974, 1976) recorded tumors on Dover sole, with prevalence of tumor bearing fish reaching as high as 9% in southern California and 6.7 % in Baja California. Surveys conducted off the Palos Verdes shelf in southern California between 1971-83 found 2.5% of all Dover sole less than 150 mm had external lesions. Many further studies have found proportions reaching over 50% (Stich and Acton, 1976, McArn and Wellings, 1971, Kimura, 1971). Therefore, percentages in Monterey Bay were not extremely high, and may even be considered low by some comparisons.

The occurrence of external lesions on Dover sole may be more of wide spread juvenile problem as cited by Mearns and Sherwood (1976) and Cross (1986). This study extends the range of Dover sole with external lesions to include Monterey Bay. Size patterns with Dover sole show that they are affected soon after recruitment. Similar patterns have been reported for Dover sole in southern California and Baja. If the sensitive period for lesion induction is during early development then knowledge of the distribution of Dover sole prior to and during metamorphosis may be of more importance than the location where the fish are caught.

The fate of fishes with X-cell lesions is as of yet unknown. There is no evidence of regression or shedding of X-cell lesions in species maintained in laboratory observations. Instead, tumors appear to enlarge with fish growth. Many studies have shown that the number of fishes with tumors steadily decline with size. Thus, it is assumed that tumored fish either die or leave the study area. The depth range and equipment used in sampling for this study allowed for the catch

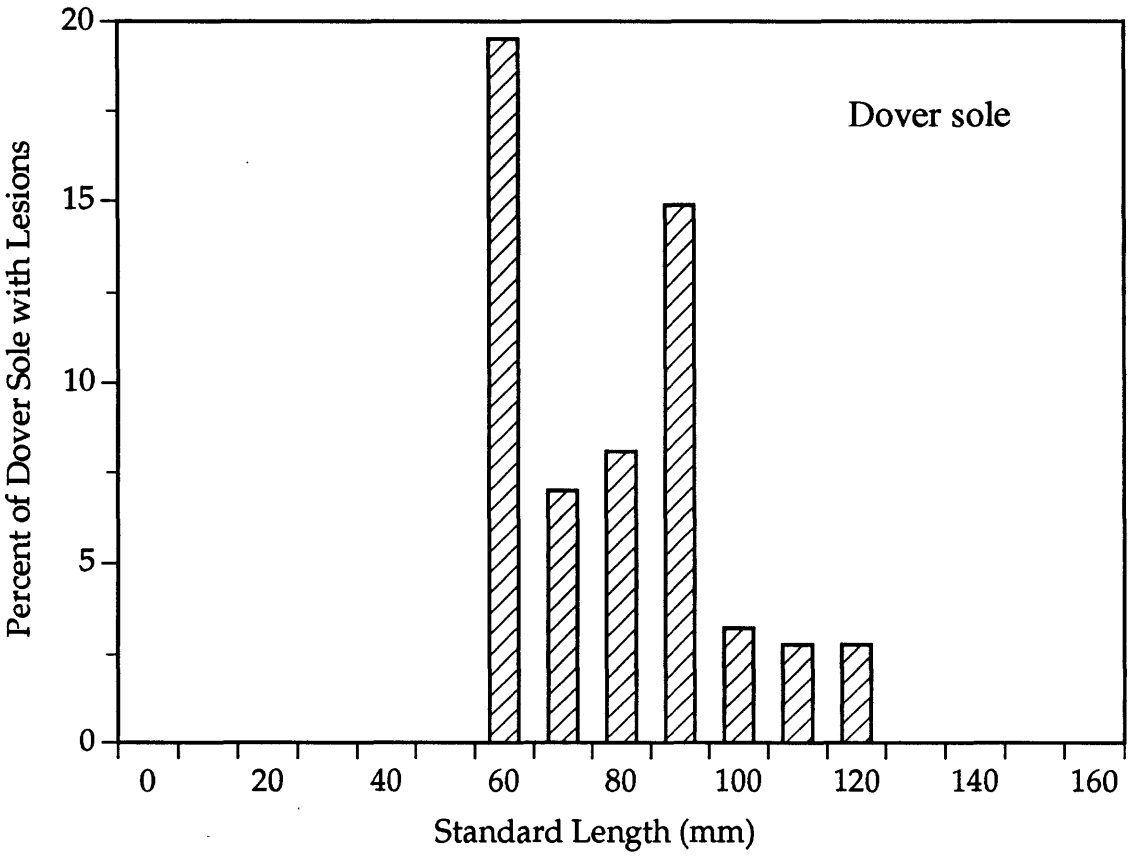

Figure 3. Percent of Dover sole affected by external lesions per 10 mm size category. Ninety-eight percent of all Dover sole sampled ranged from 60-140 mm standard length.

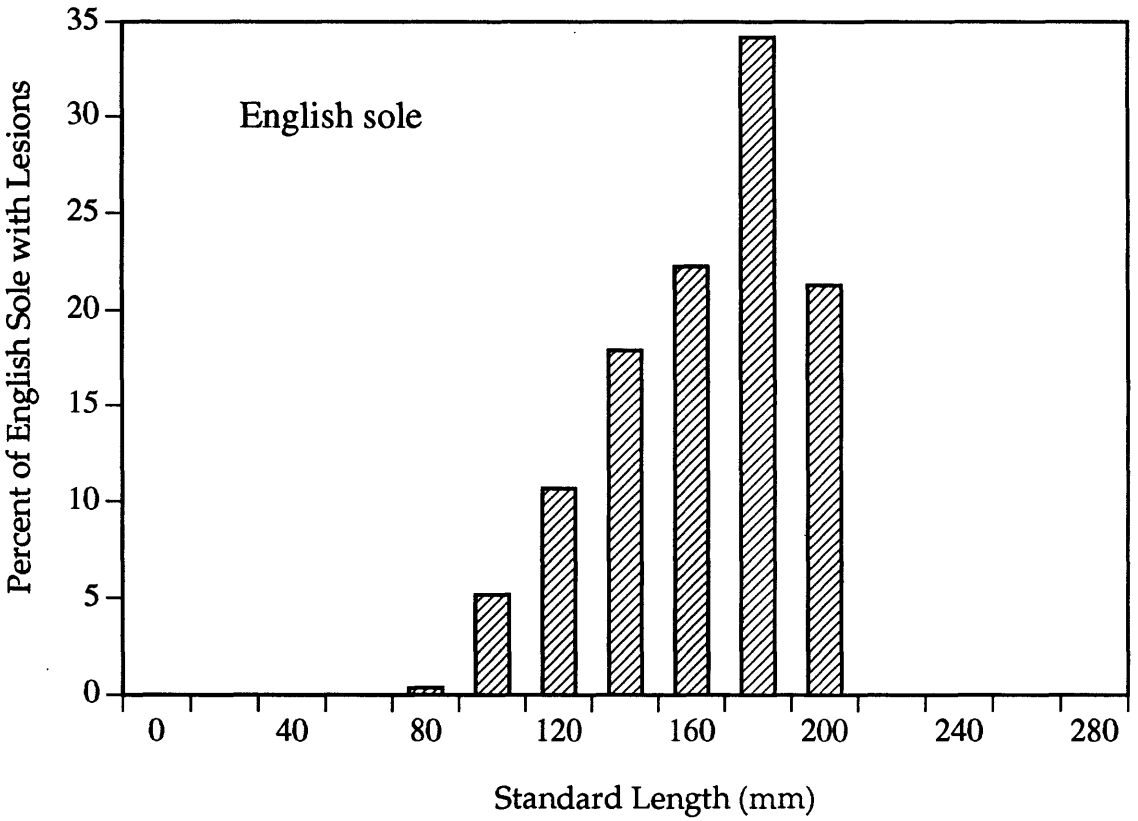

Figure 4. Percent of English sole affected by external lesions per 20 mm size category. Ninety-six percent of all English sole sampled ranged from 80-220 mm standard length.

of smaller individuals only. Further sampling is needed to determine if the trend of decreasing occurrence of external lesions in adult fish holds true for Monterey Bay. If those fishes affected by external lesions do die at an early age, then it is possible that population size could be affected.

The occurrence of trematodiasis and increasing macrophage aggregates in fishes, as seen in the English sole in this study, has increased in the past several decades. Increasing macrophage area in the spleen is currently considered pathological in several species of flatfish, such as the winter flounder, *Pseudopleuronectes americanus* (Wolke et al., 1985). This structural alteration in the spleen tissue has been considered as a monitor of fish health in relation to pollution, and has been correlated with concentrations of organic pollutants in sediments (Gardner, et.al., 1989). However, macrophage aggregate parameters may be affected by a number of factors other than pollution, including age, disease, thermal environment and season (Blazer et al., 1987).

Recent research has shown increases in fish and shellfish diseases correlating to increases in contaminants in sediments. Trematodiasis and macrophage activity are among those diseases and may have important implications for organisms of ecological concern. At this time, the reason for trematodiasis and increased macrophage areas in the English sole spleen is unidentified, primarily because baseline conditions from some reference site, and any relationship with measured chemical contaminant levels has not been established. It is generally known that fish immune systems can be weakened by pollution-induced stress, causing higher susceptibility to parasitism and elevated macrophage response.

In summary, the occurrence of external lesions on flatfishes in Monterey Bay are not significantly elevated above normal baseline levels for southern California. This study has not demonstrated a relationship between past military activities associated with FORZ and the occurrence of external lesions on fishes in Monterey Bay.

ACKNOWLEDGEMENTS

We thank Dr. John Harshbarger of the Smithsonian Institute for help with the histopathology work.

REFERENCES

Blazer, V.S. Wolke, R.E., Brown, J. and C.A. Powell, 1987, Piscine macrophage aggregate parameters as health monitors: effect of age, sex, relative weight, season and site quality in largemouth bass (*Micropterus salmoides*), *Aquatic Toxicology* , 10 (1987): 199-215.

Breaker, L.C. and W.W. Broenkow, 1994, The circulation of Monterey Bay and related processes, *Ocean Mar Bio: Annual Review* , 32: 1-64.

Campana, S.E., 1983, Mortality of starry flounders (*Platichthys stellatus*) with skin tumors, *Can J Fish Aquat Sci* , 40: 200-207.

Cross, J.N., 1986 Epidermal tumors in *Microstomus pacificus* (Pleuronectidae) collected near a municipal wastewater outfall in the coastal waters off Los Angeles (1971-1983), *CFG* 72(2): 68-77.

Eschmeyer, W.N. and E.S. Herald, 1983, A Field Guide to Pacific Coast Fishes of North America, Houghton Mifflin: Boston, 336 pp.

Gardner, G.R., Benyi, S.J., Heltshe, J.F. and J. Rosen, Pigment localization in lymphoid organs of the winter flounder (*Pseudopleuronectes americanus*) in relation to contaminated sediment, In: Society of Environmental Toxicology and Chemistry, Proceedings of 10th Annual meeting, Toronto, November 1989.

Hagerman, F.B., 1952, The biology of Dover sole, *Microstomus pacificus* (Lockinton), *CFG Fish Bull* , 85, 45 pp.

Harding-Lawson Associates, 1994a, Draft Enhanced Preliminary Assessment of Monterey Bay Fort Ord, California, Unpublished, Engineering and Environmental Services, Novato, California, USA.

Harshbarger, J.C., Spero, P.M. and N.M. Wolcott, 1993, Neoplasms in wild fish from the marine ecosystem emphasizing environmental interactions, In: Pathology of Marine and Estuarine Organisms, Edited by J.A. Couch and J.W. Fournie, U.S. Environmental Protection Agency Environmental Research Laboratory, Florida, CRC Press: Boca Raton.

Hinton, D.E., Baumann, P.C., Gardner, G.R., Hawkins, W.E., Hendricks, J.D., Murchelano, R.A. and M.S. Okihiro, 1992, Histophathologic biomarkers, In: Biomarkers: Biochemical, Physical, and Histological markers of Anthropogenic Stress, Proceedings of the Eighth Pellston Workshop, Edited by R.J Huggett, R.A Kimerie, P.M. Mehrle, Jr., and H.L. Bergman, Lewis Publishers: Boca Raton.

Kimura, J, Miyake, T. and Y. Ito, 1971, Papillomatous grouth of skin in Japanese common goby, McArn, G.E. and S.R. Wellings, 1971, A comparison of skin tumors in three species of flounders, *J. Fish Res Board Can* , 28: 1241-1251.

Levings, C.D., 1967, A comparison of growth rates of the rock sole, *Lepidopsetta bilineata*, in northeast Pacific waters, *Fish Res Board Can, Tech Rep* , 36, 43 pp.

Markle, D.F., Harris, P.M. and C.L. Toole, 1992, Metamorphosis and an overview of early-life-history stages in Dover sole *Microstomus pacificus*, *Fish Bull* , 90: 285-301.

McArn, G.E. and S.R.Wellings, 1971, A comparison of skin tumors in three species of flounders, *J Fish Res Board Can* , 28: 1241-1251.

Mearns, A.J. and M.J. Sherwood, 1974, Environmental aspects of fin erosion and tumors in Southern California Dover sole, *Trans Amer Fish Soc* , 1974(4): 799-810.

Mearns, A.J. and M.J. Sherwood, 1976, Ocean wastewater discharge and tumors in a southern California flatfish, *Prog exp Tumor Res* , 20: 75-85.

Miller, B.S. and S.R. Wellings, 1971, Epizootiology of tumors in flathead sole (*Hippoglossoides elassodon)* in East Sound, Orcas Island (Wash.), *Trans Amer Fish Soc* , 100 (2): 247-266.

Misitano, D.A., 1971, Aspects of early life history of English sole (*Parophrys vetulus*) in Humboldt Bay, Calif, M.A. Thesis, Humboldt State College, California,

Sherwood, M.J. and A.J. Mearns, 1976, Occurrence of tumor-bearing Dover sole (*Microstomus pacificus*) off Point Arguello, California and off Baja California, Mexico, *Trans Amer Fish Soc* , 1976(4): 561-5693.

Sindermann, C.J., 1979, Pollution-associated diseases and abnormalities of fish and shellfish: a review, *Fish Bull* , 76(4): 717-749.

Stich, H.F. and A.B. Acton, 1976, The possible use of fish tumors in monitoring for carcinogens in the marine environment, *Prog exp Tumor Res* , 20: 44-54.

Stich, H.F., Acton, A.B. and C.R. Forrester, 1976, Fish tumors and sublethal effects of pollutants, 1976, *J Fish Res Board Can* , 33:1993-2001.

Wellings, S.R., McCain, B.B. and B.S. Miller, 1976, Epidermal papillomas in Pleuronectidae of Puget Sound, Washington, *Prog exp Tumor Res* , 20: 55-74.

Wolke, R.E., George, C.J. and V.S. Blazer, 1985, Pigmented macrophage accumulations (MMC;PMB): possible monitors of fish health, In: Parasitology and Pathology of Marine Organisms of the World Oceans, edited by W.J Hargiss, NOAA Tech Rep NMFS 25: 93-97.

Young, P.H., 1964, Some effects of sewer effluent on marine life, CFG 50: 33-41.